Optics and Fluid Dynamics Department annual progress report for 1996

Hanson, Steen Grüner; Johansen, Per Michael; Lading, Lars; Lynov, Jens-Peter; Skaarup, Bitten

Publication date:
1997

Document Version
Publisher's PDF, also known as Version of record

Contents

1. Introduction

L. Lading
E-mail: lars.lading@risoe.dk

The department performs basic and applied research within optics and nonlinear dynamics, which includes fluids and plasmas. The scope is understanding of physical phenomena as well as development of materials and systems for specific applications. The activities are often performed in collaboration with other research groups or industry. The training of students at a graduate level is an integral part of the activities and so is the dissemination of results to research and industry.

The work is of importance to the understanding of coherent structures in fluids, plasmas and nonlinear optical systems, as well as to the understanding of optical diagnostic systems and new optical materials. However, the understanding of basic physical phenomena has to be used for devising *solutions to problems*. This is done in connection with (1) new sensors and measuring systems, (2) the processing of spatial data, (3) devising schemes for novel laser systems and (4) information storage systems. Several results are exploited by industry. The activities are supported by a number of national and international granting agencies.

The year 1996 appears to have been the most productive year in the - admittedly short - history of the department. The number of refereed publications is much higher than ever before. The basis for several patent applications has been established. The industrial collaboration has been maintained at a high level, especially within the areas of sensors and information processing. The activities on combustion diagnostics that were transferred from the now closed Combustion Research Department have been very productive both scientifically and application-wise. The work on nonlinear dynamics and scientific computing has expanded and shifted so that several optical areas are now integral parts of the activities. Collaboration with both Mikroelektronik Centret and the Institute for Electromagnetic Systems (both at the Technical University of Denmark) has been initiated on very specific areas related to optical sensors.

The department has three programme areas: (1) *optical materials* (2) *optical diagnostics and information processing* and (3) *plasma and fluid dynamics*. There is a considerable interaction between the programmes. Several activities are organised in joint projects.

The work described in this report falls within the following categories:

- nonlinear dynamics in plasmas, fluids and optical systems;
- optical materials concentrated on material physics and applications in sensors, information processing and storage;
- diagnostics and sensors for probing physical systems using diffractive optics;

- scientific computing focusing on the application of spectral models to highly nonlinear distributed systems and - as a new activity - to electromagnetic propagation and diffraction where scalar methods are invalid;
- information processing, both electronic and optical, for pattern recognition and illumination with structured light in industrial systems.

Of major results in 1996 can be mentioned:

- installation of a novel laser system for plasma diagnostics at Wendelstein 7-AS in Garching;
- numerical and experimental demonstration of pattern formation in a parabolic vessel;
- the demonstration of 'optical vortices' in nonlinear optical media;
- direct measurements of transfer matrix elements for beam coupling in photorefractive media;
- novel properties of organic materials for diffractive elements and data storage;
- nonlinear cross talk and consequential revisions of fundamental limits to storage;
- a method for the recognition of brain states by electro-encephalogram signals;
- a model for the statics and dynamics of microtubules;
- the effect of a magnetic field on the diffraction efficiency of gratings in lithium niobate;
- parametric amplification and oscillation in photorefractive media;
- gratings in thin films of indium tin oxide produced by laser ablation;
- recording of a fast Fourier transform infrared interferogram of single coal particles, thus tracking the development of a combustion process on a microscopic scale;
- a model for the propagation of light in heterogeneous media with relevance to diagnostics in human tissues;
- several new concepts for miniaturised sensors;
- a new model for window contamination in connection with non-contact optical sensing;
- experimental verification of generalised phase contrast methods for energy efficient pattern generation;
- implementation of memory-based neural networks for industrial pattern recognition;
- contributions to a feasibility study of mine detection for humanitarian demining;

- completion of several combustion research projects and the disassembly of a large facility.

Industrial collaboration is a part of several activities. A new so-called industrial postdoc scheme was introduced in 1995. The department has hosted three such postdocs in connection with joint projects with three different industrial companies.

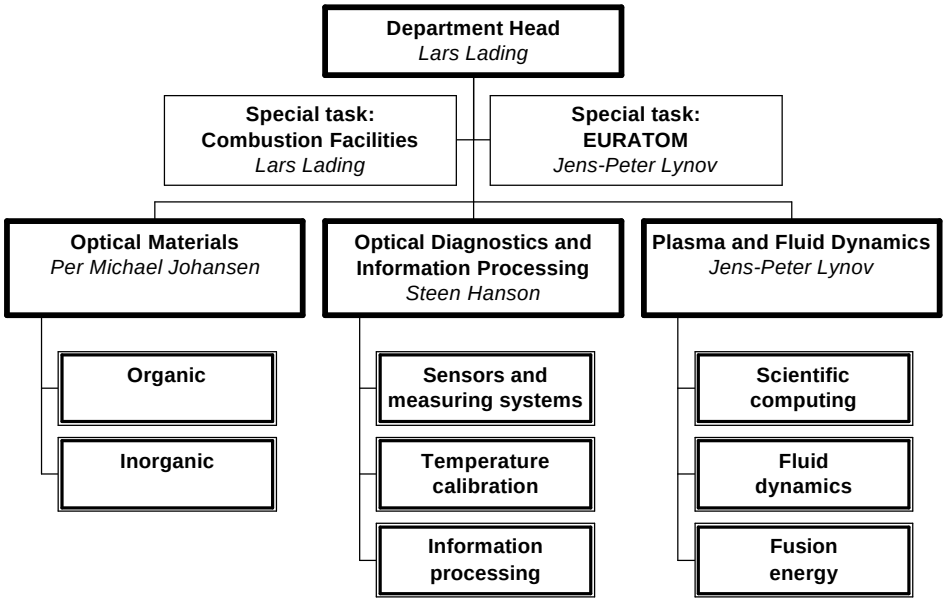

Figure 1. Organisational chart of the Optics and Fluid Dynamics Department as of December 1996. The lower boxes indicate the major areas of activity.

2. Optical Materials

2.1 Introduction

P. M. Johansen
E-mail: per.michael.johansen@risoe.dk

The research programme on *Optical Materials* was formed in 1996 to unify the growing research activities on optical materials in the Optics and Fluid Dynamics Department. The main emphasis is on the general aspects of interaction between coherent laser light as well as on various organic and inorganic optical materials. The two main lines of research are:

- development, characterisation, theoretical modelling and fabrication of new optical materials for application in optical measurement systems;
- fundamental investigations of light propagation in nonlinear dynamic optical media of both organic and inorganic nature.

Even though the research programme was not formed until 1996, very significant results have been obtained during this first year:

- In the *organic research*, significant new results relating to fabrication of diffractive elements, information storage in liquid crystalline polyesters, peptide oligomers as well as azobenzene polyesters and peptides have been achieved. These results indicate a perspective future for the organic work in the research programme.
- The *inorganic research* has mainly been conducted in the fields of photorefractive nonlinear optics and laser ablation. In the photorefractive field very important results concerning the nonlinear cross talk phenomena leading to a revision of the fundamental limit for holographic data storage have been obtained. Moreover, new and very basic results as regards the interaction of a magnetic field on the diffraction efficiency in photorefractive lithium niobate have been achieved, and two new concepts, photorefractive parametric amplification and oscillation, have been introduced. The first thin films of indium tin oxide have been produced by laser ablation and the writing of an optical grating in this material is currently being investigated.

As a whole the results mentioned above represent significant scientific achievements with a clear impact on future technology. Such results are, however, impossible to obtain without external sponsorship. Especially support from The Danish Natural Research Council, The Danish Technical Research Council, MUP2 (the Danish Materials Technology Programme), the EU and Risø National Laboratory should be acknowledged.

2.2 Organic Materials

2.2.1 Photoablative Coating for Microlithography

L. Lindvold, J. Stubager and E. Rasmussen
E-mail: lars.lindvold@risoe.dk

The activities on the fabrication of diffractive optical elements using the in-house laser microlithography system have initiated the development of resist materials that do not require wet processing. One of the materials that is currently being investigated is a photoablative coating.[1] The coating is based on a thermolabile polymer, typically nitrocellulose, doped with a dye that strongly absorbs laser light. The coating is applied as a thin film onto a glass substrate by a spin coating technique. The thickness of the film typically varies from 0.1 to 1 micron.

When the material is used in the laser microlithography system, a laser beam is focused onto the photoablative coating which causes a microexplosion in the film that closely matches the spatial extent of the focused laser beam. In theory, this makes it possible to make submicron structures when this material is utilised. Due to the explosive nature of the reaction that takes place in the focus of the laser beam, the microstructures generated by this method have very steep wall angles, see Figure 2.

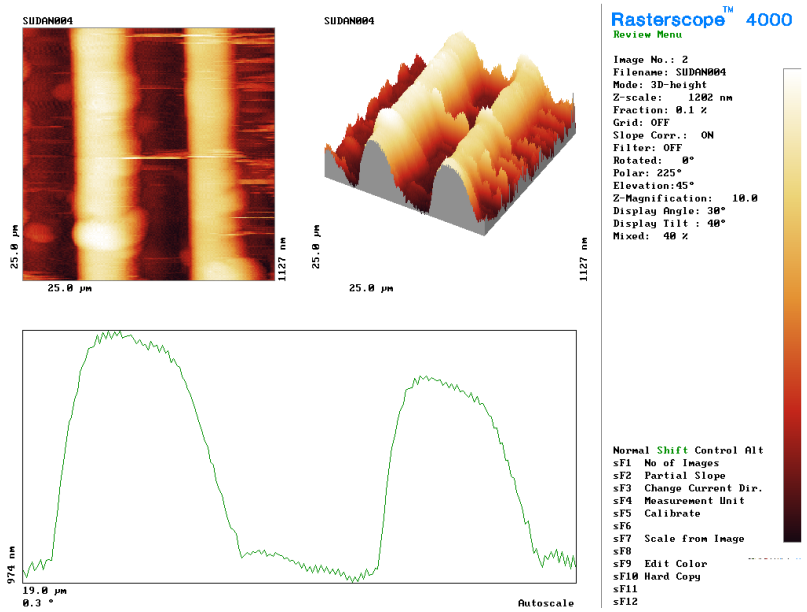

Figure 2. Atomic Force Microscopy scan of linear grating fabricated by the in-house laser microlithography system.

The advantage of using the dry resist is that it facilitates on-line monitoring during the fabrication of diffractive optical elements. Furthermore, the material is insensitive to daylight and therefore does not

require use of safelight during handling and exposure. Another promising application of the material appears to be the fabrication of master discs in compact disc manufacturing.

1. C. E. Kosmidis and C. D. Skordulis, "Dopant-enhanced ablation of nitrocellulose by a nitrogen laser", *Applied Physics A*, 64 (1993).

2.2.2 Liquid Crystalline Polyesters for Optical Information Storage (LICRYPOIS)

N. C. R. Holme, P. S. Ramanujam, E. Rasmussen, J. Stubager, S. Hvilsted[*], E. T. Kristensen[*], C. Kulinna[*] and M. Pedersen[*]
([*]Department of Solid State Physics), L. Nikolova (Bulgarian Academy of Sciences, Sofia, Bulgaria)
E-mail: p.s.ramanujam@risoe.dk

"LICRYPOIS", the focused fundamental research programme under Brite-EuRam, came to a conclusion during 1996. The aim of the project was to develop a suitable side-chain liquid crystalline polyester for erasable holographic storage. Polyesters designated P6a12 and P8a12, with (1) a tetradecanedioate main chain, (2) six and eight methylene spacers, respectively, in the flexible spacer in the side chain and (3) a cyano group as the substituent in the azobenzene were found to be ideal for holographic storage. High diffraction efficiency (> 50%), high resolution (> 3000 line pairs/mm) and long storage lifetime in the order of years were achieved under this project. The stored information can be erased globally through heat or locally through UV irradiation.[1-4] During the project, techniques for direct writing of computer-generated patterns in the film have also been developed. A remarkable biphotonic storage process, which requires the presence of a blue laser and a red laser (not necessarily simultaneously), has been discovered. Finally, a compact holographic system that contains a write laser (frequency doubled YAG laser at 532 nm), a read laser (635 nm diode laser), all the optical components and a CCD camera for the read-out has been built on an A4 size optical board.

It was also found that a large circular anisotropy can be induced in the polyester film when the polyesters are irradiated with circularly polarised light, even though they do not contain any intended chiral centres. The maximum values of the linear and the circular birefringence obtained from our experiments are $2x10^{-2}$ and $4x10^{-3}$, respectively, for a 5 μm thick film. The origin of the circular anisotropy is not clear at the moment.[5]

1. P. S. Ramanujam, C. Holme, S. Hvilsted, M. Pedersen, F. Andruzzi, M. Paci, E. Tassi, P. L. Magagnini, U. Hoffman, I. Zebger and H. W. Siesler, *Polym. Adv. Tech.***7**, 768 (1996).
2. P. S. Ramanujam, N. C. R. Holme and S. Hvilsted, *Appl. Phys. Lett.* **68**, 1329 (1996).
3. N. C. R. Holme, P. S. Ramanujam and S. Hvilsted, *Opt. Lett.* **21**, 902 (1996).
4. N. C. R. Holme, P. S. Ramanujam and S. Hvilsted, *Appl. Opt.* **35**, 4622 (1996).

5. L. Nikolova, T. Todorov, M. Ivanov, F. Andruzzi, S. Hvilsted and P. S. Ramanujam, *Appl. Opt.* **35**, 3835 (1996).

2.2.3 Holographic Storage in Peptide Oligomers

P. S. Ramanujam, R. H. Berg[*] and S. Hvilsted[#] ([*] Department of Solid State Physics)
E-mail: p.s.ramanujam@risoe.dk

We have examined a new type of oligopeptide containing azobenzene as side chain for holographic storage.[1] DNO is an oligopeptide in which the azobenzenes are placed in a configuration similar to that of the bases in DNA. It should be noted that the azobenzene is a plane aromatic π-electron system similar to the base pair in DNA. The rationale behind this architecture is that the azobenzenes in a DNO molecule should stack in a way similar to that of the base stacking in DNA, forming a helical molecule. Since the azobenzenes are helically arranged, when interacting with a light beam the molecule as a whole will not be stationary until all the azobenzenes are perpendicular to the polarisation of the incident laser light beam, i.e. the helical axis of the molecule is parallel to that of the laser beam. This was expected to minimise the number of stationary configurations possible.

DNO was synthesised by a modified stepwise Merrifield method. Films of good optical quality with a thickness of 5 μm were obtained from hexafluoroisopropanolic solutions. The films were found to be isotropic in a polarisation microscope. In these films optical storage is achieved through polarisation holography. The results have proved to be remarkable. It has been possible to achieve diffraction efficiency close to 90% in a nonpolymer organic material. We have found that an oligomer based on diaminobutyric acid with ten residuals and no spacers in the side chain gives the highest diffraction efficiency in the shortest time. A diffraction efficiency in the first order of 80% was achieved in 10 s exposure at an argon beam intensity of 2 W/cm^2. Even monomers with only a single azobenzene were found to give a diffraction efficiency of 15%. Through further modification of the DNO backbone, it has been possible to achieve rather large diffraction efficiency (greater than 60%) for a recording time less than 2 s.

The most remarkable result of this investigation is the thermal stability of the holograms. The holograms were not erased after exposure to 180^o C for a month and could be reused, albeit with lower diffraction efficiency. Holograms were found to be weakly present even after storage at 250^o C for a month. We believe that surface relief may play a role in the storage of the holograms. Furthermore, current work suggests that DNO oligomers might prove valuable also for volume holography. Thick films of DNO oligomers, immobilised within the bulk of a 65 μm thick polystyrene-polyethylene film have been fabricated to yield a diffraction efficiency of about 20%.

Further investigations of some of the DNO films using atomic force microscopy (AFM) show interesting features. The AFM pictures show

that the surface undulation increases rapidly, reaching almost 30% of the film thickness. In order to verify this result, the film was irradiated with a single beam of linearly polarised light. Again, similar to the case of the polyesters, the s-polarisation does not show any remarkable undulation. On the other hand, the p-polarisation produces a roughness that is approximately 10 times the original thickness of the film. This astonishing result is unique in optical recording. A possible explanation for this effect is that the p-polarisation has an out-of-plane component of the electric field. Irradiating the film with p-polarised light causes *trans-cis* isomerisation; it is known that the *cis* states require about twice the free volume compared with the *trans* states. (The *trans* states fill a volume of 144 $Å^3$ while an additional volume of 127 $Å^3$ is needed for the isomerisation to the *cis* state for an unsubstituted azobenzene.) In the case of peptide backbone, the azobenzenes are so tightly packed that this free volume is not available in the volume of the film; the film necessarily has to expand in order to provide space for the *cis* state. Barrett et al.[2] have calculated the resulting isomerisation pressure to be in the order of $3x10^7$ Pa in an azobenzene polymer, which is larger than the yield point of the polymer. The resulting viscoelastic flow is claimed to be responsible for surface modulation.

1. R. H. Berg, S. Hvilsted and P. S. Ramanujam, *Nature*, 383, 505 (1996).
2. C. J. Barrett, A. L. Natansohn and P. Rochon, *J. Phys. Chem.* **100**, 8836 (1996).

2.2.4 Optical Storage in Azobenzene Polyesters and Peptides

P. S. Ramanujam, N. C. R. Holme, R. H. Berg[*]*, S. Hvilsted*[*]*,*
M. Pedersen[*] *([*]Department of Solid State Physics) and L. Nikolova*
(Bulgarian Academy of Sciences, Sofia, Bulgaria)
E-mail: p.s.ramanujam@risoe.dk

Investigations of the optical storage mechanisms in side-chain liquid crystalline azobenzene polyesters were continued. Through atomic force microscopic investigations it was found that a topographic grating appeared immediately after laser irradiation. This disappeared after approximately 20 hours and was replaced by finger-like structures. However, near-field optical microscopic investigations showed that a strong anisotropy was still present in the polyester films. This is explained as the formation of aggregates in the film preserving the anisotropy over longer period of times. We have also been able to perform 10,000 write-read-erase cycles in the polyester films. The anisotropy was induced at 488 nm with an argon ion laser and was erased by irradiating the film at 350 nm with a krypton ion laser. The resultant anisotropy displayed several exponential decays, presumably associated with the alignment of the azobenzenes out-of-plane and due to temperature effects. A remarkable observation is the induction of circular anisotropy in these films when they are irradiated with circularly polarised light. The intensities of the waves diffracted in the +1 and -1 orders of diffraction

and their ratios were found to depend strongly on the reconstructing wave polarisation.

We have also tested oligomers based on a peptide-like backbone containing azobenzene chromophores in the side chain as a new class of materials for holographic storage. These oligopeptides, called Diamino-N^{α} substituted Oligomers (DNO), have been shown to have excellent holographic storage properties. An oligomer based on diaminobutyric acid with ten residues was found to give a diffraction efficiency of nearly 80% in the first order with a 10 s exposure at 488 nm, at an intensity of 2 W/cm^2. Even monomers with a single azobenzene were found to give a diffraction efficiency of 15%. The thermal stability of the holographic storage is high. Holograms were not erased after exposure to 180° C for a month, and could still be reused. Holograms were found to be weakly present even after storage at 250° C for a month. Atomic force microscopic investigations of the surface immediately after the recording show that a surface relief close to 30% of the original thickness of the film is present. Further investigations are being carried out in order to investigate the cause of the large surface relief.

2.3 Inorganic Materials

2.3.1 Photorefractive Data Storage

P. M. Petersen, P. M. Johansen, C. Dam-Hansen and H. C. Pedersen
E-mail: paul.michael.petersen@risoe.dk

Volume holographic data storage using photorefractive crystals offers many potential advantages over conventional storage systems. It enables a unique form of ultrahigh capacity data storage with fast data access and transfer times. An automated digital holographic recording device has been constructed for investigations of the fundamental limitations of photorefractive data storage. In the set-up shown in Figure 3 multiple holograms are recorded in an iron doped lithium niobate crystal by angular multiplexing. A spatial light modulator is applied to compose digital images in the photorefractive crystal. The stored information is detected with a CCD camera and a new effect - nonlinear cross talk - is analysed on a personal computer with a framegrabber. The nonlinear cross talk is an important phenomenon that takes place in the photorefractive storage medium due to the nonlinearity in the induced space-charge electric field. The nonlinear cross talk imposes fundamental limitations on the storage density and the capacity of the system. It has recently been shown experimentally that this effect can lead to more than 90% cross talk between neighbouring holograms stored in the medium and that the response times for erasure and build-up of a specific grating are also heavily influenced by the effect.[1,2] One fundamental property of the nonlinear cross talk is that it takes place even when the holograms fulfil the Bragg condition for resolving spatial information. The purpose of the

experimental investigation is to establish the fundamental nature of the cross talk, i.e. how it is controlled and how it influences the storage capability. Future work will concentrate on how the nonlinear cross talk can be used for refreshment of stored data and for selective erasure of specific holograms in the holographic memory.

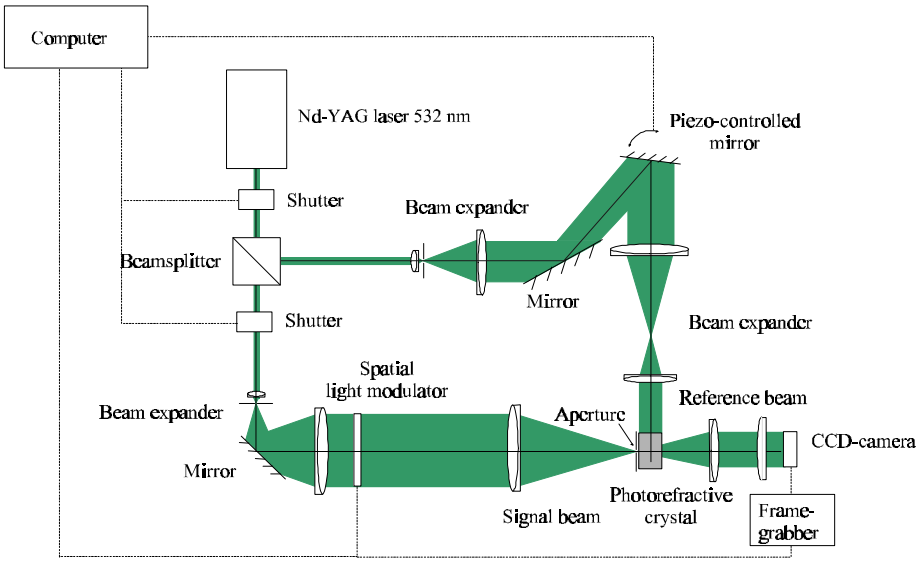

Figure 3. Experimental set-up for volume holographic data storage using angular multiplexing in photorefractive crystals.

1. H. C. Pedersen, P. E. Andersen, P. M. Petersen and P. M. Johansen, "Dynamics of nonlinear grating interaction in diffusion dominated photorefractive media: Theoretical analysis", *Opt. Soc. Am. B* **13**, 2569 (1996).
2. P. E. Andersen, P. Buchhave and P. M. Petersen, "Strong coupling between coherent gratings due to nonlinear spatial frequency mixing in $Bi_{12}SiO_{20}$", *Optics Communications* **128**, 185 (1996).

2.3.2 Photorefractive $La_3Ga_5SiO_{14}:Pr^{3+}$ Crystals and Magnetophotorefractive Effect

C. Dam-Hansen, P. M. Johansen and V. M. Fridkin (Institute of Crystallography, Moscow, Russia)
E-mail: carsten.dam-hansen@risoe.dk

Investigations of the photorefractive properties of lanthanum gallium silicate crystals doped by praseodymium ($La_3Ga_5SiO_{14}:Pr^{3+}$) have been conducted. This is a new piezoelectric crystal that exhibits a pronounced photovoltaic effect. The purpose of the work is to investigate the different charge migration processes responsible for the photorefractive effect.

Photorefractive grating formation and erasure have for the first time been demonstrated in these crystals[1] using the configuration shown in Figure 4a). An argon-ion laser at 514 nm is applied for writing and erasure while a HeNe laser is used for probing the grating. The measured

initial kinetics of the diffraction efficiency of the grating is shown in Figure 4b) as a function of the polarisation angle, β, of the writing beams. The $\cos^2(2\beta)$ dependence is due to the bulk photovoltaic effect and compares favourably with theory. The photovoltaic current along the *x*-axis is largest for β = 0° and 90°, while it vanishes for β = 45°. At this angle only the diffusion mechanism contributes to the grating formation. By changing the grating period we can control the diffusion mechanism, which provides a new possibility for separate investigations of the charge migration. From these measurements the photoconductivity and the photorefractive sensitivity have been determined.

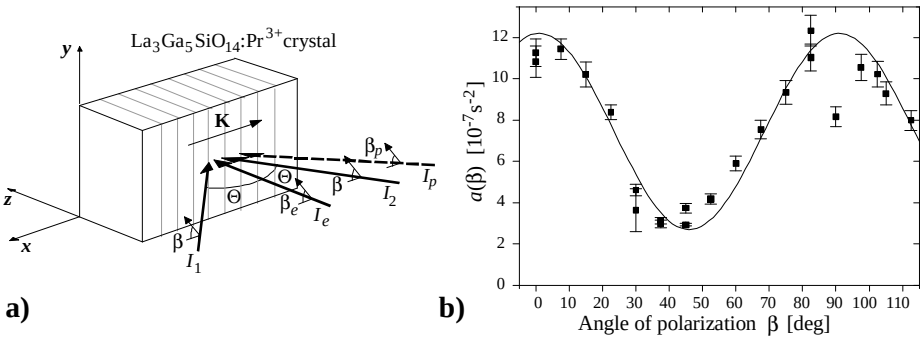

Figure 4. a) Schematic set-up used for grating formation in $La_3Ga_5SiO_{14}:Pr^{3+}$ crystals; b) measured polarisation dependence of the grating formation. The solid line is the best theoretical fit, illustrating the $\cos^2(2\beta)$ dependence.

In our work on photorefractive $LiNbO_3$:Fe crystals we have demonstrated a strong influence of an externally applied magnetic field on holographic grating formation.[2] This is due to the magnetic field interaction with nonthermalised electrons responsible for the photovoltaic effect. The developed theoretical model shows good agreement with experimental results.[3] Because of the large photovoltaic effect in the new $La_3Ga_5SiO_{14}:Pr^{3+}$ crystals, we are interested in conducting further investigations of the magneto-photorefractive effect in this material.

1. C. Dam-Hansen, P. M. Johansen and V. M. Fridkin, "Photorefractive grating formation in piezoelectric $La_3Ga_5Si:_{14}:Pr^{3+}$ crystals", *Appl. Phys. Lett.* **69**, 2003 (1996).

2. C. Dam-Hansen, "Magnetophotorefractive effect and interference filters in lithium niobate", PhD-dissertation, Risø-R-880(EN), ISBN87-550-2165-4 (Risø, 1996).

3. C. Dam-Hansen, P. M. Johansen, P. M. Petersen and V. M. Fridkin, "Magneto-photorefractive effect in $LiNbO_3$:Fe crystals: theory and experiments",*J. Opt. Soc. Am. B* **13**, 2286 (1996).

2.3.3 Parametric Oscillation and Amplification of Holographic Waves in Photorefractive Crystals

H. C. Pedersen and P. M. Johansen
E-mail: henrik.pedersen@risoe.dk

For about two decades it has been known that photorefractive crystals are suitable materials for optical information storage. If, for example, two optical beams are incident to such a material, a holographic phase grating is formed that exactly mimics the illuminating interference pattern. If, in turn, a small frequency shift (typically a few hundred Hz) is introduced in one of the laser beams, the phase grating starts running and a holographic wave is generated. In the linear case the holographic wave exactly mimics the interference pattern due to which we call this the fundamental wave, but for high contrasts of the interference pattern the crystal might start reacting in a nonlinear way. This is manifested by spontaneous formation of two so-called parametric holographic waves that have spatial frequencies that are lower than the fundamental frequency and grating vectors that are not necessarily parallel with the fundamental grating vector.[1] Hence, for different values of the optical frequency shift, different parametric waves can be seen in the medium. In Figure 5 a series of examples of diffraction patterns is shown which reflects different kinds of parametric processes. It has been shown both theoretically[2] and experimentally[3] that for different geometric configurations the parametric processes can be utilised for amplifying weak holographic waves. In this case we refer to the process as photorefractive parametric amplification.

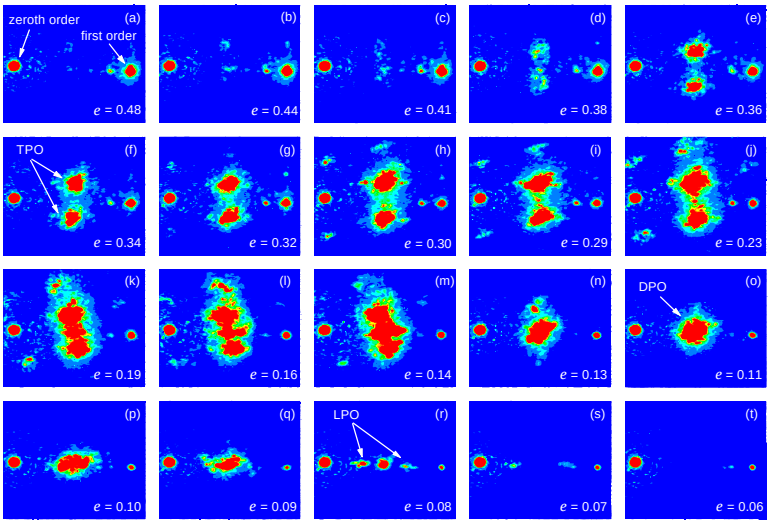

Figure 5. Diffraction patterns observed when reading out the holographic waves that are formed in a sample of $Bi_{12}SiO_{20}$. The spots on the left are directly transmitted spots whereas the spots on the right are due to diffraction in the fundamental grating. The spots/patterns in between are due to different forms of photorefractive parametric oscillation: TPO stands for transversal parametric oscillation, DPO stands for degenerate parametric oscillation, and LPO stands for longitudinal parametric oscillation.

1. H. C. Pedersen and P. M. Johansen, “Longitudinal, degenerate, and transversal parametric oscillation in photorefractive media,” *Phys. Rev. Lett.* **77,** 3106 (1996).
2. H. C. Pedersen and P. M. Johansen, “Degenerate parametric amplification in photorefractive media: theoretical analysis,” *J. Opt. Soc. Am. B* **13,** 590 (1996).
3. H. C. Pedersen and P. M. Johansen, “Observation of nondegenerate photorefractive parametric amplification,” *Phys. Rev. Lett.* **76,** 4159 (1996).

2.3.4 Holographic Gratings Induced in Laser Ablated Thin Films of Indium Tin Oxide

B. Thestrup, C. Dam-Hansen, P. M. Johansen and J. Schou
E-mail: birgitte.thestrup@risoe.dk

Diffraction from an optically induced grating has for the first time been demonstrated in a thin film of indium tin oxide (ITO) produced by laser ablation. Such a grating has recently been induced in sputtering deposited ITO films by a Greek group.[1] The ITO films are semiconducting and highly transparent in the visible range and therefore have a wide range of applications in electro-optics.

The grating is produced by two coherent beams from a Kr-ion laser at 352 nm, which is fairly close to the energy gap in ITO films. These beams are brought to overlap in the film plane and produce an interference pattern that creates the holographic grating. A weak HeNe laser beam at 633 nm is used to probe this grating.

Figure 6 shows an example of the dynamics of the first-order diffracted beam from such a grating. A photomultiplier is used to measure the diffracted power. The film was deposited on a glass substrate and has a thickness of a few hundred nm. The two Kr-ion laser beams intersect each other at an angle of 31°, giving a grating constant of 0.66 μm. The probe beam, with a power of a few mW, enters the grating normal to the film plane, giving rise to a first-order diffracted exit beam at ±75° from this normal. At time t = 0, the Kr-ion laser beams are turned on, and the grating builds up within a few minutes. At the time t = 500 s, one of the Kr-ion beams is turned off and the signal from the grating falls off. The decay is exponential containing both a fast and a slow time constant. As is seen in the figure, the grating is rather weak. Further analysis is planned in the near future to reveal the origin of the grating.

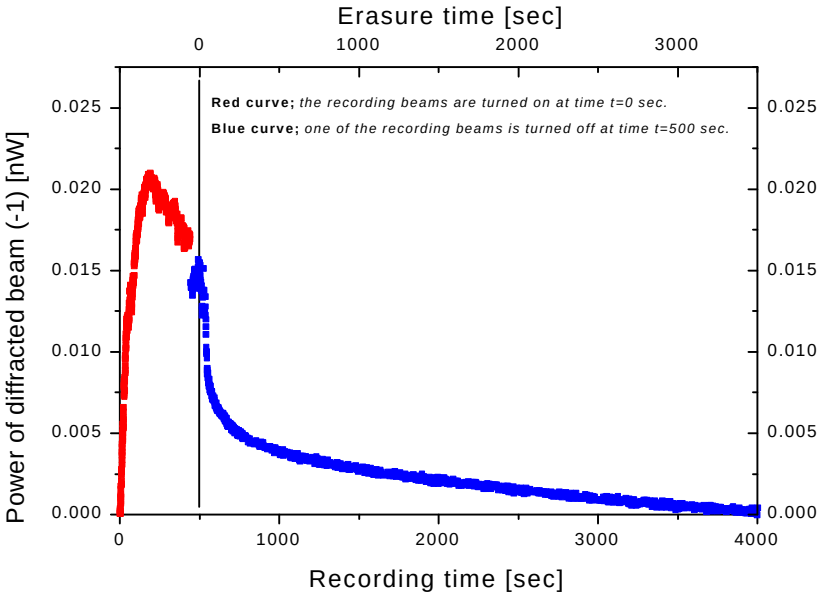

Figure 6. Dynamics of the first-order diffracted beam.

1. S. Mailis, L. Boutsikaris, N.A. Vainos, C. Xirouhaki, G. Vasiliou, N. Garawal, G. Kiriakidis and H. Fritzsche, *Appl. Phys. Lett.* **69**, 2459-2461.

2.3.5 Laser Deposited Indium Tin Oxide Thin Films

B. Thestrup, A. Nordskov, J. Schou and W. Svendsen
E-mail: birgitte.thestrup@risoe.dk

Thin films of indium tin oxide (ITO) have been deposited by laser ablation in an oxygen atmosphere. ITO thin films are both semiconducting and transparent with a variety of technological applications. With the pulsed laser deposition (PLD) technique it is possible to deposit thin films of good quality with the same chemical composition as the targets.

During irradiation of a rotating target with a pulsed beam from a quadrupled Nd:YAG laser (266 nm), a plasma plume of ions, electrons and neutrals will be emitted from the target. Thereby, target material will be transferred to a glass substrate placed in front of the target and a thin film can be deposited layer by layer. We typically use a peak power of 4 MW and a target substrate distance of 6 cm. Deposition rates, measured with a quartz crystal microbalance, are typically around 4 nm/min for an oxygen pressure about 25 mtorr. The films are analysed using XPS and AFM. Film resistivity is measured by a standard four-point probe technique and the transmittance of visible light with a spectrophotometer. The transmittance between 400 and 900 nm is usually between 70 and 90 %.

Figure 7 shows the sheet resistance for two different series of films as a function of oxygen pressure in the vacuum chamber. The base pressure is around 10^{-6} torr and the film thickness is ~110 nm. Films are deposited on substrates both at room temperature and at 200° C. The curves show strong dependence on resistivity with oxygen pressure. The dependence is

more significant for the films deposited on a cold substrate than for those deposited on a hot substrate. Furthermore, the minimum in resistivity achieved for films deposited at 200°C is significantly lower than for films deposited at room temperature. The high substrate temperature increases the migration of the different species on the substrate during ablation. As a result, the film quality can be improved and this may partly explain the behaviour seen below.

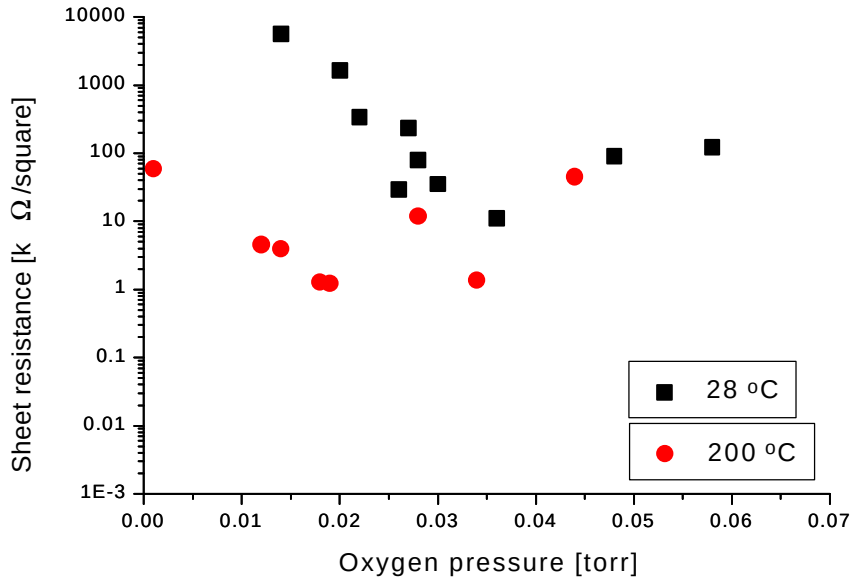

Figure 7. Sheet resistance for ITO thin films deposited at different oxygen pressures at λ = 266 nm. The film thickness is around 110 nm.

2.3.6 Ablation Rates and Angular Distribution of Ablated Atoms from Metals

J. Schou, W. Svendsen, T. N. Hansen, A. Nordskov, B. Thestrup and O. Ellegaard (University of Odense, Odense, Denmark)
E-mail: j.schou@risoe.dk

Laser ablation from metals in a newly constructed set-up has been studied. Silver and nickel have been irradiated in vacuum with a Nd:YAG laser operating at 355 nm and 266 nm with intensities ranging from 0.1 GW/cm^2 to 5 GW/cm^2. The laser strikes the target at normal incidence with a typical beam spot that varies from 0.003 to 0.1 cm^2. The ablated atoms are collected by eight quartz crystal microbalances positioned 80 mm from the target surface at different angles with respect to the target normal.

Figure 8 shows the frequency change recorded simultaneously for the eight crystals during laser irradiation of silver at 366 nm.[1] A change in the frequency of 1 Hz corresponds to a coverage of 10^{14} Ag atoms/cm^2. It should be noted that most of the particles are ejected in a direction close to the target normal. The angular distribution of the emitted particles may

be approximated well by a $\cos^p\theta$ distribution, where p = 6.1 for the data points shown in Figure 8. The total number of ablated particles can be estimated by integrating the angular distribution over the full hemisphere. At 5.3 J/cm^2 each pulse ablates 2x10^{15} Ag atoms corresponding to 330 ng/pulse. This number was checked with ordinary weight loss measurements for a long series of pulses from which we obtained 380 ng/pulse.

We have recently initiated a series of measurements of the angular distribution of the ablated particles at the wavelength 266 nm. Surprisingly, it was not possible to approximate the angular distribution with one cosine function, but we had to superimpose one strongly forward peaked distribution on top of another less forward peaked distribution.

This work has been supported by a grant from the Danish Natural Research Science Council.

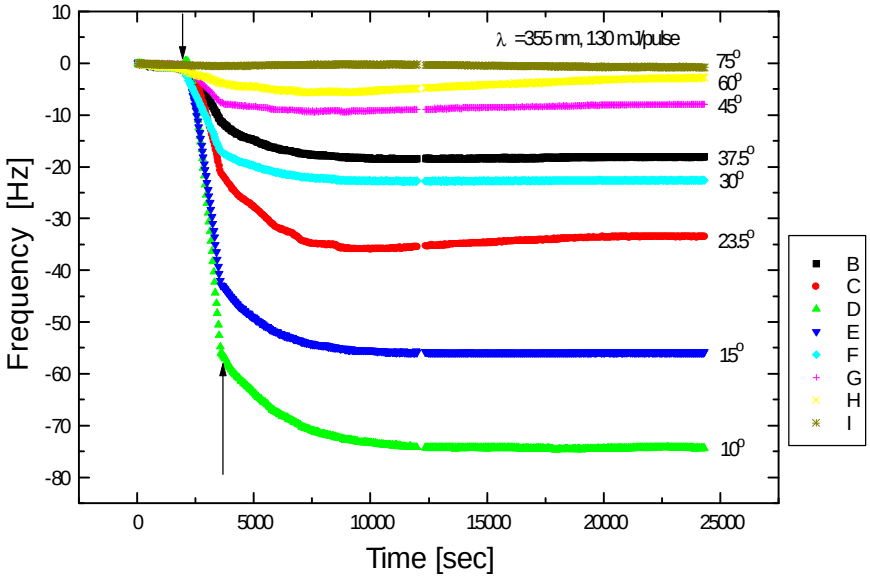

Figure 8. The frequency changes as a function of time for eight quartz crystal microbalances. The laser irradiation of the silver target took place between the arrows. The angle with respect to the normal is indicated at each curve.

1. W. Svendsen, A. Nordskov, J. Schou, B. Thestrup and O. Ellegaard, "Angular distributions and total yield of laser ablated silver", *Nucl. Instr. Meth.* (in press).

2.3.7 Investigation of Laser-induced Ejection of Organic Molecules from a Water Ice Matrix

J. Schou, A. Nordskov and L. Lindvold
E-mail: j.schou@risoe.dk

A vacuum chamber has been modified for a study on ejection of molecules embedded in a water ice matrix. The organic material is dissolved in water, which is dropped on top of a copper cylinder cooled below -50 °C. As soon as an ice layer is formed, the cylinder is inserted into a vacuum chamber, which will be evacuated to 10^{-5} torr. The ice will be irradiated by a beam at 532 nm from the existing high-power Nd:YAG laser so that the copper substrate is rapidly heated (Figure 9). The ejected species will be detected by a mass spectrometer with a mass range up to 200 amu. The study will be initiated with sodium salicylate (mass 160 amu) which is soluble in water. At a later point the method may be extended to dyes and heavy organic molecules that may be deposited on a substrate.

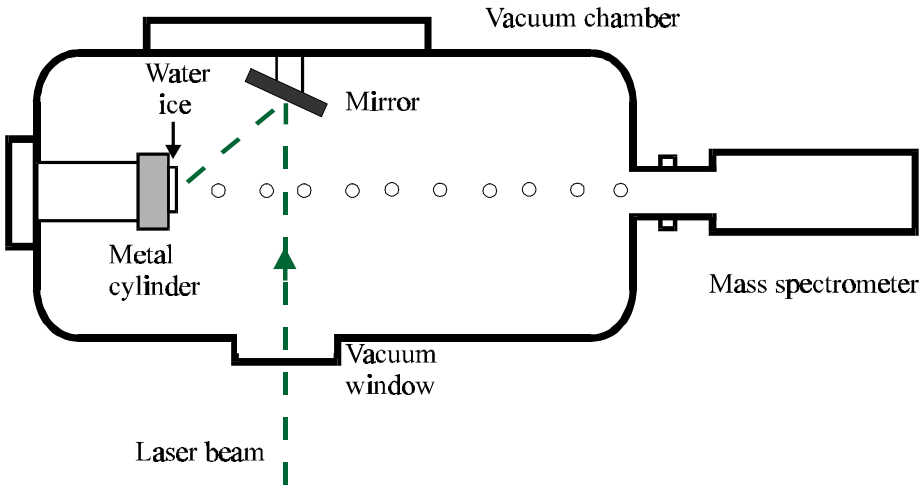

Figure 9. Vacuum chamber for laser irradiation of water ice matrices.

2.3.8 Sputtering of Solid Neon by Electrons Studied with Molecular Dynamics Simulation

L. Dutkiewicz[*]*, R. Pedrys*[*] *([*]Institute of Physics, Jagellonian University, Krakow, Poland) and J. Schou*
E-mail: j.schou@risoe.dk

Sputtering of solid neon by electrons has been studied with molecular dynamics simulation. Solid neon can be regarded as a model insulator for sputtering because the electronic excitations are predominantly localised as atomic excitons. Solid neon is a relatively simple solid, for which the interatomic potential is well known for the ground and many of the excited states. In the past, the volatile solid neon was used as a model material for studies of the even more volatile frozen deuterium at Risø.

We have constructed a molecular dynamics simulation code that describes the sputtering process from the first localisation of energy at an

atom as an exciton to the ejection of neon atoms.[2] In a system of solid neon most of the electronic excitations relax to atomic excitons. Typically, the sputtering process is initiated by an exciton located a few layers below the surface. The potential energy from the exciton that drives the ejection process is about 0.5 eV compared with a surface binding energy of 22 meV for the neon atoms. After a few picoseconds the excited neon atom (the exciton) moves towards the surface and becomes ejected. On its way out it "pushes" other atoms out of the solid as well. Several atoms can be sputtered from the solid in such an event.

This project has been supported by a grant from the Danish Natural Science Research Council.

1. J. Schou, P. Børgesen, O. Ellegaard, H. Sørensen and C. Claussen, “Erosion of solid neon by keV electrons”,*Phys. Rev. B* **34**, 93 (1986).
2. L. Dutkiewicz, R. Pedrys and J. Schou, “Molecular-dynamics simulation of ejection processes in electronically excited solid Ne”, *Europhys. Lett.* **36**, 301 (1996).

3. Optical Diagnostics and Information Processing

3.1 Introduction

S. G. Hanson
E-mail: steen.hanson@risoe.dk

At the beginning of 1996 the former Optics Programme was divided into two programmes. One programme was focused on the subject of Optical Materials, whereas the present programme, the Optical Diagnostics and Information Processing Programme, was to focus on information processing and diagnostics using optical means primarily. In connection with the splitting of the Optics Programme, the Optical Diagnostics and Information Processing Programme was strengthened by inclusion of (1) a group working with infrared spectroscopy related to combustion diagnostics and (2) a group working with temperature- and infrared radiation calibration.

The year 1996 has therefore been a year of new challenges where the inherent differences in the programme have been realised. Though the differences might seem to restrain a comprehensive effort on a single subject, the diversity will ensure an adequate collection of theoretical tools and optical methods needed for the immediate in-depth treatment of a broad variety of scientific calls. In the future the scientific diversity will be sought maintained and new challenges will be actively met.

New methods in the field of Fourier transform infrared spectroscopy (FTIR) have been employed in combustion diagnostics. For the first time it has been published that fast interferograms can be achieved on single burning coal particles, thus tracking the development of the microscopic combustion process. The same technique has been applied to determine the constituents of mixtures of solids. Here the influence of diffusely scattered radiation plays a significant role in the understanding of the measured spectra as it does when light propagates in heterogeneous media like human tissue. An industrial postdoc programme on theoretical description of light propagation in layered media, especially tissue, using the diffusion equations, has been successfully terminated. Following this work, the effort on medical optics will be pursued in the coming year combining some of the previously developed robust concepts for measuring mechanical deformations. The work on optical methods for displacement sensors has been carried on with the aim of miniaturising the sensors and preparing for industrial implementations.

Two EU-projects aimed at using memory-based neural networks for pattern recognition are close to being finished by the end of this year. In both projects our contributions consist in fast information extraction from image data to be supplied for decision taking and control. Projections of imagery either by a high-power laser source or from a white light source

have been addressed in a collaborative effort with the Japanese company, Hamamatsu Photonics K.K. Central Research Laboratory, partly supported by national funds where new and effective schemes have been presented.

3.2 Phase Contrast Image Synthesis

3.2.1 Lossless light labelling

J. Glückstad and L. Lading
E-mail: jesper.gluckstad@risoe.dk

Most applications of optical systems require that images or spatial patterns are imaged or projected onto a target. This is the case in slide and film projectors, in projection TV systems as well as in labelling systems.

Materials processing with laser light is also an area where patterns may be projected with very high levels of light power. The dissipation of light power in masks is a problem in most projection systems. This can be illustrated by the following example: Let us assume that objects - e.g. beer cans - have to be marked with production information while they are passing at high speed. A mask is illuminated with a high-power laser and the mask is imaged onto the can. In simple imaging systems much laser power (often the most) is necessarily deposited in the mask - not on the beer can. This fact implies that a very high power laser must be applied and that the masks can endure the high power level. This is expensive - if at all possible - and very inefficient in terms of energy conversion.

A very attractive method for overcoming this problem has been devised at Risø National Laboratory.[1,2] A patent application has been submitted and is the basis for a joint project with Hamamatsu Photonics K.K. Central Research Laboratory in Japan on the practical implementation of the method.[3] The basic idea is to apply a special type of phase coding of the pattern that has to be imaged on a target. A phase mask absorbs no energy. The phase distribution is converted to an amplitude distribution on the target by a nonabsorbing generalised phase contrast filter. Phase contrast is well established in microscopy for visualising very weak phase objects. However, the method is not applicable for pattern projection. The new scheme has the potential for reducing power requirements with one to two orders of magnitude making projections of images and patterns viable in many cases where it is currently either impossible or economically unfeasible. The method has been experimentally verified as illustrated in Figure 10.

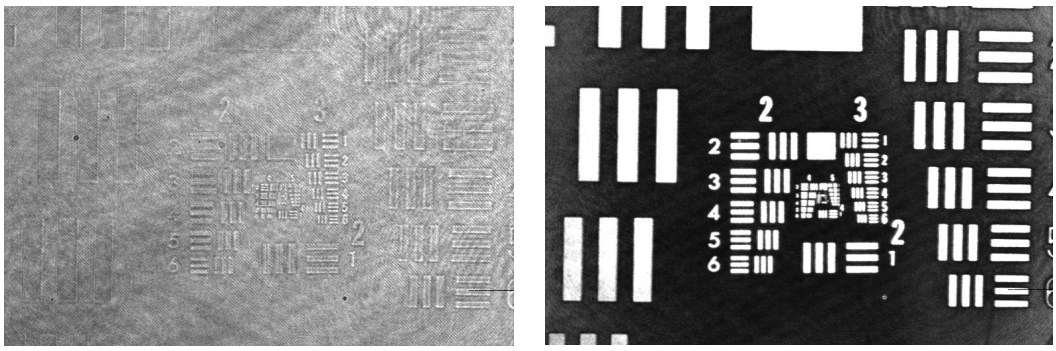

(a) (b)

Figure 10. Detected images obtained from a binary encoded π-phase PAL-SLM input pattern: (a) simple imaging with no application of a phase contrast filter; (b) imaging obtained when aπ-phase-shifting phase contrast filter is situated in the Fourier plane.

1. J. Glückstad, H. Toyoda, N. Yoshida, T. Takemori and T. Hara, "Experimental verification of phase contrast image synthesis system", in: *Optical Information Processing*, 2nd International conference on optical information processing, St. Petersburg (RU), 14-17 June 1996. Z. I. Alferov, Y. V. Gulyaev, D. R. Pape (eds.), (The International Society for Optical Engineering, Bellingham, WA, 1996) (SPIE Proceedings Series, 2969) 630-634.
2. J. Glückstad, "Phase contrast image synthesis", *Opt. Commun.* **130**, 225-230 (1996).
3. J. Glückstad, "Phase contrast imaging", WO Patent 96/34307 (31 Oct. 1996).

3.2.2 Implementation of a Dynamic Phase Contrast System

L. R. Lindvold, J. Glückstad and L. Lading
E-mail: lars.lindvold@risoe.dk

The principle of phase contrast image synthesis has previously been demonstrated by Glückstad and Lading, see section 3.2.1. In this work, a phase mask capable of performing an inverse phase-only filtering is created by inserting a Kerr-media in the Fourier plane of the optical set-up, see Figure 11. In this manner phase retardation proportional to the intensity of the light is created in the Fourier plane of the set-up. The concept of this set-up facilitates the use of pulsed lasers for material processing. Due to the high intensity in the Fourier plane a slight defocusing of the Kerr-media is necessary to avoid optical damage to the material. The materials that are currently used as Kerr-media are copper phtalocyanineand heavy-flint glass (SF 57).

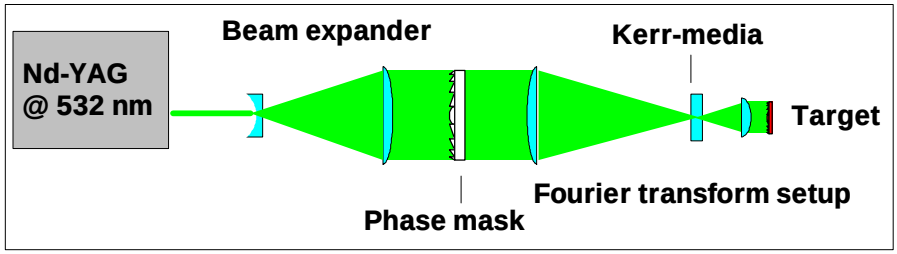

Figure 11. Practical implementation of a system for transfer of a phase mask, i.e. Fresnel zone plate, onto a polymer thin film by laser ablation. The laser is a pulsed Nd-YAG laser operating at 10 Hz with a pulse energy of 15 mJ @ 532 nm and a pulse width of 5 ns. The beam is expanded ten times to avoid optical damage on the phase mask. The Fourier transform set-up utilises a 300 mm input lens and a 50 mm output lens.

3.3 Sensors and Industrial Collaboration

3.3.1 Miniaturised Displacement Sensors

S. G. Hanson, L. Lading, B. H. Hansen and L. Lindvold
E-mail: steen.hanson@risoe.dk

Industrial applications of optical sensors for in-situ and noncontact measurement of various mechanical parameters have been investigated, including the determination of length, velocity, vibration, rotational speed and angular displacement. The theoretical work on displacement sensors has been focused on two aspects of their applications.

First, displacement sensors for industrial use are prone to contamination of the optical windows, which will usually impose limitations on the measurement accuracy or even result in unacceptable bias errors. An analytic description of the optical aberrations due to a stochastic distribution of absorbing and refracting patches on the optical window has been presented.[1] As an example, the influences on a laser transit time anemometer have been given. It has here been shown that serious bias effects may arise in case of severe window contamination.

Secondly, the use of optical sensors is not restricted to surfaces giving rise to a fully developed specular field. This will only happen if the surfaces under investigation have an rms roughness larger than the wavelength and a lateral scale smaller than the illuminated area. Several objects will have surface parameters that do not give rise to fully developed speckle. A comprehensive analytic description of the transition from a specular reflective surface to a fully diffusely scattering surface has not been obtained, but a division of the roughness domain into two areas has provided useful results for an analytic description of the performance of the laser transit time velocimeter and the laser Doppler velocimeter.[2]

Dissemination of several of the concepts for displacement sensors will call for miniaturisation of the sensors. Imbedding the emitting source(s) and the detector(s) in a monolithically integrated structure will facilitate this concept. As a step towards full integration, a solution based on one

holographic element has been presented.[3] The optical transmitter and the receiver optics are here imbedded in one single diffractive optical element fabricated as an ordinary phase hologram on a locally produced dichromated gelatine film. The simultaneous recording of the transmitter and receiver has resulted in a robust and inherently aligned optical system as shown in Figure 12.

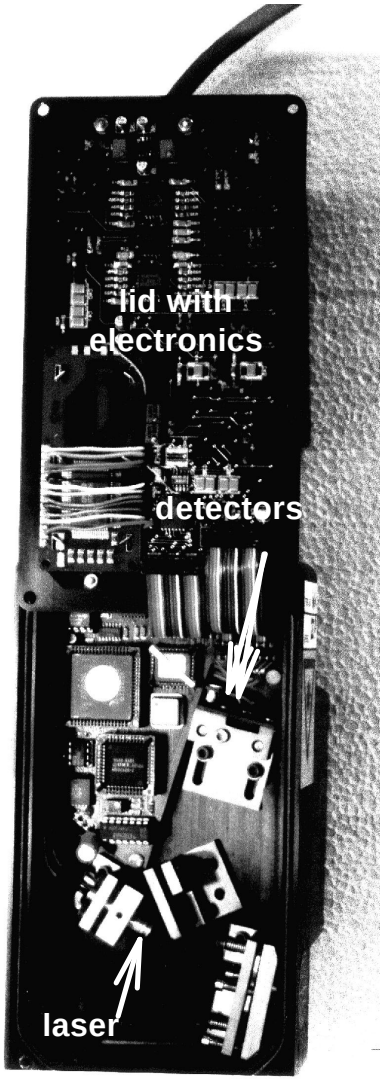

Figure 12. An integrated system based on a single diffractive optical element for noncontact measurement of velocity.

An array of optical systems for measurement of angular - and linear - velocities has been addressed, and the similarities and the differences both in the optical set-up and in the electronic processing schemes have been emphasised. Two generically different signal processing schemes are present: (1) the peak in the frequency spectrum will provide the information, or (2) the peak in the cross-covariance between two signals will contain the information. Optically, two generically different set-ups can be approached: (1) the scattered field can be imaged onto the detector(s) or (2) the Fourier transform (the far field) can be projected

onto the detector(s). This provides four different electronic/optical combinations, each of which provides a system for measurement of a certain object movement.[4] One of these systems has been treated in detail, namely a patented system for measurement of rotational speed and torsional vibrations.[5]

1. H. T. Yura and S. G. Hanson, "Effects of receiver optics contamination on the performance of laser velocimeter systems", *J. Opt. Soc. Am. A* **13,** 1891-1902 (1996).
2. H. T. Yura, S. G. Hanson and L. Lading, "Comparison between the time-of-flight velocimeter and the laser Doppler velocimeter for measurements on solid surfaces", in: *Optical Velocimetry*. OV-metry conference, Warsaw (PL), 29 May - 2 Jun 1995. M. Pluta and J. K. Jabczynski, (eds.) (The International Society for Optical Engineering, Bellingham, WA, 1996) (SPIE Proceedings Series, 2729) 91-102.
3. S. G. Hanson, L. R. Lindvold and L. Lading, "A surface velocimeter based on a holographic optical element and semiconductor components", *Meas. Sci. Technol.***7**, 69-78 (1996).
4. S. G. Hanson, and L. Lading, "Generics of systems for measuring linear and angular velocities of solid objects", in: *Optical Velocimetry*. OV-metry conference, Warsaw (PL), 29 May - 2 Jun 1995. M. Pluta and J. K. Jabczynski (eds.) (The International Society for Optical Engineering, Bellingham, WA, 1996) (SPIE Proceedings Series, 2729) 81-90.
5. S. G. Hanson, "System for noncontact measurement of torsional vibrations of shafts", in: *Optical Velocimetry*. OV-metry conference, Warsaw (PL), 29 May - 2 Jun 1995. M. Pluta and J. K. Jabczynski (eds.), (The International Society for Optical Engineering, Bellingham, WA, 1996) (SPIE Proceedings Series, 2729) 155-163.

3.3.2 Industrial Collaboration

S. G. Hanson, L. Lading, B. H. Hansen and L. Lindvold
E-mail: steen.hanson@risoe.dk

The dissemination of new technology and ideas for industrial applications[1] is one of the goals of the research programme. This goal is pursued in different ways one of which is the establishment of direct links between companies and Risø National Laboratory in the form of industrial postdocs and industrial PhDs. Direct consultancy work ordered by the company is a second way in which the twining takes place. These projects are usually considered proprietary by the company and will therefore not be described here.

In 1996, three industrial postdocs have established a close connection to three Danish companies. One of these projects related to medical optics will be described in more detail in section 3.3.4 The two other projects aim at implementing miniaturised - yet robust - velocity sensors based on optical principles.

In collaboration with Kamstrup A/S we are currently investigating the possibilities of noncontact measurement of flow velocities in pipes by way of the so-called *time-of-flight* method. Two laser beams are focused in

two spots separated along the flow direction. A scattering particle carried along with the flow will give rise to two signals as it passes each of the two spots. The time between the signals is given by the ratio of the known spot separation to the velocity. Measuring the time delay between the two pulses facilitates the velocity determination. This project is in the preliminary phase following a BSc project on the basic set-up.

The second collaborative effort between a Danish industrial partner and the department attempts to combine the local knowledge of displacement sensors with the expertise of the company, Ibsen Micro Structures A/S, on diffractive structures. This work is performed in collaboration between the industrial postdoc and an industrial PhD student. The ultimate goal is to introduce compact optical sensors with a broader range of applicability.[2] A *time-of-flight* configuration for measurement on solid surfaces has been investigated. As was the case for flow measurements, the time delay between two signals caused by scattering of two focused spots on the solid target is determined. Assuming fully developed speckle to arise from the scattering process, the signals are no longer single bursts but a continuous signal with certain statistical properties of primary interest for determining the performance of the total system. The statistical description of the signals stemming from a surface giving rise to partially developed speckle has further been developed.[3] Here a new formalism for rough surface scattering is introduced, whereby an analytic description of the transition between fully developed speckle and partially developed speckle is facilitated.

A compact laser anemometer has been put forward based on an implementation in a single chip.[4] Essential for this implementation is the possibility of combining vertical cavity surface emitting lasers (VCSELs) with a microlens array to miniaturise the system into one single chip as depicted in Figure 13.

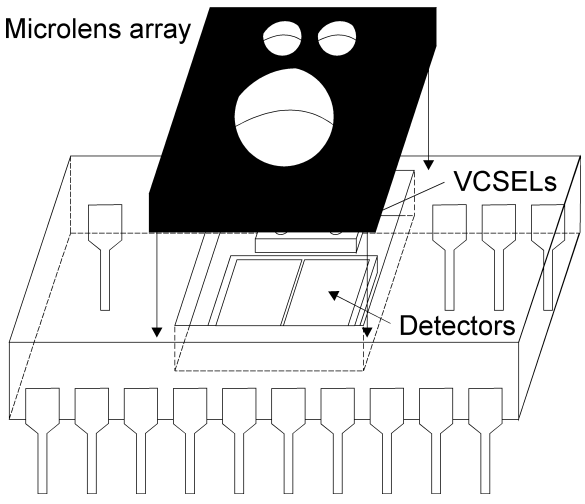

Figure 13. Miniaturised sensor concept.

The industrially oriented work will continue in the coming period addressing other kinds of sensors for noncontact determination of various mechanical parameters.

1. S. G. Hanson, L. R. Lindvold and B. H. Hansen, “Industrial implementation of diffractive optical elements for nondestructive testing”, *Vibration Measurements by Laser Techniques: Advances and Applications*, Second International Conference on Vibration Measurements by Laser Techniques, Ancona (IT), 23-25 September 1996, Tomasini, E. P. (ed.) (The International Society for Optical Engineering, Bellingham, WA, 1996) (SPIE Proceedings Series, 2868) 216-224.
2. B. Rose, H. Imam, L. Lading and S. G. Hanson, “Time-of-flight velocimetry: Bias and robustness”, *Photon Correlation and Scattering*. Summaries of the papers. Conference edition. Topical Meeting on Photon Correlation and Scattering, Capri (IT), 21-24 August 1996 (Optical Society of America, Washington, DC, 1996) (1996 Technical Digest Series, 14) 68-70.
3. B. Rose, H. Imam, S. G. Hanson and H. T. Yura, “Effects of target structure on the performance of laser time-of-flight velocimeter systems”, to appear in *Applied Optics* **36**, 10 January 1997, No. 2.
4. H. Imam, B. Rose, L. R. Lindvold, S. G. Hanson and L. Lading, “Miniaturising and ruggedising laser anemometers”, *Eighth International Symposium on Applications of Laser Techniques to Fluid Mechanics*, Vol. 2. 8. International Symposium on Applications of Laser Techniques to Fluid Mechanics, Lisbon (PT), 8-11 July 1996 (Instituto Superior Técnico. Departemento de Engenharia Mecanica, Lisboa Codex, 1996) Paper 40.2.

3.3.3 Surface Light Scattering: Integrated Technology and Signal Processing

L. Lading and J. Earnshaw (Queen’s University of Belfast, Space and Astrophysics, Belfast, United Kingdom)
E-mail: lars.lading@risoe.dk

Surface light scattering is well established for the investigation of a number of scientific problems; a wide range of systems have been studied, including pure fluids, microemulsion systems, spread monolayers of amphiphiles and polymers. In many cases unexpected phenomena have been observed. However, a number of different systems which should be of scientific interest can be foreseen. Examples include surface films with anisotropic elastic properties, or comprise anisotropic molecules for which new or radically modified surface modes should exist. Recent studies of surface waves on gelling systems are highly promising. Furthermore, the thermally excited density fluctuations of surface films remain undetectable to date although proposals for the detection have been given. In some of these cases theoretical developments are necessary; in most of them technically innovative experimental designs will be required.

Surface light scattering has matured to the extent that it is now possible to envisage the possibility of applying the technique in more demanding environments like microgravity or industrial process

monitoring. Such situations will require more compact and robust system designs than the ones that have been used in laboratory studies till now. The generic elements of a system are identified and their impact on system performance is given based on the model presented in [1]. We note that proper use of a grating provides a calibration that is independent of the wavelength. This facilitates the use of cheap unstabilised semiconductor lasers, but the optics may be rather delicate. A low-cost laser operating in a large number of axial modes may actually also provide better noise performance (Figure 14).

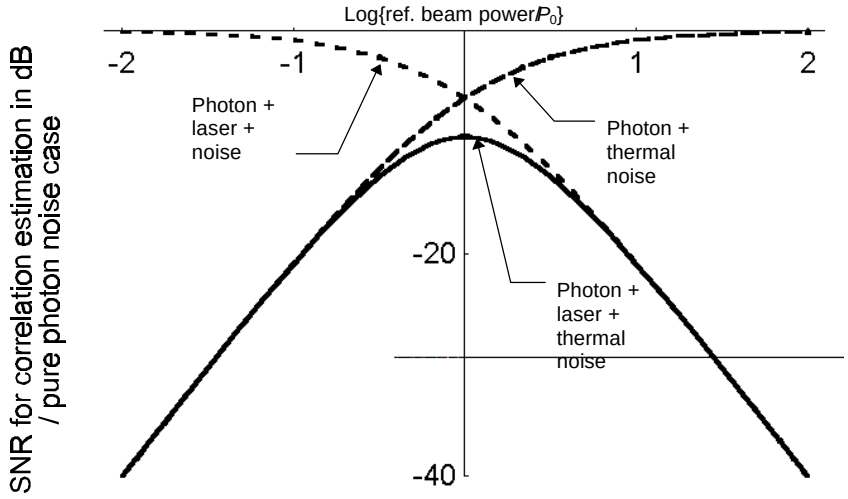

Figure 14. The signal-to-noise ratio for correlation function estimation in a system where the detection is done by optical mixing with a reference beam. In such systems it is often the fluctuations of the reference beam that limit the performance.

An implementation with holographic optical elements gives a mechanically very simple and robust system (Figure 15).[2] A concept based on fully integrated optics is obtained by combining a 2D waveguide with diffractive structures for coupling light out of and into the optical "chip". The waveguide would be combined with the lower hologram. Laser and detectors could be imbedded in the waveguide. Such a system implies a number of conflicting requirements of the integrated optics. A potential solution based on silicon and a rare earth laser is being considered. The complexity of the system may be further reduced by the application of intracavity diffractive structures. By doing this, we essentially eliminate the need for the very high diffraction efficiency required with external diffractive structures, and the laser itself may also be used as a detector. However, the simple configuration requires a spacing to the surface that is fixed within a fraction of the optical wavelength.

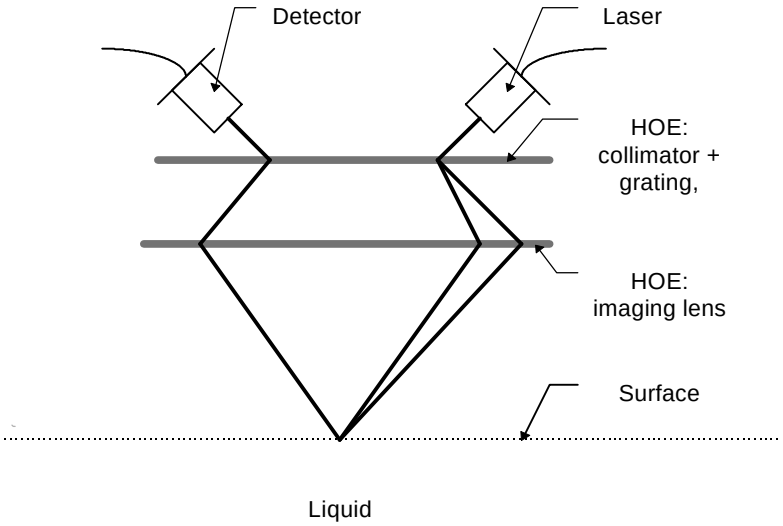

Figure 15. Surface scattering configuration based on holographic optical elements.

Signal processing is traditionally done by evaluating the correlation function of the photodetector signal. The estimated correlation function may be fitted with the expected function (this may be done in Fourier space) where the viscoelastic parameters are fitting variables. The procedure is computationally demanding for real-time measurements. A simpler approach may be based on a phase detection scheme. The signal statistics can be modelled by a narrow-band Gaussian process. The centre frequency, ω_0, is given by the mean of the derivative of the instantaneous phase, θ, which may be measured with a phase locked loop. The spectral width can be estimated from the variance of the derivative of the phase.

1. L. Lading, J. Mann, Jr. and R. V. Edwards, "Analysis of a surface-scattering spectrometer", *J. Opt. Soc. Am. A* **6**, No. 11, 1692-1700, November 1989.
2. An example of an implementation of a laser velocimeter is given by: S. G. Hanson, L. R. Lindvold and L. Lading, "A surface velocimeter based on a holographic optical element and semiconductor components", *Meas. Sci. Technol.***7**, 69-78 (1996).

3.3.4 Light Propagation in Human Tissue

*P. E. Andersen, P. M. Petersen and P. E. Fabricius**
(Bang & Olufsen Technology A/S, DK-7600 Struer, Denmark)*
E-mail: peter.andersen@risoe.dk

Understanding and modelling of light propagation in human tissue is essential for medical applications of optics in diagnostics as well as in laser therapy. Human tissue may optically be characterised by its scattering coefficient m_s [mm^{-1}], by the scattering phase function $p(\cos q)$ and by its absorption coefficient m_a [mm^{-1}]. Biological quantities, e.g. tissue glucose concentration, influence the scattering properties of the tissue through changes in the refractive index. Hence, light propagating in tissue interacts with the biological quantities through the optical

properties of the tissue. Measurements of transmitted or reemitted light from human tissue thus enable quantitative or qualitative monitoring of biological parameters.

The primary goal of our work is to establish a theoretical model for the spatially resolved diffuse reflectance from human skin tissue. The model should be capable of mimicking light propagation as the tissue glucose concentration and the blood volume change, thereby affecting the scattering and the absorption, respectively. We have developed a model for a slab geometry of finite thickness and infinite width based on the diffusion approximation to the Boltzman transport equation.[1] The incident light is a collimated beam with diameter 2*b* and the diffuse reflected light is detected at position *r* from the source, see Figure 16a. The detector has a diameter of 2*a*. We allow the tissue to have a refractive index different from the surrounding medium. In Figure 16b we have shown an example of the spatially resolved diffuse reflectance $R(r)$ calculated from the diffusion approximation, shown as the solid line, compared with Monte Carlo simulations.[2] The slab with refractive index 1.4 has a thickness of 40 mm and $a = b = 0.5$ mm. The optical properties are $m_s = 10$ mm^{-1}, $g = 0.93$ and $m_a = 0.04$ mm^{-1}.

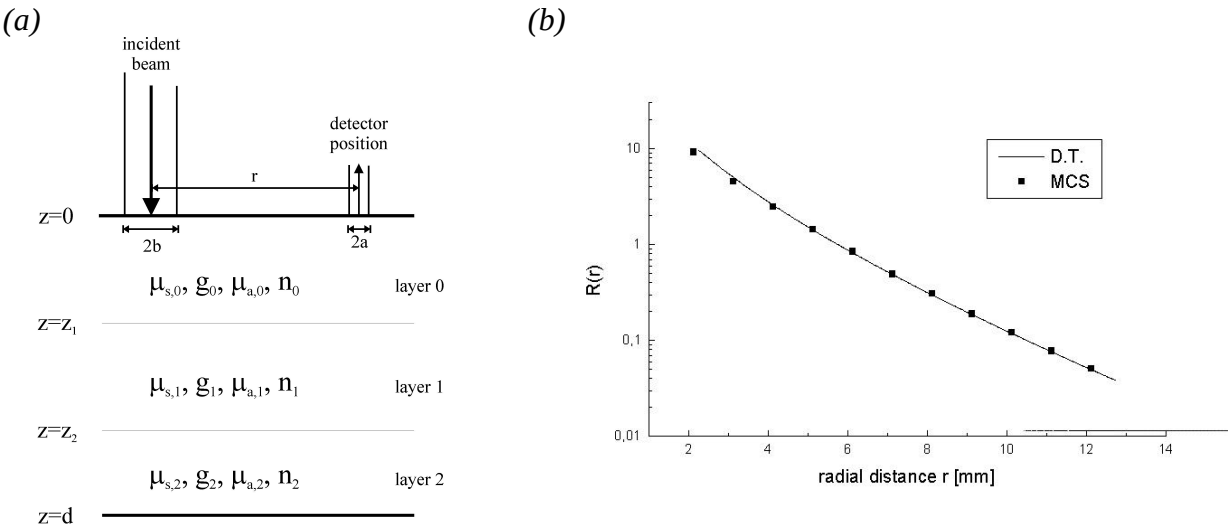

Figure 16. (a) The geometry of the tissue structure. (b) The spatially resolved diffuse reflectance $R(r)$ as a function of *r*. The solid line represents the diffusion theory and the squares represent Monte Carlo simulations.

The relationship between $R(r)$ and the underlying optical properties is complicated and therefore nonlinear data processing methods, e.g. neural networks, must be applied. We have used this model to obtain a data processing method that enables determination of the reduced scattering coefficient $m_s' = m_s (1-g)$ and m_a from steady state measurements of $R(r)$. The method involves a nonlinear curve fitting procedure applied to an analytical expression derived from the diffusion theory. It compares well with standard methods of extracting the desired optical properties. Furthermore, it is far superior to standard methods when applied on relative measurements, in which case only the shape of $R(r)$ yields information about the optical properties.[3]

Human skin consists of bounded layers with distinct optical properties. Hence, to mimic light propagation in such structures, theoretical models involving photon diffusion in multiple stacked layers should be developed. The geometry of the problem is shown in Figure 16a. Using the diffusion approximation with proper boundary and continuity equations, we have solved the light propagation for the three-layer structure. Our calculations compared favourably with Monte Carlo simulations for different skin structures. In Figure 17 we have shown a contour plot of the diffuse intensity outside the source for a three-layered tissue structure consisting of a dermal/blood layer (0.75 mm), adipose tissue layer (0.75 mm) and a muscle tissue layer (10 mm) as an example of our calculations. The optical properties are: $m_{a0} = m_{a1} = m_{a2} = 0.01$ mm^{-1}, $m_{s0} = 35$ mm^{-1}, $m_{s1} = 50$ mm^{-1}, $m_{s2} = 15$ mm^{-1}, $g_0 = 0.92$, $g_1 = 0.88$ and $g_2 = 0.85$. The refractive indices of all three layers are 1.4 and the structure is surrounded by air.

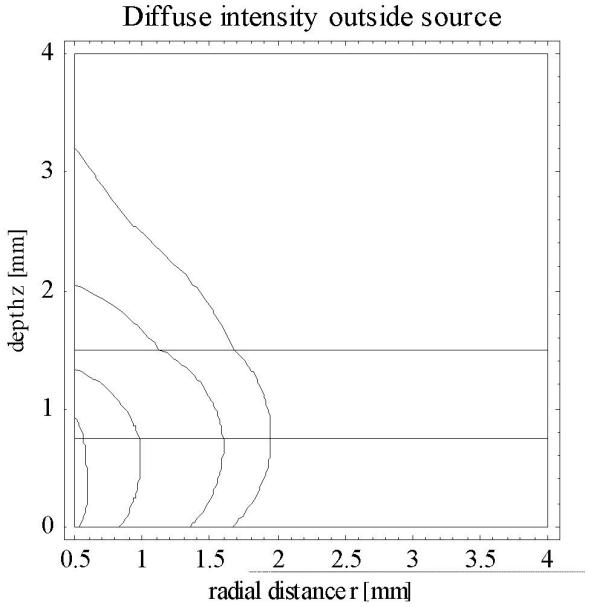

Figure 17. Contour plot of the diffuse intensity outside the source for the three-layer structure representing human skin. The source and detector radii are $a = b = 0.5$ mm (other parameters are given in the text).

By this model we have shown that the diffuse reflectance $R(r)$ in the three-layer case cannot be distinguished from the single-layer case. Moreover, we used the theoretical model to investigate the sensitivity of $R(r)$ with respect to the optical properties of each layer in different skin structures. At a single wavelength in the range 600 nm to 900 nm we found that the change in $R(r)$ due to tissue glucose concentration changes is in many cases much less than the change in $R(r)$ due to blood volume changes. Because of the complexity of multilayer models with their large number of variables, the necessity of multilayer models lies within their capability of providing a detailed description of the light-tissue interaction rather than their applicability to practical data analysis of $R(r)$ measurements.

1. A. Ishimaru, *Wave Propagation and Scattering in Random Media*, vol. I, Academic Press, New York (1978).
2. S. L. Jacques and L. Wang, "Monte Carlo modeling of light transport in tissues", Chapter 4, in *Optical-thermal Response of Laser Irradiated Tissue* (eds. A. J. Welch and M. J. C. van Gemert), Plenum Press, New York (1995).
3. J. Dam, P. E. Andersen, T. Dalgaard and P. E. Fabricius, "Determination of the reduced scattering and absorption coefficients of biological media from diffuse reflectance profiles," manuscript submitted to *Applied Optics*.
4. P. E. Andersen, J. Dam, P. M. Petersen and P. Bjerring, "Local diffuse reflectance from three-layered skin tissue models", SPIE BiOS '97, 8-14 February 1997, San Jose, CA, MS #2979-75 (1997).

3.4 Memory-based Neural Networks

3.4.1 Intelligent Machine Vision

T. M. Jørgensen, C. Linneberg and A. W. Andersen (Engineering and Computer Service)
E-mail: thomas.martini@risoe.dk

Compared with the human abilities in the area of visual processing the present capabilities of machine vision are rather primitive. In spite of this fact, there have been many successful applications of machine vision within the field of industrial inspection. When a machine vision solution is feasible, however, it has some advantages over human inspection. An automatic system is indefatigable and "objective".

Traditional machine vision solutions are hard-coded and can only solve very specific tasks in restricted environments. To cope with "real world" situations, the architectures need to be adaptive and to have the capabilities to learn. Our research efforts aim at taking the first steps towards such intelligent systems by combining traditional image analysis (morphology, edge extraction, texture analysis, etc.) with memory-based neural networks.[1]

In collaboration with Rambøll as well as Liisberg A/S we are developing a vision system for automatic detection and recognition of danger labels on containers, see Figure 18. The active vision solution uses a camera with adjustable pan, tilt and zoom. By combinations of neural nets and low-level features we locate the labels at low resolution. Due to the controllable camera it is then possible to zoom in on the detected labels and obtain high resolution images used for classifying the labels by another neural net.[2]

Figure 18. A controllable camera is used to locate and classify danger labels on containers.

Guiding of robots will probably be an important area for machine vision in the future. We are involved in an ESPRIT project the goal of which is to construct autonomous disassembly systems. The vision system operates on 2D video images as well as on depth data. The visual information is used to detect different components and to locate control points for the robot. It is always important to utilise a priori information, if possible. We have developed a tree-like structure for storing expected information concerning different TV models. This information can be updated during use of the system. To take advantage of the fact that different component are more likely to be detected in special areas we make use of coordinates normalised to the TV frame structure.[3] The partners are Siemens (D), 3D Scanners (UK) and Robotiker (E).

We also participate in a project funded by the EU Environmental Programme. The project aims at developing techniques for controlling waste incinerators. One possibility that is being considered is to develop vision sensors that can automatically classify the incoming waste into categories such as household waste, bottles, plastic, etc. The partners are Technische Hochschule Darmstadt (D) and Forschungszentrum Karlsruhe (D).

1. S. S. Christensen, A. W. Andersen, T. M. Jørgensen and C. Liisberg, "Visual guidance of a pig evisceration robot using neural networks," *Pattern Recognition Letters* **17**, 345 (1996).

2. T. M. Jørgensen, S. S. Christensen and A. W. Andersen, "Detecting danger labels with RAM based neural networks," *Pattern Recognition Letters* **17**, 399 (1996).

3. T. M. Jørgensen, A. W. Andersen and S. S. Christensen, "Neural net based image processing for disassembling TV-sets," in Proc. of the International Conf. on Engineering Applications of Neural Networks (EANN 96).

3.4.2 Memory-based Neural Networks

T. M. Jørgensen, C. Linneberg and A. W. Andersen (Engineering and Computer Service)
E-mail: thomas.martini@risoe.dk

Within the areas of machine learning and machine vision there exist different learning paradigms. Memory-based reasoning constitutes one of these approaches. The idea is to represent knowledge in terms of specific cases or patterns. When memorising the information as specific cases it can, however, be difficult to generalise to cases outside the training set unless the amount of training data is large. To avoid this shortcoming, one can instead distribute the information contained in each case by projecting the information into several subspaces. This distributed memory concept is the philosophy behind RAM-based nets. At Risø National Laboratory we have been working on a number of methods for constructing and evaluating the information contained in combinations of different subspaces. We have developed methods based on so-called cross-validation for determining the size of the RAM nets needed for proper generalisation. This corresponds to determining the number of hidden neurons in a conventional neural net. Furthermore, we use a method similar to the principal component analysis as a guide for selecting the input connections. The derived algorithms have been verified in different applications including the task of intelligent character recognition.[1]

The RAM-based net is well suited for hardware implementation. Accordingly, we have implemented the architecture in hardware to increase the speed of the training and recall process. The board can contain several RAM nets at the same time. The actual number is dependent on the sizes of the individual nets, but the maximally available number is 32 networks with 32 output classes. The total amount of memory on the board is 16 Mbytes and it is designed for a PC using a PCI-bus and running Microsoft's Windows 3.1 and 95/NT.

There are actually many similarities between the different paradigms in machine learning, and hybrid solutions are becoming more widespread. The RAM-based architecture can be viewed as a constrained feedforward neural net, but also as an ensemble of multiple decision trees. However, in opposition to normal feedforward neural nets, RAM-based nets possess some powerful features including learning of the training examples from only one pass.

1. T. M. Jørgensen, "A RAM-based neural net with inhibitory weights and its application to recognising handwritten digits," in Proc. of the 1996 International Workshop on Neural Networks for Identification, Control, Robotics, and Signal/Image Processing (1996).

3.4.3 Feasibility Study of Mine Detector for Humanitarian Demining

H. Flyvbjerg and A. Skov Jensen
E-mail: henrik.flyvbjerg@risoe.dk

This study is a continuation of a prefeasibility study financed by the Danish Ministry of Research and Information Technology, Nea-Lindberg A/S and the Centre for Advanced Technology (CAT). It is financed 80% (approx. DKK 1.8m) by the Danish Agency for Development of Trade and Industry with the Danish Ministry of Foreign Affairs as claimant, and 20% by the participating institutions.

From Risø National Laboratory the participating departments were Optics and Fluid Dynamics, The Isotope Laboratory and Solid State Physics. The Optics and Fluid Dynamics Department contributed in two ways: (1) with literature studies of infrared and nuclear methods, and (2) with project coordination within Risø.[1] The literature studies were supplemented with author contacts in order to clarify some matters, and to secure up-to-date, informal and unpublished information.

The study of infrared detection methods convincingly showed that these methods do not work for personnel mines, except under circumstances where ordinary visual inspection works as well. Extensive studies have been carried out, some of them sophisticated and in institutions devoted to the detection of mines and unexploded ordnance, i.e. in well-funded and sizeable groups that have accumulated experience for years.

Similarly, the study of nuclear methods brought out that the method is not applicable to personnel mines because they are too small and the equipment that might render them detectable would have to compensate for their smallness with prohibitive size and weight. Informal information and unpublished negative results provided by John McFee, the leader of the most advanced project in the field (Improved Mine Detection Concept, carried out in Defence Research Establishment, Suffield, Canada), were particularly useful in confirming these conclusions.

1. CAT report: "Feasibility-studie over minesøger til humanitær minerydning," parts I and II (confidential) - in Danish.

3.4.4 Prompt Recognition of Brain States by the EEG Signals

H. Flyvbjerg, B. O. Peters (Forschungszentrum Jülich, Germany) and G. Pfurtscheller (Graz University of Technology, Austria)
E-mail: henrik.flyvbjerg@risoe.dk

Noninvasive methods of investigation have distinct advantages in a number of scientific and clinical contexts. In the case of the human brain, there are obvious reasons to prefer such methods. Electro-encephalography (EEG) is one of them, and has been around for some time. It has become a widely used diagnostic and even therapeutic tool in medicine. Its fine time resolution and relatively cheap recording instrument are clear advantages of this method.

EEG recorders with up to 256 electrodes are currently in use, and experiments can produce large amounts of raw data. Thus the question naturally arises: How much can be found out about the brain's activities from all those data if they are processed optimally, and what *is* the optimal procedure for processing?

We have addressed this question of the information content of EEG signals.[1] In popular terms, this is the question of whether one can read the mind of a person by properly deciphering his EEG.

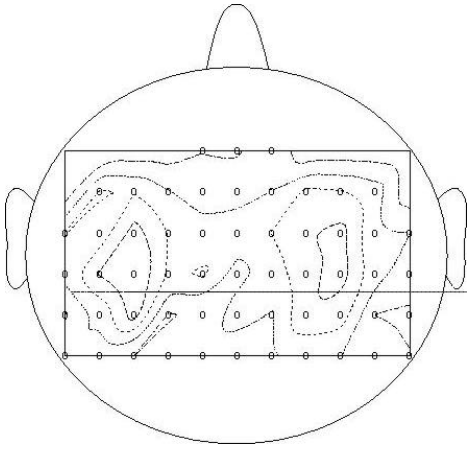

Figure 19. Map of average recognition accuracy of individual channels. Two peaks of accuracy are seen over the motor cortex, one on each hemisphere. The spacing between contour lines is 10%. Lines of 40%, 50%, 60% and 70% recognition are shown. Note that no recognition at all gives a random result, i.e. 33% recognition in this map.

It has been known for some time that this is possible, indeed, though only to a very modest extent. EEGs produced during a very limited set of mental tasks can be classified, hence recognised, according to tasks. In our investigation we have revisited the issues of how many channels to use, how to choose them, and how to use them. Since the classification capability of individual channels varies much, we applied an identical single-channel analysis to all channels in a 56-channel EEG, ranked the channels on the basis of their classification accuracy (see Figure 19 and Figure 20), formed a "committee" of the best-performing channels, and had the "committee" classify EEGs by simply summing the "opinions" of the committee members. The size of this "committee" was chosen for optimal classification accuracy, and found to be 9-12, confirming previous results obtained differently. But the classification accuracy we achieved, 83% on the basis of 1 sec short EEGs, is significantly better than what has been obtained with other procedures.[1] This result should, however, be regarded as preliminary since it was obtained for EEGs from only one subject, and needs to be confirmed on EEGs from more subjects.

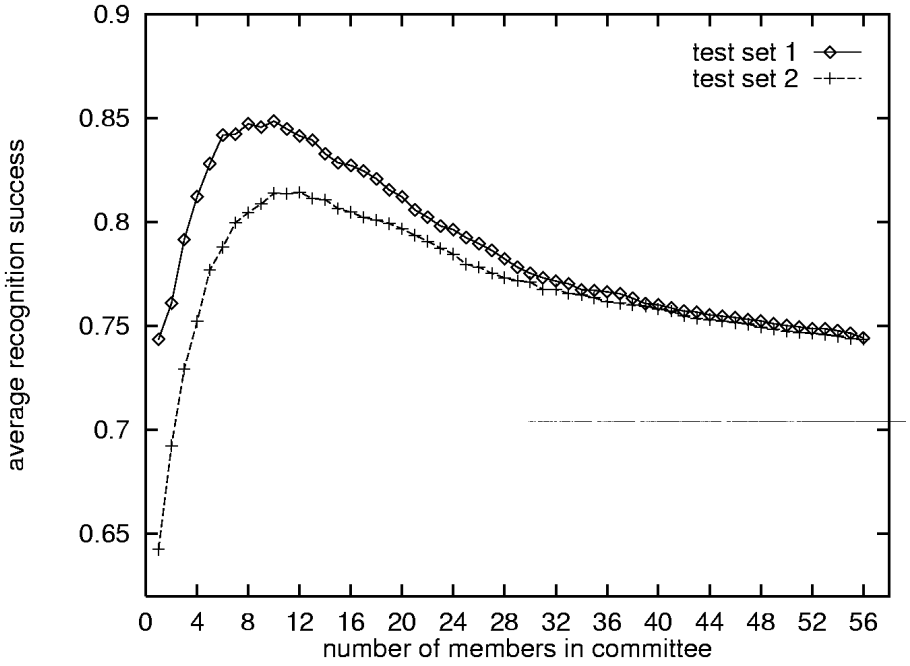

Figure 20. Classification success on test sets 1 and 2 as a function of committee size, averaged over 200 random partitions of the available trials in training, validation and two test sets. Channels were rank ordered according to their classification success on test set 1, and included in a given size committee according to rank. Consequently, the classification success of a committee is artificially high on test set 1, and its true success must be estimated by its success on an independent test set, test set 2.

1. B. O. Peters, G. Pfurtscheller and H. Flyvbjerg, "Prompt recognition of brain states by their EEG signals", submitted to *Theory in Biosciences*, special issue on brain science, to appear June 1997.

3.4.5 Statics and Dynamics of Microtubules

H. Flyvbjerg, T. E. Holy, S. Leibler* (*Princeton University, USA), I. M. Jánosi (Forschungszentrum Jülich, Germany) and D. Chrétien (European Molecular Biology Laboratory, Heidelberg, Germany)*
E-mail: henrik.flyvbjerg@risoe.dk

Microtubules are organelles common to all eukaryotic cells, i.e., "modern" cells with a nucleus, such as the cells of all multicellular organisms. They are tubular polymers of a protein, tubulin, and play a role as *universal engineering element*, used by nature in its designs anywhere rigidity is needed in eukaryotic cells: In the cytoskeleton, in cilia and flagella, in the "tracks" along which molecular motors haul vesicles containing neurotransmitters from the body of nerve cells, where they are produced, to the dendrites, where they are used. Microtubules also have dynamic properties which are very unusual for polymers, but crucial for the problems they solve in cells, such as providing rigidity to the cytoskeleton, and yet permitting cells to crawl and, most strikingly, their role during cell division, where they find and separate the chromatid pairs so that each daughter cell ends up having a complete set of chromosomes.

Pure research and important applications are never far apart in microtubule research; e.g., the so-called antimitotic cancer drugs specifically target the dynamics of microtubules, which is interrupted to arrest tumor growth.

The kinetics of microtubules that self-assemble from a solution of tubulin, was analysed phenomenologically in [1]. It was demonstrated that a unique model can be derived from the experimental time series. Figure 21 shows examples of experimental time series and fits of the model to these series.

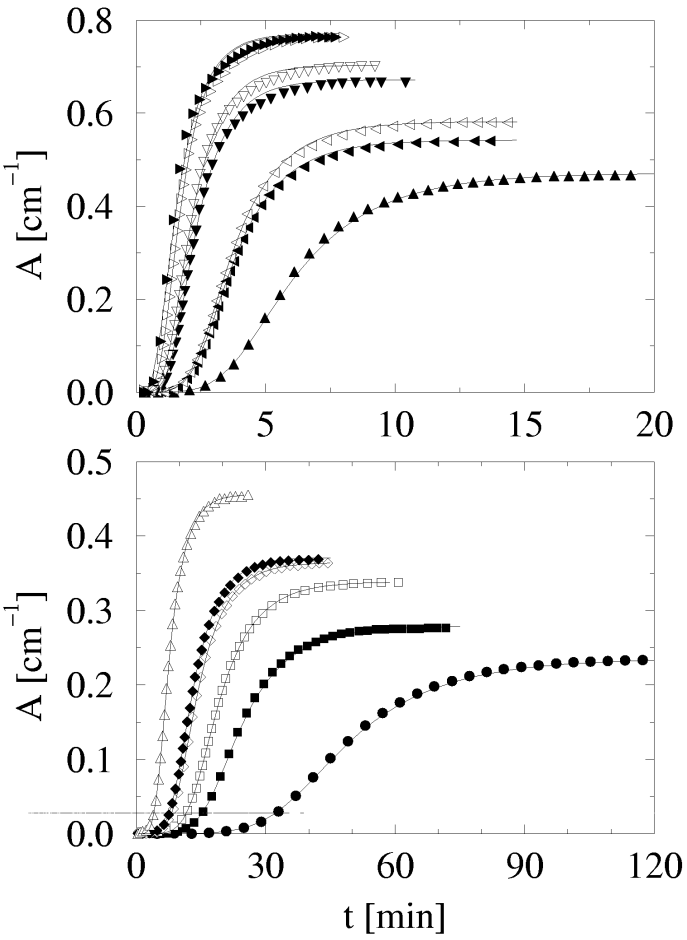

Figure 21. Turbidity versus time of tubulin solution in which a temperature jump from 0 to 37°C at time 0 has induced microtubules to self-assemble. Plotting symbols: turbidity time series for different initial concentrations of tubulin. Fully drawn curves: two-parameter fits to experimental data of theoretical turbidity series derived in [1].

The dynamics of the so-called GTP cap on growing microtubules was modelled in [2], and the rate of change from the polymerising to the depolymerising state following from the model, the so-called *catastrophe rate*, was fitted to experimental data (see Figure 22). Three different types of experiments, apparently giving conflicting results, were explained as different manifestations of one, consistent description. Figure 23 shows how the model reproduces results from one of these experiments.

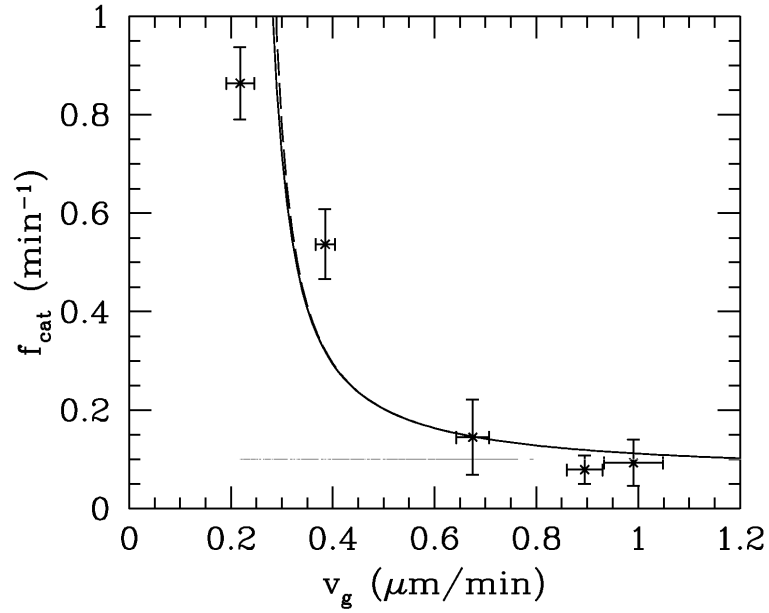

Figure 22. Catastrophic rate, f_{cat}, versus growth velocity, v_g. Dots with error bars: experimental results. Full curve: theoretical expression. Dashed curve: approximate theoretical expression; this graph is a hyperbola.

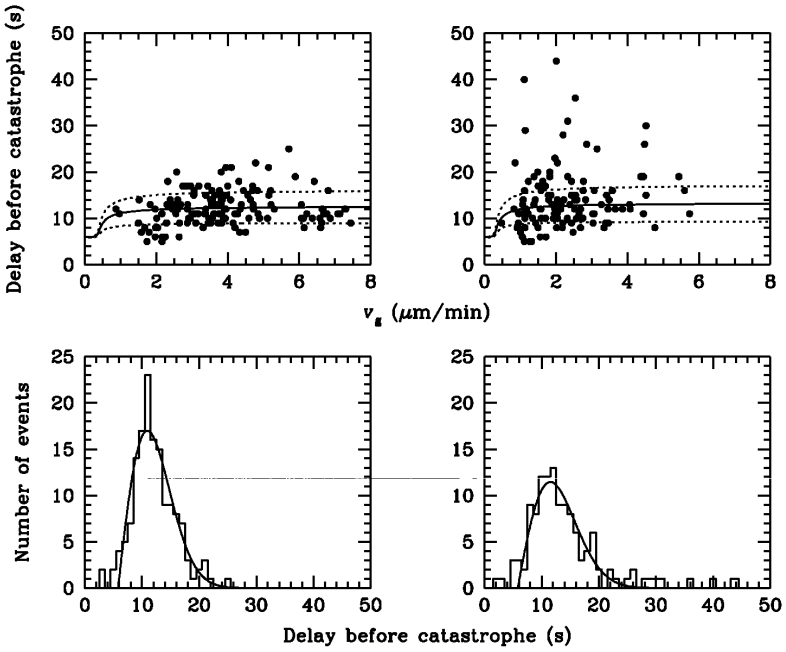

Figure 23. Delays before catastrophe following dilution of tubulin solution to stop growth. Left and right: different ends of microtubules (they are polar objects). Top: delay as a function of initial growth velocity. Each point represents a single measurement on a microtubule. Curves are theoretical mean (solid) and standard deviation (dashed) of the delay. Bottom: histograms showing the experimental distribution of delays before catastrophe. The curves are fits of the theoretical distribution. Dilution was initiated at $t = 0$ and required some time (6.1 s when used as a free parameter in our fit) for completion.

The mechanical properties of the protein sheet that forms the microtubule wall were modelled with a flexible surface with intrinsic Gaussian curvature;[3] see Figure 24.

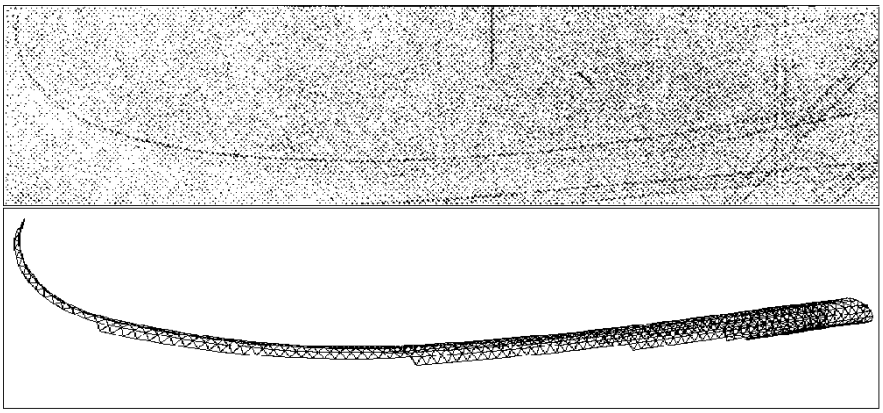

Figure 24. Top: electron micrograph of a tapered, curved microtubule end. Its shape reveals that the material of the microtubule wall has intrinsic negative Gaussian curvature. Bottom: model microtubule, surface with constant negative Gaussian curvature showing the width of the tapered end determines its curvature.

Most of these results were explained pedagogically, supposedly, in [4] and [5].

1. H. Flyvbjerg, E. Jobs and S. Leibler, "Kinetics of self-assembling microtubules: an "inverse problem" in biochemistry", communicated by M. E. Fisher in Proc. Natl. Acad. Sci. (USA), 93, 5975-5979 (1996).
2. H. Flyvbjerg, T. E. Holy and S. Leibler, "Microtubule dynamics: caps, catastrophes, and coupled hydrolysis", *Phys. Rev. E* **54**, 5538-5560 (1996).
3. I. M. Jánosi, D. Chrétien, S. Leibler and H. Flyvbjerg, "Mechanical model of microtubules", in preparation.
4. H. Flyvbjerg, "Microtubule dynamics", in H. Flyvbjerg, J. Hertz, M. H. Jensen, O. G. Mouritsen and K. Sneppen (Eds.), *Physics of Biological Systems*, Lecture Notes in Physics, Vol. 480, Springer-Verlag (Berlin Heidelberg New York 1997).
5. H. Flyvbjerg, "Modelling microtubule dynamics: doing molecular biology with the tools of theoretical physics", to appear in the published lecture notes of the IFF Spring School, 1997, Institut für Festkörperforschung (IFF), Jülich, 1997.

3.5 Infrared Diagnostics

3.5.1 Diffuse Reflectance Infrared Fourier Transform Spectroscopy (DRIFTS) of Superconducting Powders

J. Bak
E-mail: jimmy.bak@risoe.dk

Fast and sensitive optical and spectroscopic methods are as a routine used in industrial laboratories for in-line analysis of gas- and liquid samples. Optical methods for quantitative analysis of powdery materials are, however, not common. The heterogeneous nature of powder samples, i.e. particle size distribution, packing density, surface roughness, etc., makes it difficult to reproduce the measurements carried out with optical methods. Methods for analysing powder samples quantitatively as well as qualitatively are of importance because many powders, e.g. minerals, are difficult to dissolve.

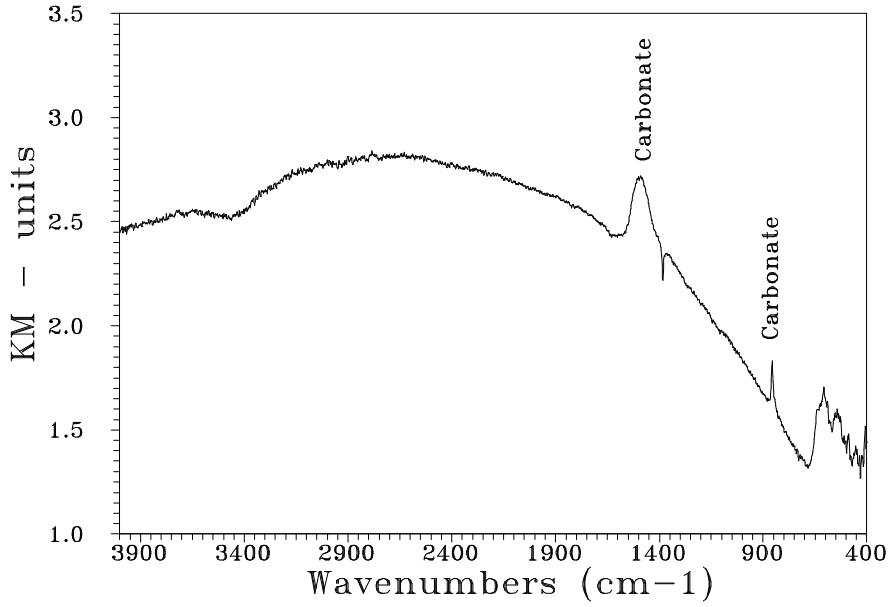

Figure 25. FTIR spectrum of a superconducting powder. Spectral peaks originating from carbonate compounds ($SrCO_3$ and $CaCO_3$) are observed at 870 cm^{-1} and 1479 cm^{-1}.

Diffuse reflectance spectroscopy has been used to determine the carbonate content in superconductor precursor powders produced at Risø. Infrared light irradiating the superconductor powder surface is partly regularly and partly diffusely reflected from the surface. The diffusely reflected light, which is multiply scattered in the upper layer of the sample and partly absorbed, is measured with a Fourier transform instrument (FTIR). Figure 25 shows the DRIFTS-spectrum of a superconductor powder. Spectral features originating from carbonate compounds are observed at 1479 cm^{-1} and 870 cm^{-1}. A qualitative

analysis shows that strontium carbonate is the major carbonate compound present in the superconductor precursor powders. It is determined quantitatively that the carbonate content is in the range of 1-2 wt %.

Tapes with superconducting properties are produced in an advanced process with repeated heating and extruding the superconductor precursor powder into a thin silver protected foil. A high content of carbonate in the superconductor precursor powders reduces the quality of the produced superconductor tapes. When heated, the carbonate present in the precursor powder liberates gaseous carbon dioxide that diffuses to the surface of the superconducting material leaving small cracks in the final superconductor tape.

1. J. Bak and B. Kindl, “Analysis of the carbonate content in air contaminated superconductor powders by DRIFTS”, to be submitted to *Appl. Spec.*

3.5.2 Improved Temperature Measurements of Burning Fuel Particles

S. Clausen and L. Holst Sørensen (ReaTech, c/o Centre for Advanced Technology, P.O. Box 30, DK-4000 Roskilde, Denmark)
E-mail: sonnik.clausen@risoe.dk

For combustion of solid particles, mass conversion and the derived heat production are the main topics. Many groups have spent large efforts to study the high-temperature devolatilisation and oxidation of coal chars. Typical high-temperature devolatilisation and oxidation measurements are conducted in experimental facilities like the flat-flame burner, the drop-tube reactor and the entrained flow reactor. Good data are valuable since they lead to better direct understanding of particle combustion and aid in the development as well as the evaluation of comprehensive combustion models.

A novel method for temperature measurements on individual burning char and coal particles with a Fourier transform infrared (FT-IR) spectrometer has been developed. The technique is demonstrated for monitoring emission spectra of individual moving particles that require a few milliseconds to pass the field of view of a conventionally scanning FT-IR spectrometer. Examples of single-particle spectra are shown in Figure 26. The accurate particle surface temperature is calculated from a best match of the measured emission spectrum to a detailed physical radiance model spectrum. The technique is applied to measure surface temperatures of 90-125 μm particles with temperatures from 1000 K up to 2200 K in an entrained flow reactor. A one-temperature calibration of the FT-IR spectrometer is sufficient for accurate measurements throughout a broad temperature range. Background radiation and a fluctuating particle feeding rate are handled by subtraction of two successive measurements. The single-particle emission spectra are useful for testing the assumptions about particle emissivity as a function of wavelength. The findings in the present work justify the greybody assumption for the burning char particles as well as the burning coal

particles. Under sooting conditions particle temperature errors of about 300 K were observed. The burn-offs for four coal samples are analysed and compared with particle temperatures at 1, 3, 6, 12 and 21 vol% oxygen, see Figure 27. In addition to giving important information on the modelling of the combustion process, the particle temperature measurements and the burn-off give information that can be used for ranking of coal samples with respect to reactivity.

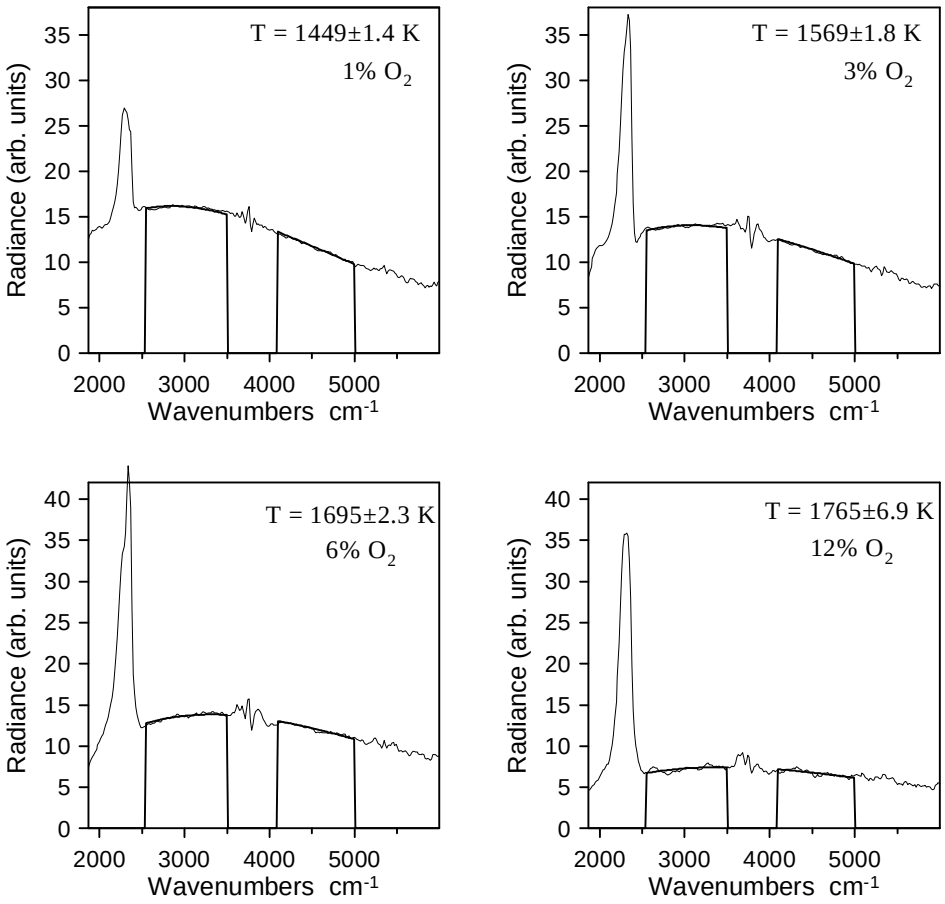

Figure 26. Examples of single Cocerr coal char particle emission spectra and the corresponding least squares fit curves. The spectral resolution is 32 cm^{-1}.

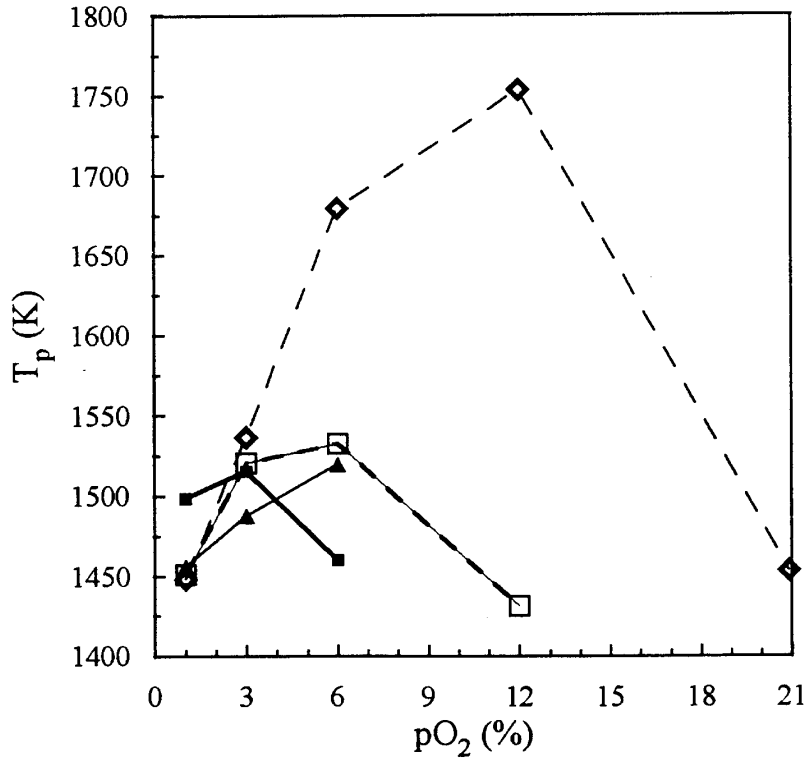

Figure 27. 90-125 µm particle mean temperature as a function of oxygen particle pressure. Reactor temperature T_{set} = 1603 K and residence time is t = 191 ms. ■: Idpina, □: Aublat, ▲: Samidd, ◊: Cocerr.

1. S. Clausen and L. H. Sørensen, "Measurement of single moving particles temperatures with an FT-IR spectrometer", *Applied Spectroscopy* **50**, 1103-1111 (1996).
2. S. Clausen and L. H. Sørensen, "Improved temperature measurements of burning char and coal particles using an FTIR spectrometer", *Energy & Fuels* **10**, 1133-1141 (1996).
3. L. H. Sørensen, S. Clausen, P. Astrup, O. Rathmann, O. Biede and J. S. Lund, "Experimental high-temperature investigations of coal particles", Risø National Laboratory Report Risø-R-871(EN) (1996).
4. S. Clausen, "Measurements of particle temperature under combustion", Risø National Laboratory Report Risø-R-861(EN) (1996).

3.5.3 Optimisation of a Grate Fired Biomass Furnace with an Infrared Fibre-optic Probe

S. Clausen
E-mail: sonnik.clausen@risoe.dk

In any combustion system the gas temperature and the gas composition are parameters of great importance. The gas temperature is usually measured with a suction pyrometer with a slow response time. The true gas temperature fluctuations are thereby mostly unresolved for turbulent

flows. The measurements of instant local flame temperatures are interesting with regard to understanding the process and the chemical reactions that take place.

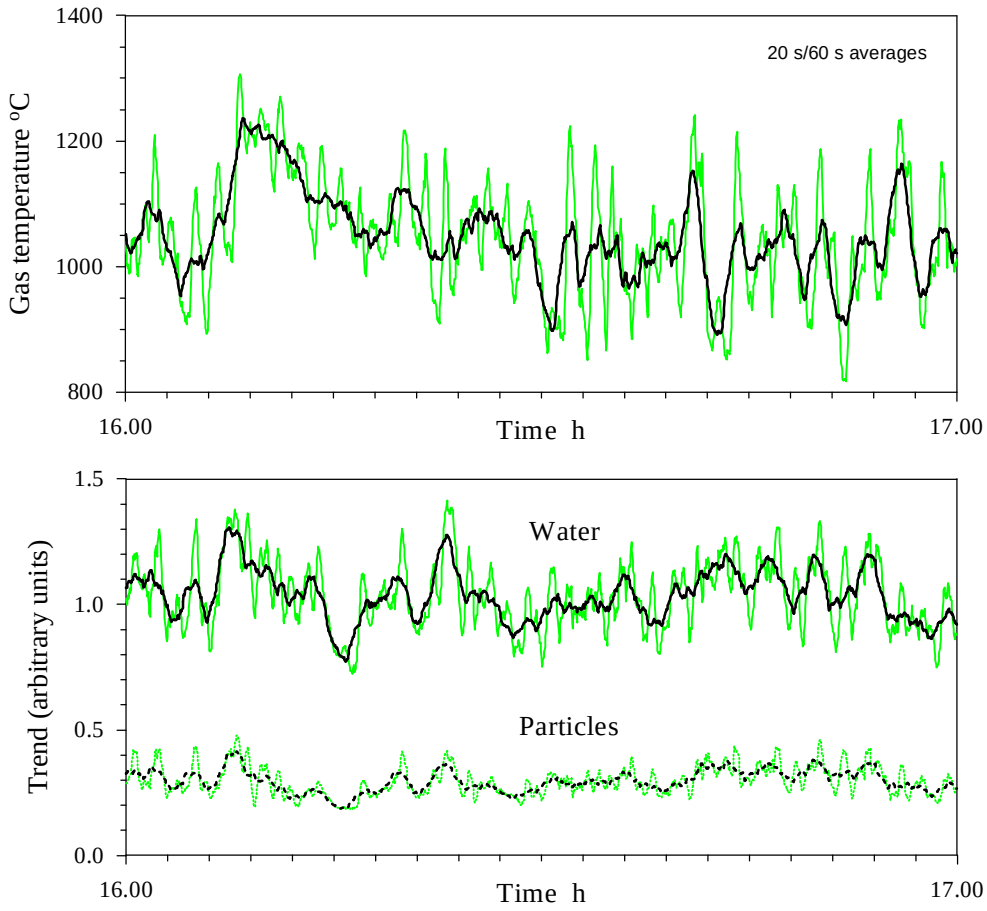

Figure 28. Upper curves: gas temperature; lower curves: trend curves of the flue gas composition in straw- and wood-fired furnace. The bold lines are 60 s averages; the grey lines are 20 s averages calculated from flue gas emission spectra (40 scans per minute).

Fourier transform infrared (FT-IR) emission spectroscopy is a flexible and powerful technique for studying energy transfer from surfaces and through media that absorb, emit and scatter radiation. Many common gases, e.g. H_2O, CO_2, CO and C_xH_y formed under combustion, have absorption bands in the spectral range of the instrument, and the gas temperature as well as the gas concentration might in principle be determined experimentally. An infrared fibre-optic probe has been applied for measuring the flue gas temperature and the trend curves of gas composition in a 21-MW straw- and wood-fired furnace. The principal feature of the new method is that several important parameters can be extracted on-line, instantly and simultaneously from the infrared spectra. The thermal radiation from the flue gas across the furnace at the exit of the intense combustion zone is collected with the infrared fibre-optic probe, and the emission spectra are measured with an FT-IR spectrometer. The performance of the infrared method is illustrated by measurements that reveal details that can be tracked back to the behaviour

of the combustion process and the operation of the furnace, see Figure 28. It was observed that the vibration of the grate and the reorganisation of the fire on the grate result in large gas temperature fluctuations. Flue gas temperature fluctuations with a period of about 1 minute were measured in the first experiment. The amplitude of the temperature fluctuations was reduced with a factor of 2-4 after the interval between vibration of the grate and the frequency of the vibration was optimised. Furthermore, it is shown that variations in the steam production from the boiler are closely linked to variations in fuel load through changes of the gas temperature and the gas composition. The future prospects regarding applications of infrared measuring devices and sensors for active control and regulation of combustion systems are promising.

1. S. Clausen “Local measurement of gas temperature with an infrared fibre-optic probe”,*Meas. Sci. Technol* **7**, 888-896 (1996).
2. The method for gas temperature measurements was presented at the 3rd Workshop on Infrared Emission Measurements by FTIR, Quebec, 7-9 February 1996.

3.6 Calibration

3.6.1 Temperature Calibration and Measurements

N.E. Kaiser, M. Kirkegaard and F. Andersen
E-mail: n.e.kaiser@risoe.dk

For more than 30 years the department’s thermometry laboratory has calibrated temperature sensors for use in Risø's own test facilities.

The laboratory was accredited in 1978 and has been approved in the Danish Accreditation Scheme, DANAK, to issue certificates for calibration of temperature measurement equipment. DANAK certificates are the only Danish certificates that are accepted in connection with ISO-9000 certification.

The instruments in the laboratory are traceable to international standards. The reference thermometers are regularly calibrated at the National Physical Laboratory in London to secure accordance with the International Temperature Scale, ITS-90.

Accredited calibrations can be made in the temperature range -150°C - 1100°C with an uncertainty better than ±0.008°C - 0.018°C up to 550°C and ±0.5°C further up to 1100°C. Available in the laboratory is a set of liquid bath thermostats and electric furnaces to establish any temperature in the accredited temperature range.

Temperature measurements are made in situ in waste incineration plants, furnaces, power plants, autoclaves, etc. If the plant instrumentation has electrically available outputs, these signals can be collected simultaneously with the signals from Risø's sensors by Risø's computer-based data acquisition system. This allows direct comparison between Risø's measurements and the readings of the plant instruments.

3.6.2 Infrared Temperature Calibration

S. Clausen
E-mail: sonnik.clausen@risoe.dk

A reference laboratory for calibration of infrared instruments was established at Risø in 1996 with support from the Danish Agency for Development of Trade and Industry. Traceable calibration of pyrometers and infrared thermometers is made with blackbodies in the temperature range -50 °C to 1600 °C. The work affects the following four main topics to reduce noncontact temperature measurement uncertainties:

- calibration service of infrared thermometers;
- research and development of improved methods for temperature measurements;
- measurements for customers;
- consultative service and information.

The research activities include methods for measurements of surface, particle and gas temperatures. The measurements of particle and gas temperatures are described in sections 3.5.2 and 3.5.3, whereas the measurements of surface emissivity and temperature are described below.

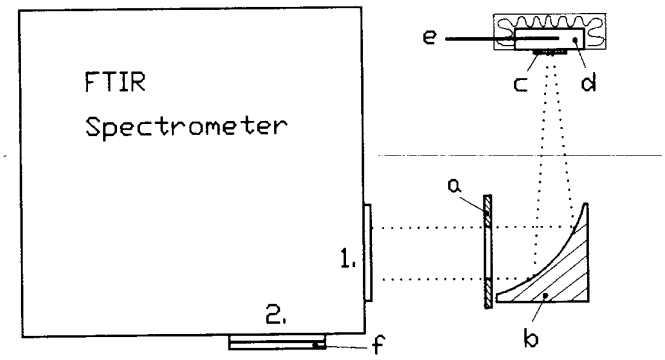

Figure 29. Experimental set-up for measuring the spectral emissivity of a sample. 1.: emission port used; a: 25 mm aperture; b: focusing mirror (f =152.4 mm); c: sample; d: insulated heated aluminium block; e: thermocouple for measuring the temperature of the aluminium block.

The Fourier transform infrared (FT-IR) spectrometer is a powerful tool for measuring emittance spectra at good spectral resolution. Instrumentations and methods for measuring the spectral emissivity of surfaces have been developed, Figure 29. However, the values measured for the same material by different investigators may sometimes differ considerably. One of the most difficult problems that arises when surface emissivity is measured is the accurate surface temperature determination; the difficulty stems from temperature gradients that exist close to the surface of a freely radiating body or from disturbances introduced by using a contact sensor. Surface temperatures are estimated with great precision based on a multitemperature method for FT-IR spectrometers. The

method is based on Planck's radiation law as well as on a nonlinear least squares fitting algorithm applied to two or more spectra at different sample temperatures and a single measurement at a known sample temperature, for example, at ambient temperature. The temperature of the sample surface can rather easily be measured at ambient temperature. The spectrum at ambient temperature is used to eliminate background effects from spectra measured at other surface temperatures. The temperatures of the sample are found in a single calculation from the measured spectra independently of the response function of the instrument and the emissivity of the sample. The spectral emissivity of a sample can be measured if the instrument is calibrated against a blackbody source. Temperatures of blackbody sources are estimated with an uncertainty of 0.2 to 2 K. The method is demonstrated for measuring the spectral emissivity of a brass specimen and an oxidised nickel specimen. The spectral emissivity for a nickel specimen is shown in Figure 30.

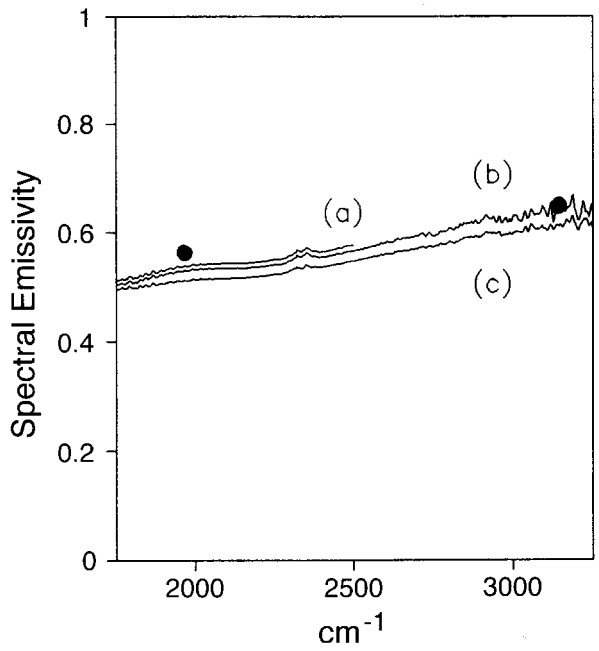

Figure 30. Calculated normal spectral emissivity of oxidised nickel specimen. a: T_1 = 319.3 K and T_2 = 351.7 K; b: T_1 = 319.6 K and T_2 = 352.3 K; c: T_1 = 320.2 K, T_2 = 353.4 K and T_3 = 389.0 K. The two dots indicate the values measured by NPL at 773 K.

1. S. Clausen, A. Morgenstjerne and O. Rathmann, "Measurement of surface temperature and emissivity by a multitemperature method for FT-IR spectrometers", *Applied Optics* **35**, 5683-5691 (1996).
2. S. Clausen, "Praktisk måling af overfladetemperaturer med IR-termometer", Måleteknisk temadag omhandlende temperatur, DTI, 30 April 1996 (in Danish).
3. S. Clausen, "Kalibrering af infrarødt udstyr", Den 18. nordiske konference: Måleteknik og kalibrering, 24-27 November 1996 (in Danish).
4. S. Clausen, "Infrarød temperaturmåling", Risø National Laboratory Report Risø-R-862(DA) (in Danish) (1996).

4. Plasma and Fluid Dynamics

4.1 Introduction

J. P. Lynov
E-mail: jens-peter.lynov@risoe.dk

A unifying topic for the research performed under the Plasma and Fluid Dynamics programme is the dynamic behaviour of nonlinear continuum systems. The continuum systems under investigation cover fluids, plasmas and optical media, and the studies are focused on fundamental dynamic processes related to self-organisation, pattern formation and various types of wave localisation and collapse.

A long-term objective of the research is to utilise the acquired knowledge to synthesise and optimise new devices and systems of benefit to society and industry. The development of a new and virtually inexhaustible energy source based on fusion is an example of such a goal, as is the development of novel optical devices based on controlled pattern formation. The investigations are performed through close interplay between theoretical, numerical and experimental studies.

Although many of the problems studied in 1996 were of fundamental and generic nature and of relevance to many physical systems, a division of the research projects has been introduced grouping the projects into three different subgroups that mainly relate to specific physical systems. The results obtained during 1996 can be summarised as:

- *Fusion research*. Based on a novel measurement technique developed at Risø, a laser diagnostic has been constructed for use in fusion energy research. This diagnostic was successfully installed on the Wendelstein 7-AS stellarator in Garching, Germany, and commissioning of the system has been initiated. The diagnostic project is supported by theoretical and numerical studies of the formation of large-scale, coherent structures in drift wave turbulence. Coherent structures are also found in fundamental drift wave experiments conducted in a simple magnetised torus at the University of Tromsø, Norway.
- *Fluid dynamics*. Detailed experimental investigations of pattern formation by shear flow instability in a parabolic vessel have been performed and the experimental results closely reproduced by numerical simulations. The evolution of vortex rings in viscoelastic as well as stratified fluids has been studied experimentally, and large-scale numerical simulations based on highly accurate spectral codes have been conducted concerning fundamental processes, including particle mixing, involved with coherent structures under various degrees of turbulence and in different flow geometries.

- *Nonlinear optics*. Experimental and numerical results have been obtained for 'optical vortices' and elliptical solitons in photorefractive crystals, while experimental results have been established for optical pattern formation by noncollinear pump beams and for the transfer of temporal fluctuations by beam coupling in photorefractive media. Fully three-dimensional, dynamic simulations have been performed for the anisotropic, nonlinear Schrödinger equation, and theoretical and numerical results have been obtained for the nonlinear interaction of light with media possessing different types of nonlinearity.

4.2 Fusion Energy

4.2.1 Collective Scattering Turbulence Diagnostic at the W7-AS Stellerator

M. Saffman, B. Sass, W. Svendsen, J. Thorsen, W. Junker and H. Larsen (Engineering and Computer Service)
E-mail: mark.saffman@risoe.dk

The preparation of a two-point collective scattering diagnostic for spatially localised turbulence measurements was completed in 1996, and the instrument was installed at the W7-AS stellerator experiment at the Institute for Plasma Physics in Garching, Germany, in July-August 1996. A view of the diagnostic concept is shown in Figure 31. The instrument, which is based on a two-point correlation measurement technique, has been designed to give enhanced spatial resolution of large-scale turbulence. Commissioning and initial testing of the diagnostic are currently in progress.

As installed at the W7-AS experiment the diagnostic is a complex system that comprises mechanical, optical, electronic and computer components. A detailed description of the system design has been given in [1]. Only the primary features of the installed system will be described here. The optical train includes a transmitter table with 25 W CO_2 laser and beam forming optics located in the basement underneath the torus, and a receiving table mounted on the top of the torus. The optical path length between the transmitting and receiving tables is approximately 9 metres, and human communication between the two tables is via walky-talky since there is no direct line of sight.

The optical access and mechanical mounting has been designed to allow translation of the measurement volume throughout a large portion of the plasma cross-section. The four optical beams (two strong primary beams, and two local oscillator beams) traverse along a vertical chord through the plasma. Optical access is through 200 mm diameter ZnSe windows located on the lower and upper torus ports separated by 2 m. Large diameter windows have been mounted to enable radial adjustment of the measurement volume in the plasma by up to +/- 5 cm. The radial adjustment is achieved by tilting mirrors located below and above the

plasma. Continuous vertical adjustment from 60 cm below to 60 cm above the plasma midplane has been obtained by mounting the primary focusing and receiving lenses on long travel translation stages. The measurement direction in the horizontal plane can be varied continuously by rotation of dove prisms located on the transmitting and receiving tables. The combined effect of the available adjustments is that transport along both radial and poloidal directions can be investigated.

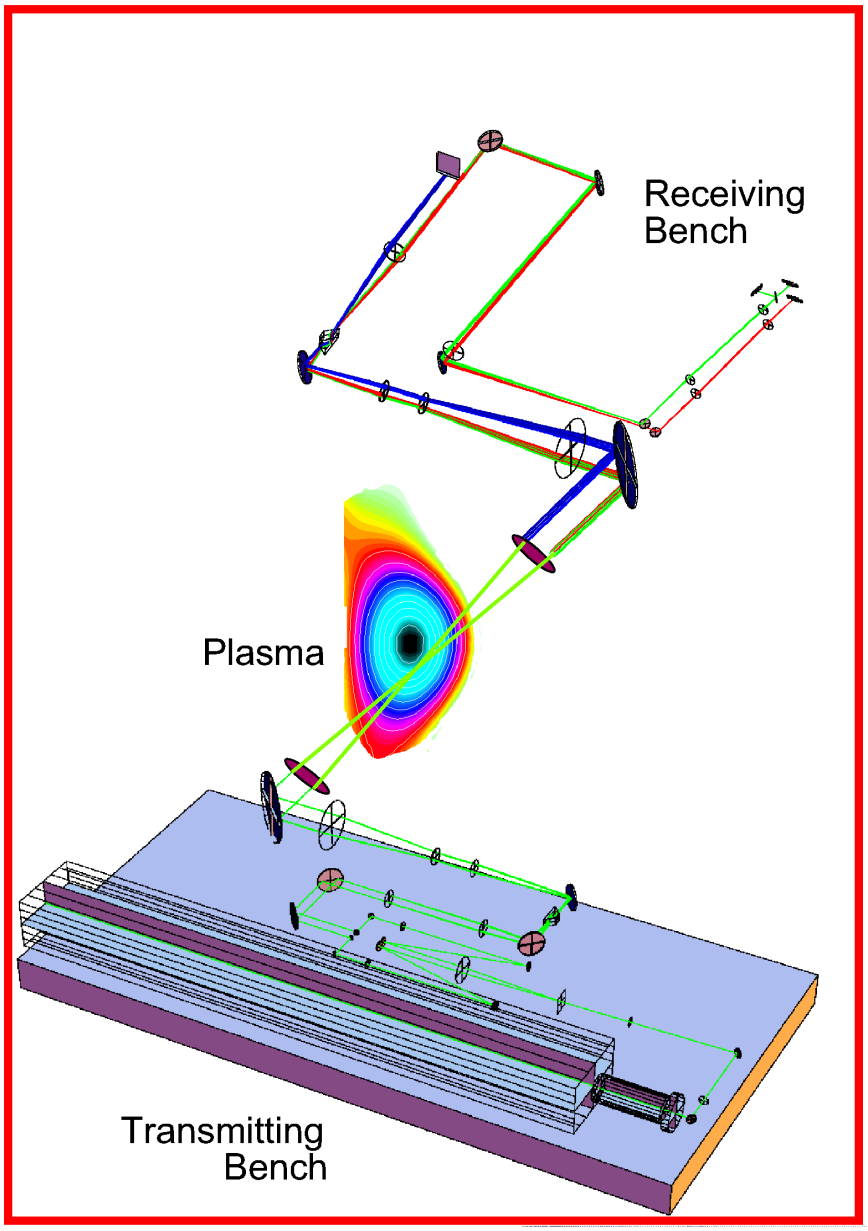

Figure 31. Layout of the collective scattering diagnostic installed at the W7-AS stellerator.

The electronics consists of a primary rack located next to the transmitting table, and a smaller rack located next to the receiving table. Data acquisition is via a dedicated dual-channel, digital quadrature demultiplexer designed and built by Risø's Engineering and Computer

Service. The quadrature demultiplexer is contained on a single PCI card located in a Pentium computer in the primary electronics rack. Digitised data are transferred directly to the computers main memory which has been expanded to 80 Mbytes to allow for up to 0.75 sec of two-channel 16 MHz bandwidth quadrature data. Power spectra and correlations are calculated off-line between plasma discharges. Data acquisition and mechanical adjustments are controlled remotely from a computer in the W7-AS control room. Connection to the computer in the torus hall takes place via an optical ethernet link.

Initial tests have concentrated on verifying mechanical stability and susceptibility to noise pickup from other electronic equipment in the torus hall. Mechanical stability has been investigated by intentionally modulating the local oscillator beams at 3 kHz and measuring the detected signal levels. Preliminary results indicate acceptable mechanical stability during a plasma discharge, as well as good long-term mechanical stability. The system maintained good mechanical alignment during the six-week summer shutdown of W7-AS from August to September.

Susceptibility to noise pickup has been more troublesome, due to several factors. The detected signals receive a high level of electronic gain to match them to the sensitivity of the quadrature demultiplexer, and there is about 25 m of cable between the detectors and the quadrature demultiplexer. Measurements have shown unacceptably high levels of parasitic pickup. This has necessitated improvements to the electromagnetic shielding used for the detectors and preamplifiers. Tests performed in December 1996 have shown that the improved electronics is now effectively isolated from parasitic interference. Commissioning of the system will continue in 1997.

1. Association Euratom - Risø National Laboratory Annual Progress Report 1995, Risø-R-897(EN).

4.2.2 Spatially Resolved Turbulence Measurements on an Air Jet

M. Saffman and W. Junker
E-mail: mark.saffman@risoe.dk

For direct verification of the spatial resolution of the scattering diagnostic installed at the W7-AS stellarator, experiments using a turbulent air jet as a source of fluctuations were performed at Risø. By placing the nozzle of the air jet several millimetres from the measuring volume and translating the jet parallel to the axis of the laser beams, the spatial response of the diagnostic was mapped out.

Figure 32 shows turbulence spectra recorded 5 mm downstream from the 1 mm diameter nozzle of an air jet. The three spectra were recorded at different axial locations *z*, for fixed turbulence intensity from the jet. The strong peak is due to local oscillator leakage at 40 MHz, and the turbulence spectra extend over a bandwidth of several MHz.

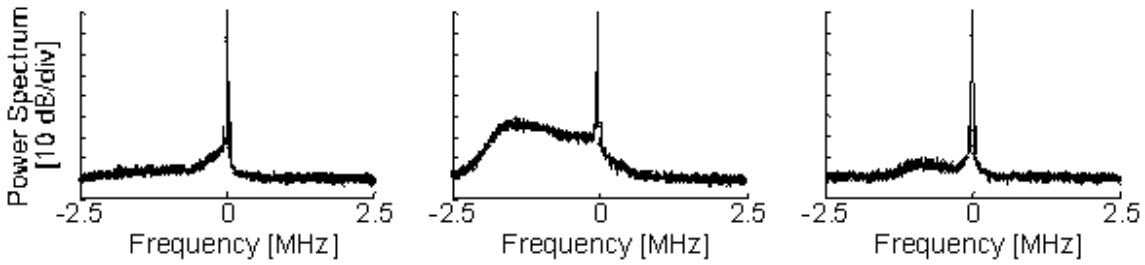

Figure 32. Turbulence spectra recorded at z = +9 cm (left), 0 (centre) and -9 cm (right).

The measured axial resolution may be compared with a simple theoretical estimate. Assuming that the peak level of the measured spectrum is proportional to the peak value of the optical intensity squared gives an axial response function proportional to $1/(1+(z/z_R)^2)^4$. The measurements were performed with a Gaussian laser beam radius in the measurement volume of $w = 0.64$ mm giving $z_R = pw^2/l = 12$ cm. Figure 33 shows the theoretical curve and the experimental points, normalised to a peak turbulence intensity of 1. There is rough agreement between the two figures. Ongoing work will compare more detailed measurements with a complete model of the spatial response characteristics of the scattering diagnostic. Nonetheless, simple estimates of spatial resolution based on Gaussian beam optics have been verified as being essentially correct.

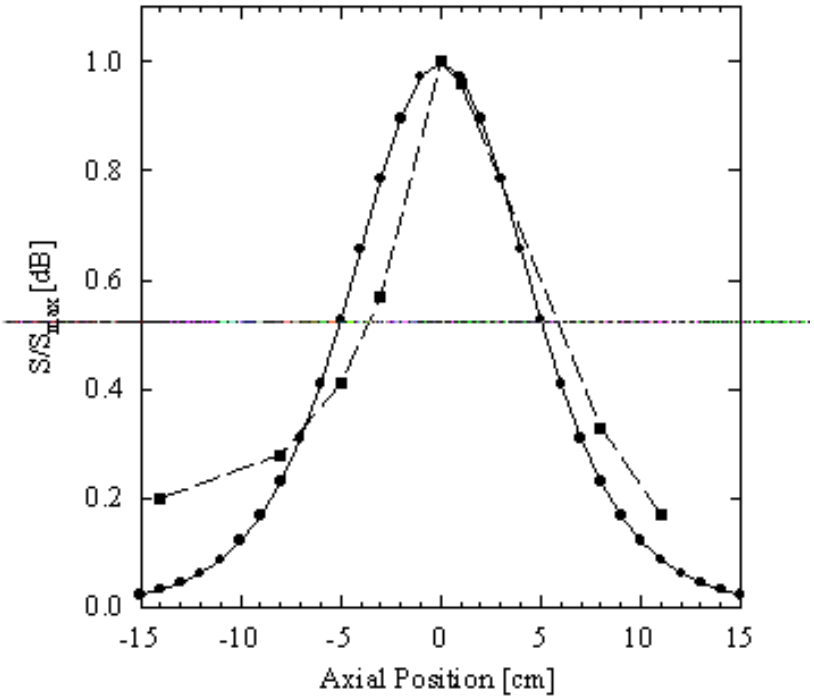

Figure 33. Comparison of theoretical instrument response (solid line) and measured instrument response (dashed line).

4.2.3 Localised Vortex Structures in Inviscid Plasma Flows

T. Jessen and P. K. Michelsen
E-mail: poul.michelsen@risoe.dk

A new highly efficient spectral computer code for two- and three-dimensional simulation has been developed. The main objective is to obtain a code for simulation of the response of a two-point collective scattering laser diagnostic to various types of plasma turbulence. As an initial test of the code the Euler equation was solved in a two-dimensional box using double periodic boundary conditions. Part of the verification procedure included the study of generation and breakdown of localised vortex structures. A variety of stable or long-lived structures has been observed. These include dipoles and also higher order poles, which have recently been observed in a number of experimental and numerical studies. Azimuthal perturbation of an initially radially shielded vortex is found to be a rich setting for generation of localised vortex structures. We perform the first systematic scan of parameter space, thereby outlining the basins of attraction of various vortex structures.

4.2.4 Resistive Coupling in Drift Wave Turbulence

P. K. Michelsen, T. Sunn Pedersen and J. Juul Rasmussen
E-mail: poul.michelsen@risoe.dk

Investigations of the two-dimensional Hasegawa and Wakatani model[1] for nonlinear plasma drift waves were continued with the main purpose of getting an improved understanding of drift wave turbulence and the related cross-field particle transport. In this model the drift waves are linearly unstable and after a period of exponential growth, a nonlinear quasi-stationary turbulent state is achieved. The model equations were solved numerically in a two-dimensional domain of size $L_x \times L_y$. A reformulation of the model equations clearly brings out the effects of the coupling between the density and the electrostatic potential, due to the parallel electron coupling. The coupling can be reduced to a coupling constant if it is assumed that only one mode k_z exists in the parallel direction. The value chosen for the coupling coefficient C reflects a specific choice of the values of the parallel resistivity and the parallel wave number. The plasma turbulence was investigated for various values of the coupling coefficient.

In Figure 34a spectra of the total energy for various values of the coupling coefficient for a domain size of $L_x = L_y = 50$ are shown. It is seen that a maximum is obtained around $k = 1.0$ for small values of C and that the maximum occurs at lower $k-$values for larger values of C. The energy spectrum for $C = 10$ and $L_x = L_y = 150$ shown in Figure 34b was calculated to see the effect of the domain size. The statistics give some fluctuation in this spectrum; however, it seems clear that there is still a maximum that appears around $k = 0.2$.

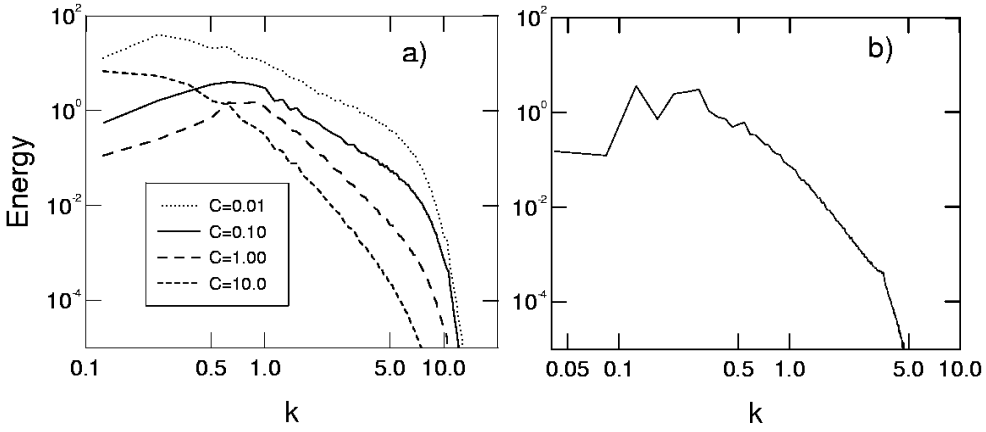

Figure 34: Spectra of total energy for various values of coupling coefficient and domain size. a) $L_x = L_y = 50$ and b) $L_x = L_y = 150$ and C = 10.

1. A. Hasegawa and M. Wakatani, *Phys. Rev. Letters* **50,** 682 (1983).

4.2.5 Contribution of Coherent Structures in Drift Wave Turbulence to Particle Transport

V. Naulin and K. H. Spatschek (Heinrich-Heine Universität, Düsseldorf, Germany)
E-mail: volker.naulin@risoe.dk

Anomalous transport in magnetically confined plasmas is still not a phenomenon that is well understood. Basic processes have to be studied in reduced simple models. As drift waves are often made responsible for transport in the scrape off layer (SOL), we here concentrate on the turbulent dynamics of drift waves and the coherent structures that emerge in the turbulent flow.

A one-field model for driven drift wave turbulence[1] that describes the universal and the drift dissipative instability is considered, and the equation is solved numerically.

The saturated turbulent state consists of random fluctuations and long-lived structures. The dynamics and properties of the latter coherent structures are of special interest. It is possible to identify coherent structures in the turbulent flow using the Weiss field.[2] Therefore, for the statistical evaluation of the motion of structures we search for all of them in each time step of the numerics and follow their movement over time. When monitoring structure displacements, however, we only consider events that last longer than an eddy turnover time. Using position vectors pointing to the structures, considering density humps/dips separately and, finally, weighting the contribution of each hump (or dip) by the corresponding trapped density, a mean position vector for maxima and minima, respectively, is defined.

The *x*- and *y*-coordinates of the structures that have thus been statistically averaged show that both maxima and minima move in the *y*-direction at the same (diamagnetic) velocity, whereas in the *x*-direction they move oppositely to each other (maxima down the density gradient;

minima up the density gradient). As a result the structures are not dipole-like and do indeed account for transport as they move the particles trapped within them in the direction of the density gradient.

We are led to the following scenario for the particle transport: One contribution is the fluctuation induced transport which is due to a (slight) phase shift between density and potential fluctuations. The second component of the transport is caused by the movement of coherent structures in x-direction.

Estimates show that the coherent transport might become of the same order as the fluctuation induced component. However, we were able to derive an approximate relation between both kinds of transport; an approximation that states that the coherent flux should be a fraction δ of the fluctuation induced flux, with δ being a measure of the non-adiabaticity of the electron density response.

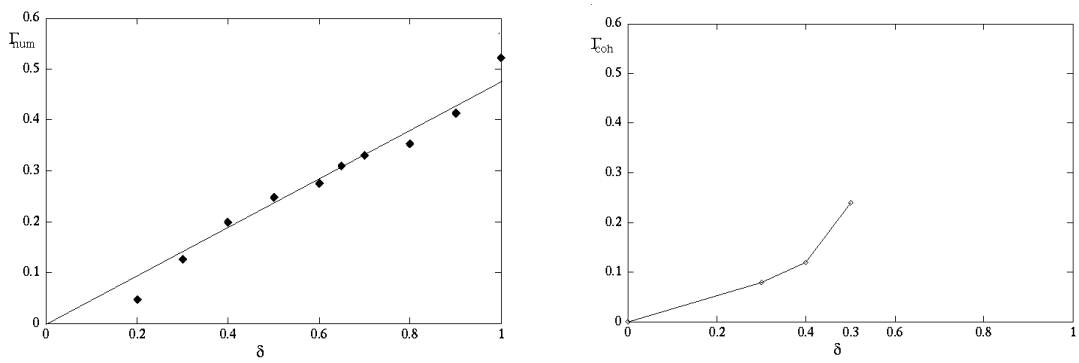

Figure 35. Fluctuation induced (left) and coherent (right) particle flux over deviation from adiabaticity δ. The fluctuation part shows $\sim\delta$ behaviour, while the coherent transport is $\sim\delta^2$.

The numerical results shown in Figure 35 support this finding, but we should bear in mind that here we present only a rough estimate of the coherent transport as a more detailed theory for the dynamics of coherent structures in turbulent flows is still missing.

1. Volker Naulin, *Nichtlinearer Transport in ebenen Drift-wellenmodellen*, PhD thesis, Heinrich-Heine Universität, Düsseldorf, 1995.
2. J. Weiss, *Physica D*, 48:273, 1991.

4.2.6 Extended Models of Flute- and Drift Modes in Plasmas Confined by Curved Magnetic Fields

K. Rypdal, O. E. Garcia (University of Tromsö, Norway), V. Naulin and J. Juul Rasmussen
E-mail: kristoffer.rypdal@risoe.dk

Experimental observations from various magnetically confined plasmas show plasma turbulence that consists of large coherent structures immersed in a background of turbulence, which may well be of drift wave

type. The flute structures are driven by the interchange instability, which is due to magnetic field curvature and a density gradient. The drift waves are driven unstable by density and/or temperature gradients in combination with a finite parallel resistivity. A model of the flute modes has been developed in [1], and a relevant model of the resistive drift waves is the well-known Hasegawa-Wakatani equations.[2] In the present work we develop a three-field model that contains both these models as special cases. In its most general form the model also allows for fluctuations in electron temperature in addition to plasma potential and electron density. By formulating this extended model the range of validity of the various reduced models can be investigated, and a proper reduction can more easily be found to describe a given experimental situation. A number of such reductions are under consideration.

1. K. Rypdal, H. Fredriksen, J. V. Paulsen and O. M. Olsen, *Physica Scripta* **T63**, 167-173 (1996).
2. A. Hasegawa and M. Wakatani,*Phys. Rev. Lett.* **50**, 682 (1983).

4.2.7 Detection of Coherent Plasma Structures: Verification of Experimental Methods by Application to Simulation Data

K. Rypdal, V. Naulin, P. K. Michelsen J. Juul Rasmussen, A. H. Nielsen and O. M. Olsen (University of Tromsö, Norway)
E-mail: kristoffer.rypdal@risoe.dk

Observations from Q-machines and plasmas confined in simple toroidal geometries reveal plasma turbulence consisting of large coherent structures immersed in a background of turbulence. Methods applied for detection of these structures include bispectral analysis of time series from a single probe,[1] and conditional averaging of time series data obtained from a fixed reference probe and a movable probe.[2] Improved understanding of the information obtained by these techniques can be gained by applying them to data where the full space-time information has been recorded. In plasma experiments such information would require a dense array of probes recording simultaneous time series, which is very difficult to achieve. However, in numerical simulations of models describing plasma turbulence such data can be recorded and it is possible to check for coherent structures using the Weiss field[3] and wavelet analysis.[4] In the present work the validity of existing detection methods will be put to a test by applying them to simulation data of drift wave turbulence as well as to simulation data of fluid turbulence. The latter will contribute to the understanding of the differences between these two types of turbulence.

1. K. Rypdal and F. Øynes,*Phys. Lett.* **A 184**, 114 (1993).
2. F. Øynes, H. L. Pécseli and K. Rypdal,*Phys. Rev. Lett.* **75**, 81 (1995).
3. J. Weiss,*Physica* **D 48**, 273 (1991).
4. Proceedings of the IEEE, Special Issue on Wavelets, April 1996.

4.2.8 Spiral Collapse and Turbulent Equilibrium of the Simple Magnetised Torus

K. Rypdal and O. E. Garcia (University of Tromsö, Norway)
E-mail: kristoffer.rypdal@risoe.dk

The notion of a simple magnetised torus covers the plasma configurations where a plasma is confined by an axisymmetric toroidal magnetic field, without any poloidal field component. Although this configuration is known not to possess an MHD-equilibrium, it has proved to be very suitable for experimental investigation of waves, coherent structures, turbulence and anomalous transport. In fact, the configuration serves as a paradigm for those naturally occurring and man-made situations where plasmas are confined by curved magnetic fields, and where no rotational transform exists to prevent interchange instability. Experimental investigations have revealed the quasiperiodic occurrence of a large flute-like dipole vortex rotating poloidally with the flow of the bulk plasma. This vortex is found to be very active in mediating transport.

In the present work numerical simulations of a 2D fluid model show that the emergence of such a dipole structure could be the early stage of a driven collapsing spiral vortex. Just as in other more familiar wave collapse phenomena, the early stage of the collapse reflects a physical reality, but the later stage is the result of imperfections of the model. In our case such an imperfection is the assumption of flute-like perturbations. This is probably not a valid assumption when very large density gradients develop. Inclusion of resistive dynamics parallel to the magnetic field would drive drift waves and ion acoustic waves unstable, and would thereby open a channel for dissipation of energy that could lead to burnout of the spiral vortex. Such a burnout would pave the way for a new vortex and, hence, a quasiperiodic occurrence of these structures.

The fluid equations are solved numerically in an entire poloidal cross-section and an example of the results is shown in Figure 36. The fluid equations are solved without many of the scaling assumptions and linearisations made in the standard models of drift waves and flute modes. Such models become invalid if the perturbations grow to a level where they strongly alter the background profile. In our model the free energy derives from explicit sources of plasma and electric charge, not from a fixed equilibrium profile. This corresponds closely to the experiments in question, which are steady state discharges produced by electron emission from a hot, negatively biased cathode.

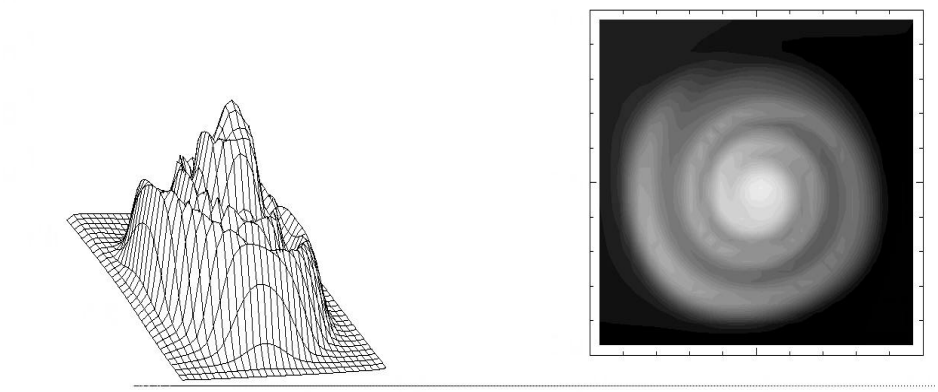

Figure 36. Simulation of fluid equations showing the electron density distribution (both as a three-dimensional and a contour plot) in a poloidal cross-section of a simple magnetised torus at a given time.

1. K. Rypdal, H. Fredriksen, J. V. Paulsen and O. M. Olsen, *Physica Scripta* **T63**, 167-173 (1996).

4.2.9 Two-dimensional Electron Magnetohydrodynamic Turbulence

N. Chakrabarti (Institute of Plasma Physics, Bhat, India),
P. K. Michelsen, J. Juul Rasmussen and K. Rypdal
E-mail: poul.michelsen@risoe.dk

Recently, special interest in electron magnetohydrodynamic turbulence has arisen to model collisionless reconnection that may be the origin of strong magnetic activity in nearly collisionless plasmas. Both two-dimensional high resolution and three-dimensional low resolution simulations have revealed that strong turbulence is excited by the current density gradients in the reconnection region, which gives rise to anomalous electron viscosity (see, e.g., [1]). In order further to study this turbulence together with vortex propagation and interaction, a model for the electron magnetohydrodynamics was investigated theoretically and numerically. The 2D model equations for the electron magnetohydrodynamics may be written in terms of two scalar quantities, the flux function y describing the magnetic field in the plasma $\mathbf{B} = \hat{\mathbf{z}} \times \nabla y$ and a stream function b describing the poloidal electron flow $\mathbf{v} = \hat{\mathbf{z}} \times \nabla b$, which is proportional to the poloidal current density. The ions are assumed to be infinitely heavy so only the high frequency electron dynamics is considered. The evolution of stationary dipole solutions to the model equations is investigated.

1. D. Biskamp, E. Schwarz and J. F. Drake, *Phys. Rev. Letters* **76,** 1264 (1996).

4.2.10 Shear Flow Effect on Ion Temperature Gradient Vortices in Plasmas with Sheared Magnetic Field

N. Chakrabarti (Institute of Plasma Physics, Bhat, India),
J. Juul Rasmussen and P. K. Michelsen
E-mail: jens.juul.rasmussen@risoe.dk

The effect of velocity shear on ion temperature gradient (ITG) driven vortices in a nonuniform plasma in a curved, sheared magnetic field is investigated. In absence of parallel ion dynamics the toroidal branch of the ITG mode vortices is studied analytically assuming a Gaussian equilibrium profile of the density. It has been shown that the coupled potential and pressure equations exhibit solutions in the form of tripolar vortex-like structures. These structures are special cases and arise at resonance (when the flow velocity matches the velocity of the propagating vortex). For the general case, however, we include parallel ion dynamics, and the equation describing the stationary ITG vortex has the structure of a nonlinear Poisson-like equation. For a simplified case, the analytic solution indicates the existence of a monopolar vortex structure away from the velocity shear layer. The most general solution is solved numerically. It is shown that, for a critical value of the velocity shear, asymmetric dipolar vortices can arise. At resonance these vortex structures are strongly modified and a localised vortex chain may be formed. For large velocity shear these structures are destroyed and ultimately lead to a shear driven structure with a dominating monopolar part. The effect of magnetic shear on velocity shear induced vortices is also studied. Qualitative results indicate that magnetic shear destroys these structures in the sense that no localised stationary solutions seem to exist when the magnetic shear strength exceeds a (low) threshold value.

Preliminary investigations of the dynamic evolution and stability of the velocity shear vortex structure by numerically solving the evolution equations indicate that they are unstable, at least for the strong shear cases.

4.2.11 Relations to Authorities, the Press and the Public

V. O. Jensen
E-mail: vagn.o.jensen@risoe.dk

In the Ministry of Research and Information Technology a standing reference group on fusion has been formed whose main responsibility is to advise Danish representatives in various high ranking committees dealing with the European fusion programme. As representative for the Fusion Research Unit and being specialised in fusion research the author has the responsibility for explaining the physical and technical content of the fusion research programme in the reference group.

A number of journalists from technical journals and newspapers have written about fusion energy research. Many of them have asked for and have received advice in the Fusion Research Unit. As a result their articles have had a high technical standard.

The exhibition “FUSION EXPO: Harnessing the energy of the sun” was shown at the Elmuseum in Bjerringbro, Jutland, from mid-August to the end of September 1996. As *local organiser* the Fusion Research Unit was responsible for reediting and translating into Danish the brochures that describe the exhibition, the panel texts and the multimedia texts. Some effort was spent in educating the staff at the museum about fusion research in order to make them well equipped to introduce the exhibition to the visitors.

4.3 Fluid Dynamics

4.3.1 Shear Flow Instability in a Parabolic Vessel

J. A. van de Konijnenberg, T. Stoltze Laursen, A. H. Nielsen, R. de Nijs, J. Juul Rasmussen and B. Stenum
E-mail: bjarne.stenum@risoe.dk

The instability of forced, circular shear layers in a shallow layer of water in a parabolic vessel has been studied experimentally. The shape of the bottom of the vessel corresponds to the shape of the free surface layer of water rotating at 71.9 rpm; the inner diameter of the tank is 560 mm at the top. In the shallow layer of water, a shear layer can be produced by differential rotation of the central part of the vessel. Above a critical value of this inner rotation, the shear layer becomes unstable and evolves into a number of equally signed vortices. The mode number of the vortex chain has been studied as a function of the inner rotation rate at different depths and background rotations. In all cases, the number of vortices was seen to decrease with increasing shear, ranging from 14 slightly above the threshold of instability to two at a high inner rotation. The critical value of the Reynolds number for the onset of the instability was found to be almost independent of the rotation rate and the depth of the fluid layer. At a rotation rate of 71.9 rpm the variation of the Coriolis parameter with the radial position in the vessel - the beta effect - is cancelled by the radial variation in depth, and the mode number is symmetric with respect to the direction of the inner rotation. At a background rotation faster than 71.9 rpm, asymmetry appears: the mode number is found to be higher at an inner rotation opposite to the background rotation, and lower at an inner rotation in the same direction as the background. At a background rotation slower than 71.9 rpm this picture is reversed.

The experimental results have been compared with results of numerical simulations, see Figure 37. In the simulations the combined effect of the variations of the Coriolis force and the depths has been modelled by an effective beta effect. The results of the simulations are found to be in good qualitative agreement with the results of the experimental studies. See also section4.3.9.

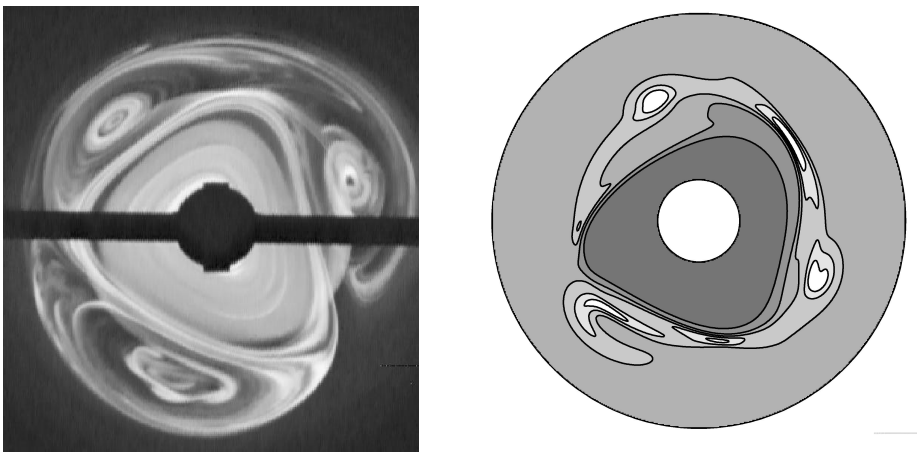

Figure 37. Oscillating pattern of three anticyclonic vortices in a rotating fluid according to dye visualisation (left) and numerical simulation (right).

4.3.2 Evolution of Forced Monopoles in Rotating Shallow Water

T. Stoltze Laursen, J. Juul Rasmussen, B. Stenum and E. N. Snezhkin
(Kurchatov Institute, Moscow, Russia)
E-mail: bjarne.stenum@risoe.dk

The generation and evolution of monopolar vortices in shallow water in the rotating parabolic tank (see section 4.3.1) have been studied. The bottom of the tank is shaped as the free surface of water rotating at 71.9 rpm (= 7.53 rad/s, the nominal rotation rate). The vortices were produced by a pumped in- or outwards flow of a tube rotating relative to the tank itself. The vortices were followed resonantly by the tube maintaining the pumping. The outlet of the tube was situated at a distance of 20 cm from the axis of rotation; normally, 2 mm above the surface of the tank. An outwards flow produces a small elevation around the tube and, thereby, an anticyclonic vortex due to the Coriolis force contrary to an inwards flow that produces a depression and a cyclonic vortex. By means of the depth measurements, the perturbations of the layer thickness were found to increase less than proportional to the flow rate. Using the shallow water approximation, the internal velocities of the vortices could be determined from the thickness perturbations. The maximum internal rotation rate of the anticyclones seems to be almost constant, about 4 cm/s, for flow rates larger than 0.3 l/min. The dependence of the vortices' drift velocities on the flow rate has been studied at different background rotations. The drift velocities were measured as the angular rotation rate of the tube. The background rotation is given as the shift from the nominal rotation rate (see Figure 38). The drift velocities of the anticyclones depend almost linearly on the flow rate and were found to be larger than the Rossby velocity for high flow rates. The Rossby velocity is a typical drift velocity of nonlinear vortical structures. In a paraboloid the angular Rossby velocity is equal to the shift from the nominal rotation rate.[1] The drift velocities of the anticyclones were found to increase with increasing thickness of the water layer at the nozzle position but only

weakly influenced by the width of the nozzle opening and the position of the nozzle above the bottom of the tank. Although there appear to be regimes where the cyclones have slightly higher velocities than the Rossby velocity for the case characterised by positive Rossby velocities, the anticyclones were found to be more robust than the cyclones. This finding seems to be a general feature.

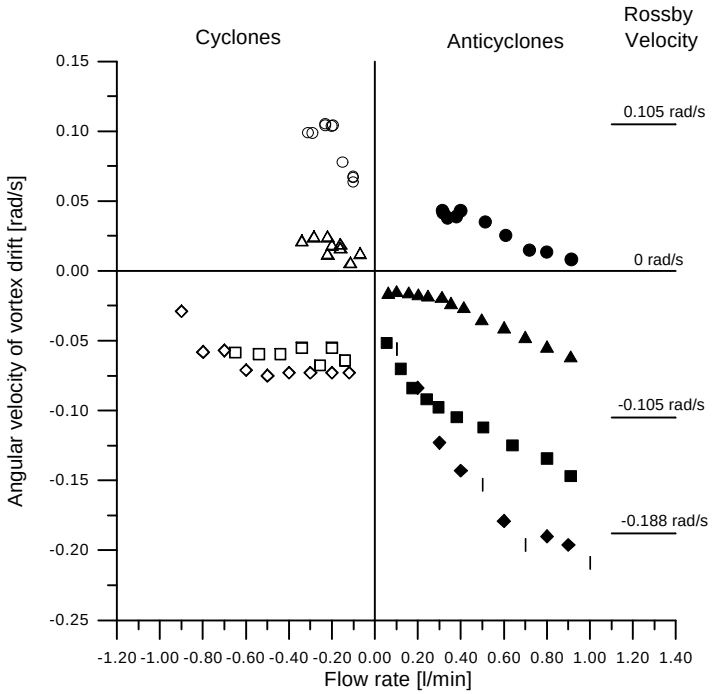

Figure 38. Drift velocities of forced vortices versus flow rate at different background rotation rates. The circles, triangles, squares and diamonds indicate rotation shifts of 0.105, 0, -0105 and 0.188 rad/s, respectively. The drift velocities are measured relative to the rotating tank. The positive drift is in the direction of the background rotation. The positive direction of the flow rate is outwards the tube.

1. M. V. Nezlin and E. N. Snezhkin, *Rossby Vortices, Spiral Structures, Solitons* (Springer, Berlin, Heidelberg, New York) (1993).

4.3.3 Evolution of a Vortex Ring in a Viscoelastic Fluid

L. Lindvold, J. Juul Rasmussen and B. Stenum
E-mail: bjarne.stenum@risoe.dk

The temporal evolution of a flow field produced by a vortex ring ejected horizontally into a viscoelastic fluid has been studied using a dye marker technique. The inlets of water puffs are controlled by a linear motor that ensures well defined inlets. The water puffs were injected through a circular tube with an inner diameter of 1.5 cm into a water tank with a length of 30 cm, a width of 10 cm and a depth of 25 cm. The viscoelastic fluid is an aqueous solution of two salts, viz. cetyltrimethylammonium bromide (CTAB) and sodium salicylate (Na-sal) in a 1:1 molar ratio. At room temperature such a solution will form rod-shaped micelle aggregates in periodic structures at concentrations between 0.05 and 0.1 mol/l. This fluid is viscoelastic at high

shear rates, whereas it behaves as a Newtonian fluid at low shear rates. The formation of a propagating vortex ring in the viscoelastic fluid was found to be almost similar to that in a homogeneous Newtonian fluid. However, in the viscoelastic fluid the propagation speed of the vortex ring is slowed down due to the viscoelastic forces. Later the vortex ring stops and the structure starts to move backwards keeping a coherent form (see Figure 39) with internal rotation directed opposite to the injected vortex ring. The backwards directed propagation as well as the internal rotation speed is significantly smaller than the initial velocities. The backwards motion seems to stop close to the inlet tube for formation of the vortex rings. Apart from its peculiar flow properties, the viscoelastic solution also exhibits shear induced birefringence. This property could possibly be used as a means of flow visualisation.

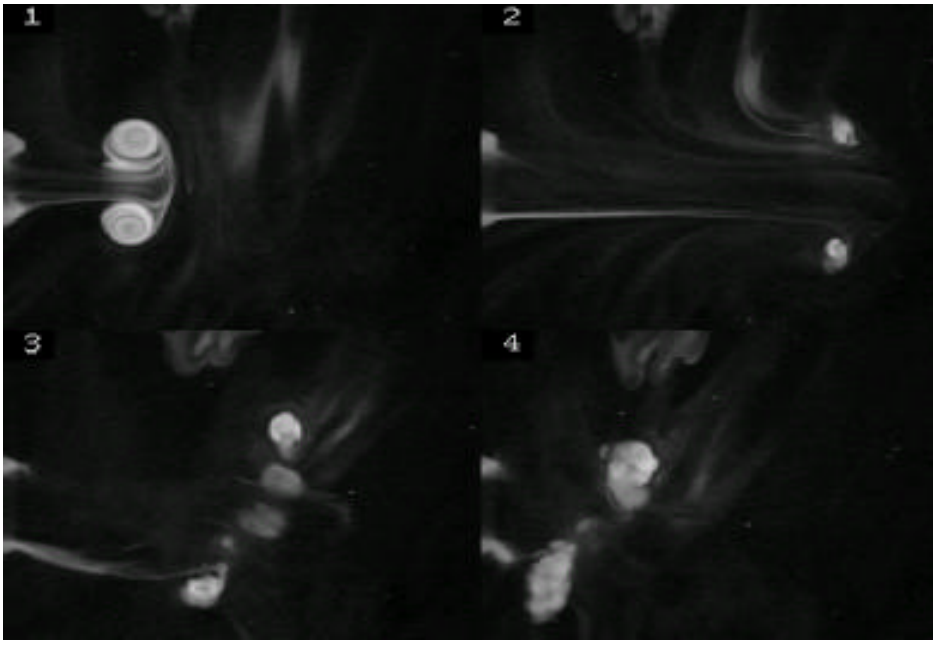

Figure 39. Time evolution of a vortex ring ejected into a viscoelastic fluid. Frame 1: 1 s after injection; frame 2: 8 s after injection; frame 3: 40 s after injection; frame 4: 70 s after injection.

4.3.4 Evolution of a Vortex Ring in a Stratified Fluid

T. Stoltze Laursen, J. Juul Rasmussen, B. Sass, B. Stenum and D. R. McCluskey (Dantec Measurement Technology A/S)
E-mail: bjarne.stenum@risoe.dk

The collaboration between Dantec Measurement Technology A/S and Risø National Laboratory has been continued by studying the dynamics of vortex rings. The collapse of a three-dimensional vortex ring injected horizontally into a stratified fluid has been investigated to reveal the detailed collapse mechanism. A new vortex ring generator has been constructed. The inlets of water puffs are now controlled by a linear motor that ensures well defined inlets. The water puffs were injected through a circular tube with an inner diameter of 1.5 cm into a water tank

with a length of 30 cm, a width of 10 cm and a depth of 25 cm. The stratified fluid was produced by the two-tank method. The temporal evolution of the vortex ring ejected horizontally into the stratified fluid can be divided into three stages (see Figure 40). After its formation the propagation speed of the vortex ring is initially slowed down by generation of baroclinic vorticity and, thereby, generation of secondary vortical structures. Later, when the vortical structure has broadened and the propagation speed has been slowed down sufficiently, the vortex ring couples to internal waves and the propagation speed is additionally reduced. At this stage, energy is radiated away via internal waves. Finally, the structure collapses into a two-dimensional dipolar structure, which is translating much slower than the original vortex ring.

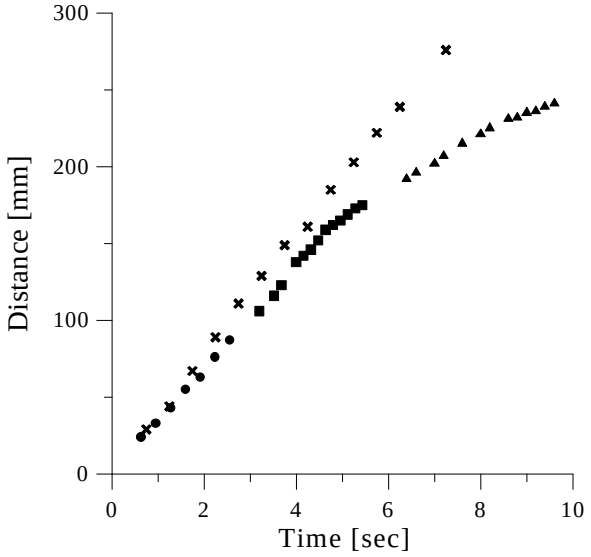

Figure 40. The propagation distance for identical vortex rings injected into stratified (closed circles, squares and triangles) and homogeneous fluid (crosses) versus time. The circles, squares and triangles indicate different runs and measuring areas.

A small transportable vortex ring generator has been built for demonstration of the Flowmap system developed at Dantec Measurement Technology.[1] In this case the piston is lifted by an electronic magnet and the inlet is driven by gravity ensuring a simple and robust system.

1. D. R. McCluskey, T. S. Laursen, J. J. Rasmussen and B. Stenum, "Evolution of vortical flow fields measured by real-time PIV system", ASME Fluid Engineering Summer Meeting 1995.

4.3.5 Formation of Vertical Geological Structures by Vortex Ring Structures

B. Stenum and J. P. Jensen (Højgård og Schultz a/s)
E-mail: bjarne.stenum@risoe.dk

Vertical cylindrical structures (VCSs) with coaxially organised sediment layers have been observed in the Køge Esker.[1] In size the VCSs normally vary from a few centimetres to a few metres in diameter and from about 1

to 6 m in height. Inside the VCSs the largest and most dense particles are concentrated around the axis. The particle size is decreasing outwards and the VCSs are enclosed by a layer of very fine sediments. The origin of the VSCs is not known. It is suggested that the VCSs are formed by pressure driven injection of water/sediment puffs from below. The puffs organise in vortex ring structures. The upwards drifting vortex ring carries the fine sediments upwards and towards the outer periphery of the vortex ring structure whereas the large sediments are left behind the ring structure. Applying Stokes law to the upwards directed flow, an estimate of the order of magnitude of the flow velocities can be obtained.

1. J. P. Jensen and J. Miller, "Vertical cylindrical structures in Danish quaternary (Weichselian) glaciofluvial deposits: their description and genesis",*Bull. Geol. Soc.* **38**, 59-67 (1990).

4.3.6 Numerical Studies of Two Oppositely Signed Shielded Monopolar Vortices

A. H. Nielsen, J. Juul Rasmussen, M. R. Schmidt, M. Becker and G. J. F. van Heijst* (*University of Technology, Eindhoven, The Netherlands)*
E-mail: michel.schmidt@risoe.dk

We have performed a number of numerical studies of shielded monopolar vortices in two-dimensional fluids governed by the incompressible Navier-Stokes equations. Two oppositely signed shielded vortices, initially closely located, will interact. The typical evolution is the roll-up of the shielding, which is effectively removed from the intermediate range. The two cores of rotation will then contract and form a relatively compact dipolar structure. The dipolar structure will self-propel, i.e. translate, through a homogeneous medium. The details of the final dipolar structure depend on the initial conditions: the initial profile of the vorticity distribution and the separation distance compared with the widths of the two structures. For small initial separation distances, the dipolar structure will obtain a linear relation between the stream function and the vorticity, i.e. it resembles the classical Lamb dipole. For larger initial separation distances, the dipolar structure becomes less compact and obtains a nonlinear relation. It seems as if the shielding is actually very important to the formation of the final dipolar structure. Thus, no unique profile of the dipolar structure exists.

We have compared our numerical parameter study with experimental data from the university in Eindhoven. Experimental data have been read by a Navier-Stokes solver and have been integrated on a time scale in which the real flow has been followed. The experiments are performed in a two-layer tank: the lower layer consists of salted water, whereas the upper layer consists of fresh water. In principle, the monopoles are generated at the interface of the two layers by injection of fluid in two metal cylinders, which are subsequently removed. The equations include an Ekman type of damping to model the friction with upper and lower layers.

$$\frac{\partial \omega}{\partial t} + J\{\omega, \psi\} = \upsilon \nabla^2 \omega - \lambda \omega \ , \qquad \text{where } J\{\omega, \psi\} \equiv \frac{\partial \omega}{\partial x}\frac{\partial \psi}{\partial y} - \frac{\partial \omega}{\partial y}\frac{\partial \psi}{\partial x}$$

$$\omega = -\nabla^2 \psi$$

ω is the vorticity, ψ is the stream function, ν is the kinematic viscosity and λ is the effective Ekman coefficient determined by the experiment. Then it becomes possible to compare the 2D numerical approximation directly with the laboratory results. An example of the numerical results is shown in Figure 41. The agreement between the numerical and the experimental results concerning the gross dynamics is excellent, even though no term in the numerical integration accounts for the vertical diffusion of vorticity, which is the most important loss mechanism in the experiment. Scatter plots and graphs with decay of peak values obtained in the experiments and in the numerical simulations show close resemblance.

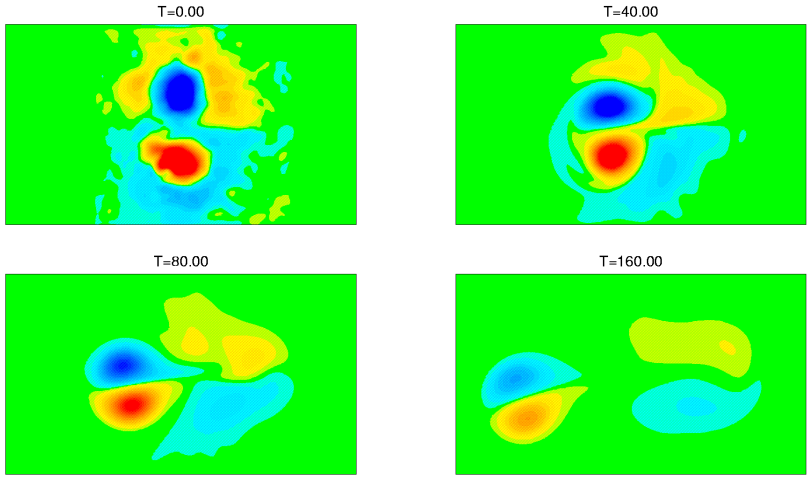

Figure 41. Contour plots of vorticity for different times. The initial data are the measured values obtained from experiments in a stratified fluid after removal of the metal cylinders. The shielding is shed off and the two cores form a dipolar structure, which propels itself forward until viscosity and vertical diffusion have damped the structure.

4.3.7 Vortex Merging and Corresponding Energy Cascade in Two-dimensional Turbulence

A. H. Nielsen, J. Juul Rasmussen and M. R. Schmidt
E-mail: anders.h.nielsen@risoe.dk

For two-dimensional turbulence it is well established that the energy is cascading towards larger scales resulting in the build-up of large-scale structures. This inverse cascade is believed to be mediated by merging of like-signed vortices. The enstrophy (mean squared vorticity), on the other hand, cascades directly towards smaller scales. To provide detailed understanding of this cascading process we have investigated the simple case of the merging of two equally signed monopoles with Gaussian

distributed vorticity by numerically solving the Euler equations by a high resolution double-periodic spectral code.

The temporal evolution of the vorticity together with the Weiss field, $s = ¼(\sigma^2-\omega^2)$, is shown in Figure 42. During the merging process the spiral filaments in the vorticity are created, which are stretched infinitely in the straining field resulting from closer interaction of the monopoles. From the Weiss field we see that the cores of the monopoles are rotation-dominated, $s < 0$, whereas just outside the monopoles a strong straining field is present, $s > 0$. Our simulations also identify that the enstrophy cascade is most active on the disordered vortex boundaries and to a certain degree also in the filaments, with a localised energy spectrum, $E(k) \approx k^{-4}$, developed at high wave numbers. A similar spectrum will be obtained if, instead of only two like-signed monopoles, we were initialising a large number of monopoles with different sizes and polarities.

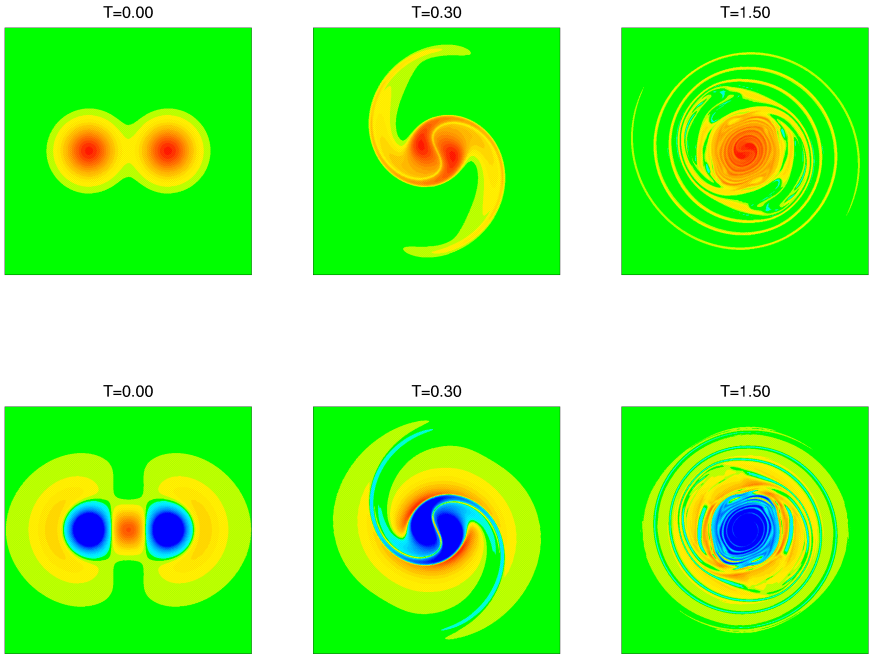

Figure 42. Computer simulation of the merging of two identical monopoles with Gaussian distributed vorticity. The first row displays the temporal evolution of the vorticity while the second row displays the corresponding Weiss field, $s = ¼(\sigma^2-\omega^2)$. Full lines are for positive values; dashed lines are for negative values. A resolution of 1024 x 1024 and a sixth-order hyper viscosity with $\mu = 10^{-18}$ were used.

4.3.8 Particle Tracking in a Two-dimensional Flow Field

A. H. Nielsen
E-mail: anders.h.nielsen@risoe.dk

Particle tracking in fluid dynamics is an important tool for determining the transport properties of a flow field. Generally, we solve the Navier-Stokes equation in the Eulerian framework where the flow field is known at all times in a (fixed) spatial grid. The fluid inside a small fluid element located at a grid point will consist of different fluid particles at different times.

The information about how these particles are transported or convected by the flow field is not directly present in this framework.

We have solved the two-dimensional Navier-Stokes equation numerically using spectral methods. The domain could either be double-periodic or an annulus with one bounded direction and one periodic. For the periodic directions we use Fourier modes as expanding functions, whereas for the bounded direction we use Chebyshev polynomials. To follow the trajectories of the particles we evaluate the full spectral expansion of the velocity field. Thereby we use all the information stored in the flow field. Such evaluations are quite expensive in terms of computer time, and 200-300 particles take as much CPU time as solving the Navier-Stokes equation itself. We have therefore implemented the computer code on an SP2 parallel supercomputer located at UNI*C, Lyngby, Denmark.

An example of our particle simulation is shown in Figure 43. Here the interaction between a Lamb dipole and a no-slip wall is shown both in terms of vorticity and for 3,000 particles initialised inside the dipole. During interaction, strong boundary layers that split the dipole into two are created, and at the end of the simulation these two monopoles are shielded from each other and the wall by a strong vortex sheet originating from the boundary layers. For the evolution of the particles we observe that they are all convected towards the wall by the Lamb dipole and that even during the strong interaction with the wall most of them stay trapped inside the vortex structures - i.e. the mixing is in this case quite weak.

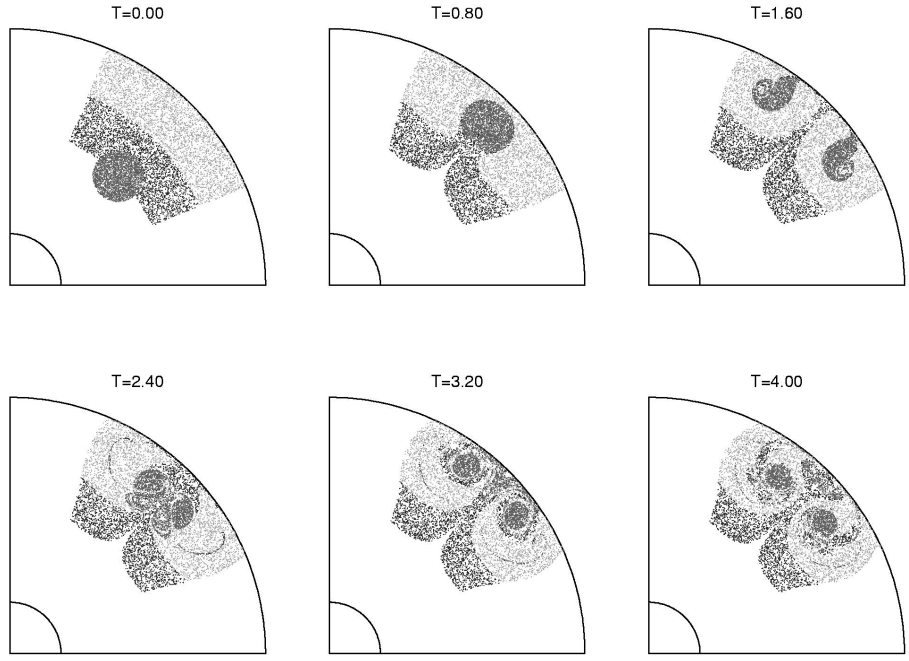

Figure 43. Particle simulation for the case of a Lamb dipole interaction with a no-slip wall. In the figure 3 x 3,000 particles have been distributed in three different regions, where the darkest points are particles all initialised inside the dipole.

4.3.9 Spin-up and Spin-down Transitions in Circular Shear Layers

K. Bergeron (USAF Academy, Colorado, USA), E. A. Coutsias (University of New Mexico, Albuquerque, USA), J. P. Lynov and A. H. Nielsen
E-mail: jens-peter.lynov@risoe.dk

The dynamic properties of circular shear layers have been the subject of detailed studies at Risø National Laboratory over several years. The background for this interest is that circular shear layers are well suited for controlled experiments and numerical simulations of fundamental dynamic properties related to self-organisation, pattern formation and symmetry braking transitions in fluid dynamics. These properties have strong impact on the flow and transport properties of many different systems of physical and technical significance, ranging from geophysics over aerodynamics to fusion plasma physics.

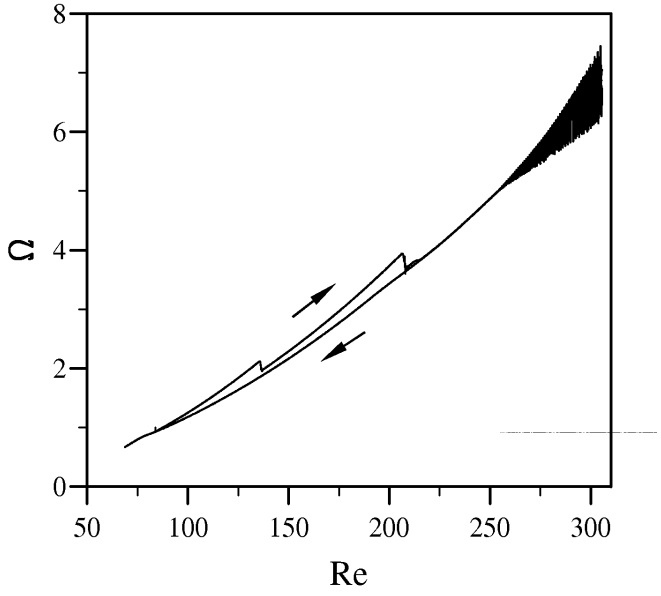

Figure 44. Evolution of the total enstrophy, Ω, in a circular shear as a function of the Reynolds number, Re, during a complete spin-up and spin-down cycle. The jumps in Ω during spin-up at near Re = 145 and Re = 210 correspond to mode transitions from n = 7 to 5 and n = 5 to 4, respectively. Above Re = 270 a temporal state with both mode 4 and mode 2 is created. During spin-down the system remains in the n = 4 mode with gradually diminishing amplitude until an axisymmetric (n = 0) state is reached at Re ≈ 70.

A characteristic feature of a circular shear layer is its capability of forming a stable, circular array of coherent vortices. The number of vortices in the array depends on the geometry of the shear layer (mainly through the aspect ratio) and on the Reynolds number related to the shear forcing. By changing the Reynolds number, the system can undergo symmetry breaking transitions in which the number of vortices in the array changes. In this work, the details of these transitions during both spin-up and spin-down have been investigated numerically. An example of the evolution of the total enstrophy in the system is shown in Figure 44. Our

results reproduce the strong hysteresis effect observed in fluid experiments. The effects of the rate of change of the Reynolds number of the external noise have been investigated in detail. These effects have strong impact on the Reynolds number at which a transition occurs. However, it was found that both the instantaneous energy and the enstrophy of the total system are well defined functions of the Reynolds number once the symmetry of the flow is given. See also section 4.3.1.

4.3.10 Nonlinear Boundary Dynamics in Two-dimensional Flows

S. Lomholt and J. P. Lynov
E-mail: jens-peter.lynov@risoe.dk

The nonlinear dynamic evolution of the two-dimensional Couette and Poiseuille flows in periodic channels has been investigated by direct numerical simulation using a highly accurate spectral scheme.[1] In the two-dimensional Couette flow, an asymptotic turbulent state was not found, even though very large initial disturbances were applied. After a period of vigorous boundary layer detachments, the inverse cascade process, characteristic of two-dimensional flows, becomes dominant leading to the formation of isolated, coherent vortices. These vortices are located midway between the walls of the channel and have the same rotation as the background flow. The vortices interact only very weakly with the boundary layers, and on a viscous time scale they decay, leaving the flow fully laminar.

For the Poiseuille flow, two different boundary conditions corresponding to a constant pressure drop and a constant flow rate have been investigated. For subcritical flows (Re = 4,000) in short channels a stationary state can appear. This state can be created for both types of boundary conditions and is characterised by an array of vortices of alternating signs located near the channel walls. The stationary state only appears at specific periodicity lengths of the channel. Away from these ‘resonant’ lengths, a decay to a laminar flow is observed. For long channels satisfying the ‘resonance condition’, the array of vortices is no longer stationary but is subject to modulational instability. For the subcritical flows, the difference in the results for the two different boundary conditions could be explained by different scalings of the flow which give rise to different definitions of the Reynolds number.

For supercritical Poiseuille flows (Re = 10,000), quasi-stationary states are developed that are not fully rescalable between the pressure driven and the flow rate driven cases. An example is shown in Figure 45. In all the cases considered, it was found that the results from pure two-dimensional simulations were quite different from experimental results obtained in quasi two-dimensional systems where the dynamics in the third dimension have not been completely suppressed.

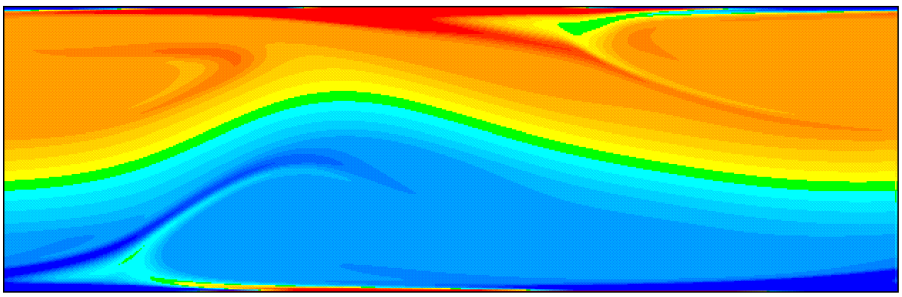

Figure 45. Snapshot of the quasi-stationary vorticity field in a Poiseuille flow driven by a constant flow rate in a periodic channel of length 2π and with Re = 10,000, where Re is defined by the flow rate and the channel half-width.

1. E. A. Coutsias, J. S. Hesthaven and J. P. Lynov, “An accurate and efficient spectral tau method for the incompressible Navier-Stokes equations in a planar channel”, in “Proceedings of the Third International Conference on Spectral and Higher Order Methods” (Houston Journal of Mathematics), 39-54 (1996).

4.4 Nonlinear Optics

4.4.1 Optical Pattern Formation in the Field of Noncollinear Pump Beams

M. Saffman, A. V. Mamaev (Institute for Problems in Mechanics, Moscow, Russia)
E-mail: mark.saffman@risoe.dk

There are several reasons for the high level of current interest in pattern formation in optical systems. Nonlinear optics has proved to be an attractive medium for studying symmetry breaking and dynamics in nonequilibrium systems. Results obtained in optics parallel corresponding observations from fluid and other systems, as in the case of formation of hexagons, but also reveal exotic spatiotemporal structures not seen elsewhere. There are also intriguing prospects of applications of pattern formation to information processing[1].

A generic mechanism leading to optical pattern formation is transverse modulational instability of pump beams counterpropagating in a medium with cubic nonlinearity. For collinear pumps there is cylindrical symmetry about the *z*-axis (propagation), and hexagonal patterns are typically observed. It is known that misalignment of the pump beams breaks the phase matching condition in the plane containing the pumps, and leads to collapse of the hexagonal pattern into a one-dimensional roll pattern in the plane perpendicular to the plane of the pump beams.

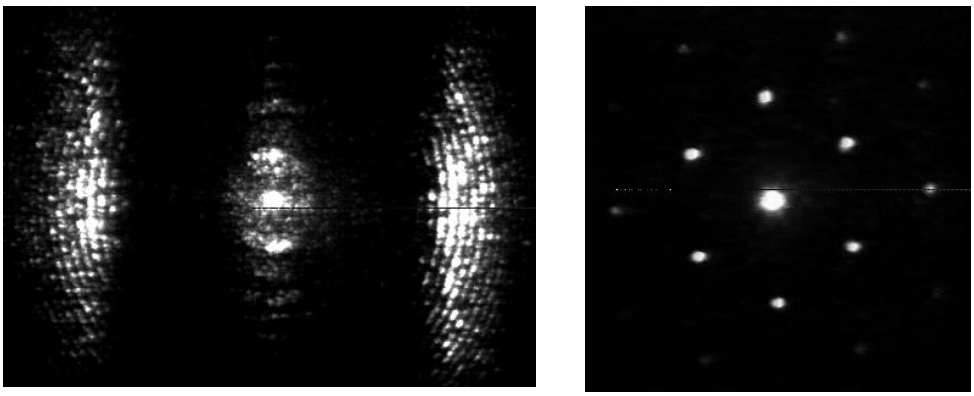

Figure 46. Lines observed for intermediate misalignment (left), and squeezed hexagons observed for large misalignment (right). The pump beams are misaligned along the horizontal axis.

We show here[2] that introducing pump misalignment, while allowing instability in both transverse dimensions, leads to the generation of previously unobserved patterns. For intermediate values of the misalignment we observe lines perpendicular to the misalignment plane. Simple theoretical arguments show that the angular separation of the lines is inversely proportional to the degree of misalignment, and quantitative measurements are found to be in good agreement with the theory. Modulational instability of the lines leads to a two-dimensional transverse pattern with rhombic symmetry. For small misalignment we observe both rolls and squeezed hexagons, and for relatively large misalignment, where the angle at which the lines are generated is comparable with the normal angle for hexagon generation, we observe squeezed hexagons. Examples of the observations for intermediate and for large misalignment are given in Figure 46.

This work was supported by the Danish Natural Science Research Council.

1. M. A. Vorontsov and W. B. Miller, Eds., *Self-organization in Optical Systems and Applications in Information Technology,* (Springer-Verlag, Berlin, 1995).

2. A. V. Mamaev and M. Saffman, "Modulational instability and pattern formation in the field of noncollinear pump beams", *Opt. Lett.* to appear in 1997.

4.4.2 Transfer of Temporal Fluctuations by Beam Coupling in Photorefractive Media

S. Juul Jensen and M. Saffman
E-mail: mark.saffman@risoe.dk

The temporal dynamics of two-beam coupling in photorefractive media have been the subject of numerous studies. Since no general analytical solution is available, either numerical solutions or approximate analysis must be used. In the undepleted pump limit a transfer function describes the temporal behaviour of the signal beam, while for arbitrary pump to

signal ratios a transfer matrix describing the coupling of fluctuations between the pump and signal beams must be used. An analytical study of the stability of several photorefractive resonator circuits based on the transfer matrix formalism was previously found to be consistent with experimental observations. Nonetheless, a direct experimental measurement of the transfer matrix elements has been lacking. We have now shown[1] that direct measurements of the four matrix elements are in close agreement with the analytical expressions.

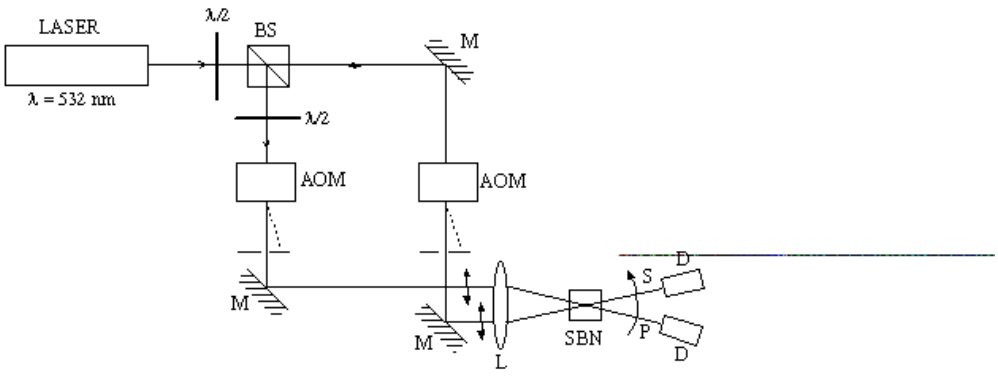

Figure 47. Experimental set-up.

The matrix elements were measured using the two-beam coupling set-up sketched in Figure 47. Two linearly polarised beams from a 532 nm laser were coupled in a strontium-barium niobate (SBN) crystal with a 100 mm focusing lens. Each beam was passed through an acousto-optic modulator that diffracted a small part of the beam at a selected frequency. Thus, the transmitted beams consisted of DC and AC components. After coupling in the crystal the beams were detected by two photodiodes followed by a spectrum analyzer. Figure 48 shows measured and calculated values for the transfer of perturbations from pump to signal beams, for three values of the input beam ratio, as a function of $\Omega\tau$ (perturbation frequency times material time constant).

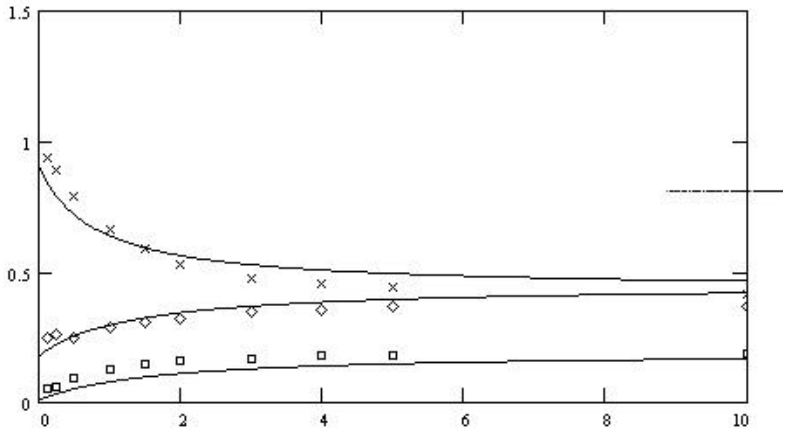

Figure 48**.** Measured values of the perturbation matrix elements compared with the corresponding theoretical expressions.

This work was supported by a grant from the Danish Natural Science Research Council.

1. S. J. Jensen and M. Saffman, “Transfer of temporal perturbations in photorefractive two-beam coupling”, submitted (1996).

4.4.3 Self-focusing and Formation of Elliptical Solitons in Anisotropic, Nonlocal Nonlinear Media

A. V. Mamaev (Institute for Problems in Mechanics, Moscow, Russia), A. A. Zozulya, D. Z. Anderson* (*JILA, University of Colorado, USA) and M. Saffman*
E-mail: mark.saffman@risoe.dk

In typical nonlinear optical media the material responds to the presence of the optical field $B(\mathbf{r})$ by a nonlinear change in its refractive index dn that is an algebraic (local) function of the light intensity. In its simplest case $dn \approx |B(\mathbf{r})|^2$ this local response results in the canonical nonlinear Schrödinger equation for the amplitude of light propagating in the medium. Higher-order nonlinearities result in various forms of local saturable response. In photorefractive media the change in the refractive index is proportional to the amplitude of the static electric field induced by the optical beam. Finding the material response therefore requires solving globally an elliptic-type equation for an anisotropic electrostatic potential with a source term due to light-induced generation of mobile carriers that has no direct analogs in nonlinear optics. The closest structurally similar counterparts are probably Davey-Stewartson equations describing nonlinear dispersive waves in fluid dynamics or Zakharov equations for parametrically coupled electromagnetic and Langmuir waves in plasmas.

Media with a photorefractive nonlinearity turn out to be convenient for studying complex spatial dynamics. These include formation of patterns, self-focusing, and transverse modulation instability of solitary stripe beams with formation of optical vortices. We have performed a theoretical and experimental study of self-focusing and soliton formation in photorefractive media with anisotropic and nonlocal response.[1] We give an approximate analytical solution that demonstrates the possibility of elliptically shaped solitary waves, find them exactly using a numerical approach and verify their existence experimentally. The rate of convergence of round input beams to elliptical solitons is governed by the ratio of the optical intensity to the saturation intensity in the medium. In the high saturation limit ($|B|^2 >> I_{sat}$) convergence is slow and the beam shape oscillates, see Figure 49(a), while for moderate saturation ($|B|^2 \approx I_{sat}$) there is relatively rapid convergence to the elliptical soliton, see Figure 49(b).

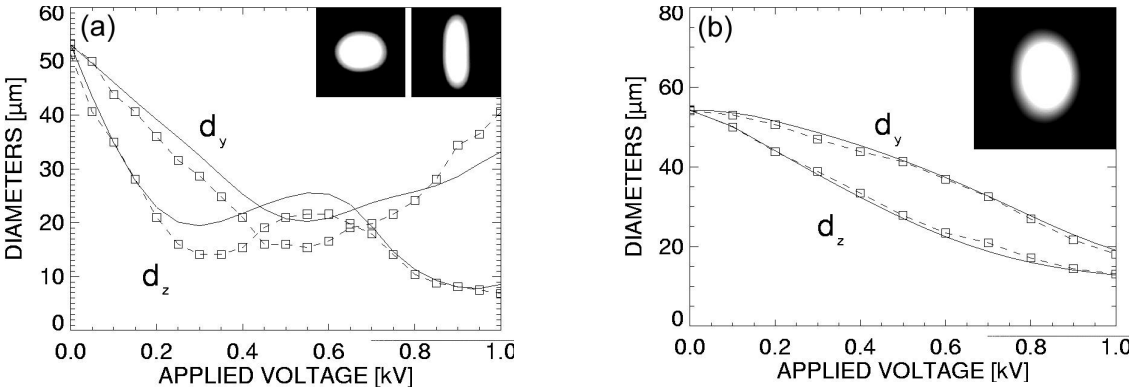

Figure 49. Experimental (squares) and theoretical (solid line) evolution of beam diameters in the high saturation regime (a) and the moderate saturation regime (b). The insets show the intensity profile of the output beam at selected values of the applied voltage.

This work was supported by the Danish Natural Science Research Council.

1. A. A. Zozulya, D. Z. Anderson, A. V. Mamaev and M. Saffman, "Self-focusing and soliton formation in media with anisotropic nonlocal material response", *Europhys. Lett.* **36**, 419-424 (1996).

4.4.4 Propagation of Optical Vortices in Anisotropic, Nonlocal Nonlinear Media

A. V. Mamaev (Institute for Problems in Mechanics, Moscow, Russia), A. A. Zozulya (JILA, University of Colorado, USA) and M. Saffman
E-mail: mark.saffman@risoe.dk

Vortex solitons exist in media with a defocusing nonlinearity. Their stability depends on the structure of the nonlinearity and the dimensionality of the medium. Evolution in a medium with cubic nonlinearity in the limit of one transverse dimension is described by the (1+1)D nonlinear Schrödinger equation, which is integrable, and admits solitary wave solutions for both focusing and defocusing nonlinearities. Planar (1+1)D solutions are modulationally unstable in bulk media described by a (2+1)D system of equations. This was known theoretically at an early stage, and has been seen experimentally in water waves and in nonlinear optics both in atomic vapours with a Kerr-type response and in photorefractive media. Three-dimensional solitary vortex solutions of the nonlinear Schrödinger equation were first considered in the context of superfluidity and have attracted a great deal of recent interest in nonlinear optics. Kerr-type optical media with a cubic, isotropic and local nonlinearity support (2+1)D vortex solitons.

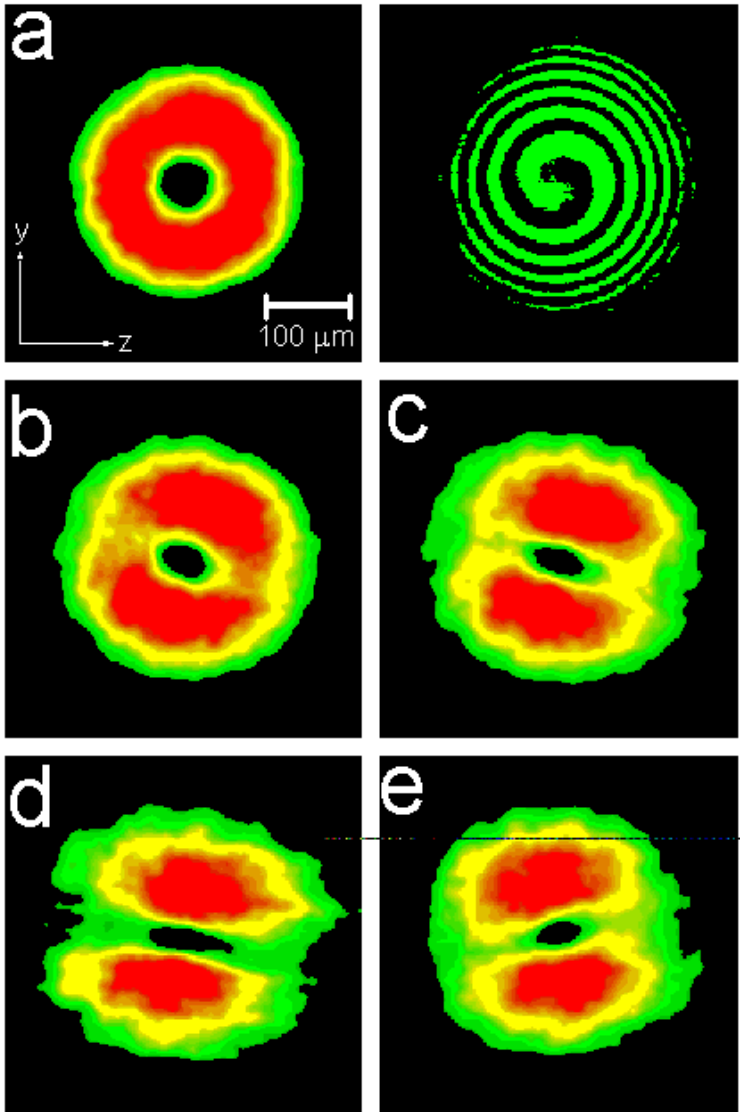

Figure 50. Evolution of a charge-one vortex for applied voltages of 0 (a), 200 (b), 400 (c) and 800 V (d). Frame (e) is analogous to (c) but for opposite vortex sign. The frame to the right of (a) is the interference pattern of the output field (a) and a spherical reference wave.

A Kerr-type nonlinearity is, however, a simplified idealised model of a nonlinear response. The evolution of vortices in media with a more complex nonlinear response has not been studied extensively. The bulk photorefractive nonlinear medium used in the experiments reported here exhibits a nonlinearity that is both anisotropic and nonlocal. This leads to some remarkable qualitative differences in the spatial dynamics of light beams. In particular, an optical vortex with initial circular symmetry rotates and stretches, aligning itself so that its major axis coincides with the direction of greatest material nonlinearity. The stretching proceeds unchecked so that the vortex becomes more and more delocalised. Both theory and experiment indicate that, in contradiction to results reported earlier by other groups, localised optical vortex solutions and, especially, soliton vortex solutions of unit topological charge do not exist in these

media.[1] The nonexistence of localised vortex solutions is not a simple consequence of the anisotropy alone since, in related work done with the same material but with a self-focusing nonlinearity, we have demonstrated convergence to elliptical soliton solutions,[2] see also section 4.4.3.

Figure 50 shows experimentally observed spreading and delocalisation of an input vortex beam in a photorefractive crystal. The input vortex was created by diffraction from a computer-generated hologram prepared at Risø. As the nonlinearity (proportional to the applied voltage) is increased, the vortex spreads and rotates. As shown in frame (e) the sign of rotation is determined by the charge of the vortex.

This work was supported by the Danish Natural Science Research Council.

1. A. V. Mamaev, M. Saffman and A. A. Zozulya, "Vortex evolution and bound pair formation in anisotropic nonlinear media", *Phys. Rev. Lett.* **77**, 4544-4547 (1996).
2. A. A. Zozulya, D. Z. Anderson, A. V. Mamaev and M. Saffman, "Self-focusing and soliton formation in media with anisotropic nonlocal material response", *Europhys. Lett.* **36**, 419-424 (1996).

4.4.5 Decay of High-order Optical Vortices in Anisotropic Nonlinear Media

A. V. Mamaev (Institute for Problems in Mechanics, Moscow, Russia), A. A. Zozulya (JILA, University of Colorado, USA) and M. Saffman
E-mail: mark.saffman@risoe.dk

Vortical excitations with quantised circulation appear in superfluids, superconductors and nonlinear optics in the presence of a repulsive or self-defocusing nonlinearity. The nonlinear Schrödinger equation with cubic nonlinearity has been used extensively to describe vortex solitons in two transverse dimensions, as was done first in the context of vortex lines in superfluids by Ginzburg and Pitaevskii. Much recent attention has been attracted by vortices and vortex solitons in nonlinear optics. Idealised Kerr-type optical media with a cubic, isotropic and local nonlinearity have been shown experimentally to support stable (2+1)D vortices.

While vortices with unit topological charge have been studied extensively, much less is known about higher-order vortices. The cubic nonlinear Schrödinger equation supports higher-order vortex solutions with integer charge *m*.

As was shown by Ginzburg and Pitaevskii, a high-order vortex of charge *m* is energetically unfavourable compared with *m* vortices of unit charge. It is therefore often assumed that high-order vortices will always decay. Nonetheless, the mode of decay of a high-order vortex has not been established, and recent calculations suggest that in the context of the cubic nonlinear Schrödinger equation high-order vortices are metastable. The nonlinear metastability of high-order vortices in Kerr media may be viewed as evidence for the weak interaction of unit-charge vortices in such media. It has been shown that for large intervortex separation the dynamics of vortices satisfying the cubic nonlinear Schrödinger equation

correspond to point vortex dynamics in an ideal two-dimensional fluid. A pair of point vortices with equal vorticity in an ideal fluid rotates about their mutual centre while maintaining a constant separation. The corresponding rotation of quantised vortices with the same charge and a relatively large separation has been observed in both linear and nonlinear optics.

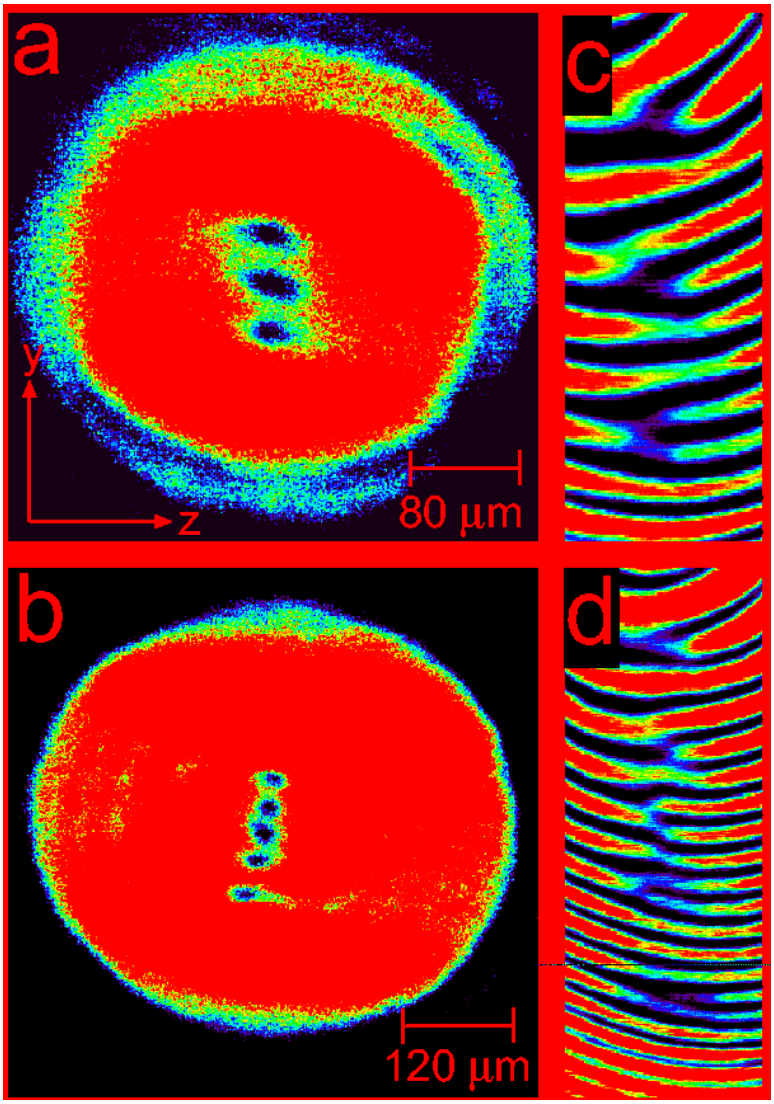

Figure 51. Experimentally observed decay of charge 3 (a) and charge 5 (b) vortices. Frames (c) and (d) show the corresponding interferograms.

We show here[1] that the weak interaction of optical vortices with the same topological charge, and the close analogy with point vortices in a fluid are not general results. We present the first experimental demonstration of the decay of a high-order vortex in a nonlinear medium with nonlocal anisotropic response. Examples are shown in Figure 51. Upon breakup of the input high-charge vortex, the resulting charge-one vortices repel each other and form an array aligned perpendicularly to the anisotropy axis. The same scenario holds for several closely spaced charge-one vortices launched into the medium. They repel each other, and their characteristic

separation at the final stages of the instability may exceed their initial separation by orders of magnitude.

This work was supported by the Danish Natural Science Research Council.

1. A. V. Mamaev, M. Saffman and A. A. Zozulya, "Decay of high order optical vortices in anisotropic nonlinear optical media", submitted (1996).

4.4.6 The Anisotropic Three-dimensional Nonlinear Schrödinger Equation

M. R. Schmidt and J. Juul Rasmussen
E-mail: jens.juul.rasmussen@risoe.dk

The anisotropic three-dimensional cubic Schrödinger equation models a slowly varying amplitude field of electromagnetic waves in media where the refractive index depends linearly on the field intensity, i.e. a Kerr-type media. The equation reads:

$$i\frac{\partial\psi}{\partial t}+\nabla_\perp^2\psi+s\frac{\partial^2\psi}{\partial z^2}+p|\psi|^2\psi=0\ ,\ \text{where}\ \nabla_\perp^2\psi\equiv\frac{\partial^2\psi}{\partial x^2}+\frac{\partial^2\psi}{\partial y^2}$$

ψ is the complex field and z is the direction of propagation. The second term models the diffraction in the transverse plane; the third term models the dispersion along the axis of propagation (s > 0 yields anomalous dispersion, s < 0 yields normal dispersion). The last term on the left-hand side models the Kerr effect, where p > 0 corresponds to focusing, and p < 0 corresponds to defocusing. As the equation is nondimensionalised, only the signs of s and p are important, giving four regimes with different dynamics. Most previous studies were based on the assumption of isotropy in the media, or radial symmetry in the solution.

To study the complete three-dimensional dynamics of fields governed by the cubic Schrödinger equation, we have implemented a pure spectral code that solves it in a triple periodic geometry with time integration performed by a third-order Adam-Moulton predictor-corrector scheme with fixed time step. We have also studied a split-step and a stiffly stable time integration instead of the Adam-Moulton scheme. Especially the split-step scheme is appropriate for the cubic Schrödinger equation, as it conserves the invariants, and change of time step is possible without loss of accuracy and computational time.

We have conducted preliminary investigations of the internal dynamics of light beams (light bullets) in idealised, homogeneous media. An interesting phenomenon in anisotropic media with s < 0 is the competing mechanisms of splitting in the *z*-direction (the direction of propagation) and self-contraction in the transverse plane, here p > 0. It is well established that self-focusing in two and three dimensions in media with s > 0 can lead to a so-called "collapse" or "blow-up", where the field becomes singular. This takes place in finite time, provided that the beam intensity exceeds some critical value inside an effectively bounded area. It is also quite well established that for s < 0 beams focusing in two

dimensions will split along z into smaller structures, which can successively undergo further splitting. The splitting process stops when the intensity of the involved structure decreases below a critical value. Our preliminary results indicate that splitting takes place before the field (a spherical Gaussian light bullet) can collapse. However, a more detailed study is necessary to validate the observation.

4.4.7 Amalgamation of Interacting Light Beamlets in Kerr-type Media

L. Bergé (CEA/Limeil-Valenton, Villeneuve-Saint-Georges cedex, France), M. R. Schmidt, J. Juul Rasmussen, P. L. Christiansen and K. Ø Rasmussen* (* IMM, The Technical University of Denmark, Lyngby, Denmark)*
E-mail: jens.juul.rasmussen@risoe.dk

Self-trapping and self-focusing of intense optical beams propagating in nonlinear, weakly dispersive media have been widely investigated since the 1960s. In particular, self-trapped beams evolving in three spatial dimensions (3D) are well-known to be unstable within an ideal Kerr medium and to break up into a train of 3D solitary waves. In the absence of saturation, the resulting filaments self-focus until they collapse at a finite propagation distance, when their individual power is such that the nonlinear effects continuously dominate over the natural dispersion of the wave. In this regime, the "energy" - or Hamiltonian - integral associated with the filaments is negative and the transverse power of the input beam must exceed a critical threshold. These results apply to individual light beams. Often a number of light filaments are formed as a result of the modulational instability of a broad light beam. These filaments are observed to interact, but up to now no quantitative investigation of this interaction dynamics has been performed.

The aim of our work is to contribute to the theory of interacting light beams by considering the possible interaction regimes for two optical filaments in a self-focusing Kerr medium. The nature of the interaction is shown to vary with the incident individual powers and relative phases of the beamlets. By means of virial arguments supported by numerical results it is found that three distinct evolution regimes characterise two in-phase interacting filaments: (i) When each of the filaments has a power below $N_c/4$, where N_c is the critical self-focusing threshold for a single beam, they both disperse along their propagation axes. (ii) When their respective powers lie between $N_c/4$ and N_c, they fuse into a single central lobe which may self-focus until collapse, depending on their initial separation distance; this distance below which the central lobe forms and can collapse is estimated analytically. An example of this behaviour is shown in Figure 52. (Here $N_c = 4\pi$.) (iii) When their incident powers both exceed N_c, initially separated filaments individually self-focus without mutual interaction. In contrast to in-phase beamlets, two light cells with opposite phase are shown never to coalesce. The extension of these self-focusing dynamics to optical filaments in bulk media with anomalous group velocity dispersion is also discussed.

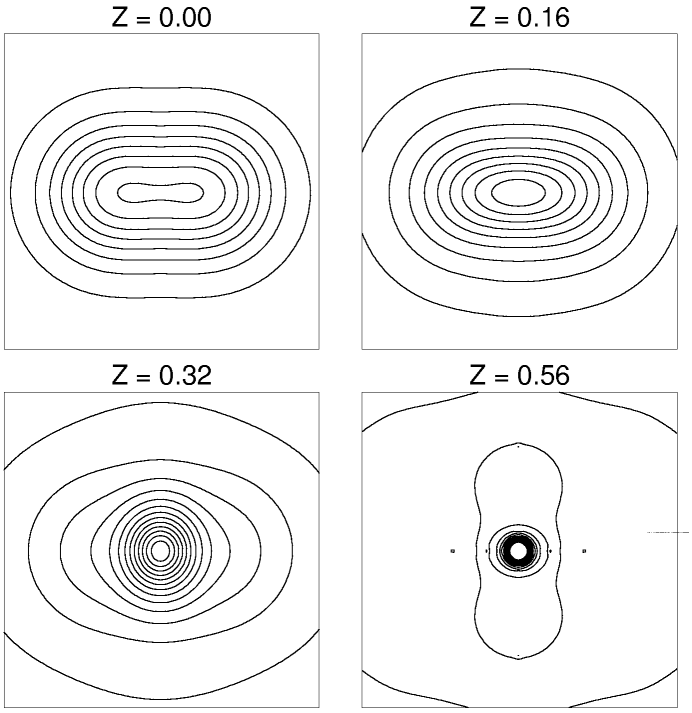

Figure 52. Contour plots for the amplitude field of two interacting beamlets. Each beamlet has a power of 2π; isolated they would spread out. Together, however, the total power of the two beamlets, including the interaction between them, exceeds 4π. This causes them to fuse into one central lobe and collapse at the propagation distance z = 0.58.

4.4.8 Numerical Studies of the Dynamics of Localised Wave Fields in the Raman-extended Derivative Nonlinear Schrödinger Equation

J. S. Hesthaven (Division of Applied Mathematics, Brown University, Providence, RI 02912, USA), J. Juul Rasmussen, L. Bergé (CEA/Limeil-Valenton, Villeneuve-Saint-Georges cedex, France) and J. Wyller (Department of Mathematics, Narvik Institute of Technology, Narvik, Norway)
E-mail: jens.juul.rasmussen@risoe.dk

The evolution of localised solutions to the Raman-extended derivative nonlinear Schrödinger (R-EDNLS) equation is investigated numerically using a stable pseudospectral multidomain method. The R-EDNLS equation describes, e.g., the evolution of the envelope, *u*, of a nonlinearly modulated wave train in optical waveguides. With suitable normalisations it reads:

$$u_t + iu_{xx} + |u|^2 u_x + ig\left(|u|^2\right)_x u + i|u|^4 u = 0, \qquad (4.1)$$

where γ is a real constant measuring the Raman effect. For Eq. (4.1) in general only the "wave action" $N = \int |u|^2 dx$ is conserved.

We have in particular investigated which initial conditions lead to collapse and noncollapse. The results are found to correspond well with theoretical predictions based on a Lagrangian approach and through comparison with the dynamics of the critical nonlinear Schrödinger equation.[1] Without the Raman effect $\gamma = 0$, initial conditions with $N > N_c$ are found to collapse; here N_c is slightly larger than the value of the "wave action", N_s, for the soliton solution. Inclusion of the Raman effect ($\gamma \neq 0$) is found to inhibit finite-time collapse for $\gamma < 0$. For $\gamma > 0$, on the other hand, collapse is only inhibited for $\gamma > \gamma_c$, where γ_c depends on the value of N. This is illustrated in Figure 53 (a,b). Here we have $N = 1.1\ N_s$ for which we observed a collapse for $\gamma = 0$. In the case of $\gamma = 1.0$ the collapse is stopped. This is not the case for $\gamma = 0.5$, where the wave field collapses.

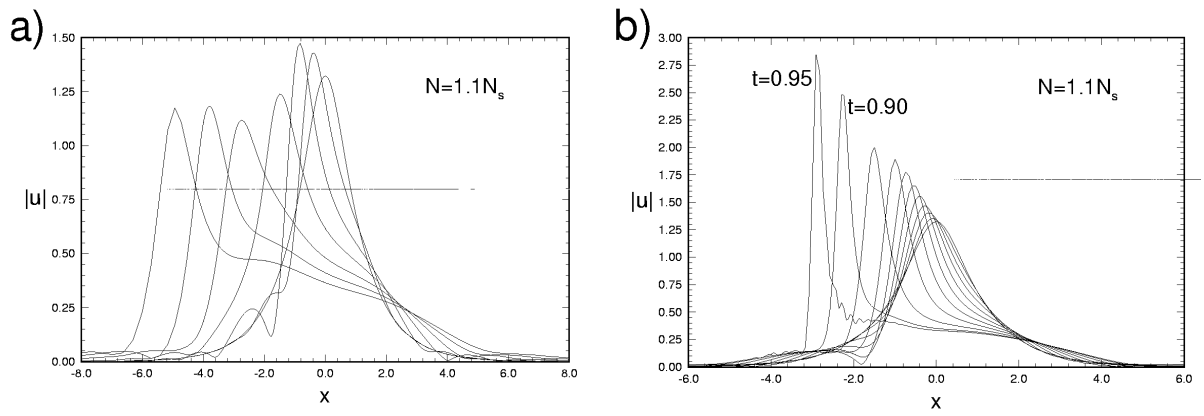

Figure 53. a) shows the decaying and spreading wave field for $\gamma = 1$. The solution is shown for $t = 0.0$ - 1.2 at intervals of 0.2. b) shows the collapsing wave field for $\gamma = 0.5$ for $t = 0.0$ - 0.95 at intervals of 0.1 with the exception of the explicitly marked ones.

1. L. Bergé, J. Juul Rasmussen and J. Wyller, *J. Phys. A.: Math. Gen.* **29**, 3581 (1996).

4.4.9 Self-focusing and Soliton-like Structures in Materials with Competing Quadratic and Cubic Nonlinearities

L. Bergé (CEA/Limeil-Valenton, Villeneuve-Saint-Georges cedex, France), O. Bang (The Australian National University, Canberra, Australia), J. Juul Rasmussen and V K Mezentsev (Institute of Automation and Electrometry, Novosibirsk, Russia)
E-mail: jens.juul.rasmussen@risoe.dk

In bulk media of a material with inversion symmetry and, consequently, a purely cubic (or $\chi^{(3)}$) nonlinearity, it is well known that light beams will either diffract or self-focus until a destructive collapse occurs at a finite propagation distance, depending on whether the input power is below or

above a given threshold. In contrast, it was shown that in materials with strongly asymmetric crystal structures and, thus, purely quadratic (or $\chi^{(2)}$) nonlinearities, a catastrophic collapse can never occur.[1]

In most materials the nonlinearity will both have a component that is quadratic and a component that is cubic in the field amplitude. Obviously, the competition between the two kinds of nonlinearities will affect the properties of beams propagating in such $\chi^{(2+3)}$ media. The dynamic equations for 1+1 dimensional temporal and spatial evolution of waves in $\chi^{(2+3)}$ media have recently been derived,[2] and investigations of modulational instability and the existence of solitary waves have been performed.

We have generalised these equations to describe the evolution of wave beams in systems of two transverse dimensions (D = 2) and have performed a detailed analytical and numerical analysis of the self-focusing characteristics and soliton stability for various parameters. For attractive potentials with positive coupling parameters, we have shown that mutually trapped waves can self-focus until collapse, whenever their respective powers exceed some threshold value. However, the $\chi^{(2)}$-nonlinearity was found to have a stabilising influence in the sense that it increases the collapse threshold as compared with the case with a pure $\chi^{(3)}$-nonlinearity. In contrast, for D = 1 we found that coupled waves may evolve towards stable soliton-like structures. For D = 2 we further found regimes (below the self-focusing threshold) of stable soliton-like structures.

1. L. Bergé, V. K. Mezentsev, J. J. Rasmussen and J. Wyller, *Phys. Rev. A* **52**, R28 (1995).
2. O. Bang, *J. Opt. Soc. Am. B* (in press) (1997).

5. Combustion Facilities

A. Olsen
E-mail: aksel.olsen@risoe.dk

In the long-term, pressurised combustion and gasification technologies are expected to have the largest potential as regards high energy efficiency and low environmental impact. During 1996, the combustion and gasification laboratory at Risø National Laboratory has investigated fuel reactivity under pressurised conditions - experimentally as well as theoretically. A number of different fuels have been investigated, including different types of coal, wheat straw, barley straw, willow and giganteus. The experimental part, which has been completed, covered pressures up to 10 bar and temperatures up to about 1400°C. Analysis of the experimental data is in progress.[1] This work is supported by the Danish utility organisations ELSAM and ELKRAFT as well as by the Danish Ministry of Energy and the Environment.

Furthermore, for two European projects, which describe the state-of-art of biomass utilisation for heat and energy production in small systems, Risø's contribution has been finished. Risø has primarily been describing the combustion and gasification process.[2-4] The Danish conclusion for this part of the work is that at present there are no commercial gasification solutions available and it will probably take several years before they have been developed.

The tar production is a problem in certain types of low temperature combustion of grass and straw. An experimental set-up has been built and the first experiments covering partial oxidation of the tar have been performed. The measurement technique - gas chromatography/mass spectroscopy - has been established and compared satisfactorily with results from other sources.

1. O. Rathmann, "Steam gasification of wheat straw, barley straw, willow and giganteus, Risø-R-944(EN), November 1996.
2. P. Stoholm and A. Olsen, Eurec Network on Biomass (Bio-Electricity), Biomass Combustion, November 1996.
3. P. Stoholm and A. Olsen, Eurec Network on Biomass (Bio-Electricity), Biomass Gasification, November 1996.
4. P. Stoholm, "Analysis and co-ordination of the activities concerning gasification of biomass", Summary Country Report, Denmark and Norway. Concerted Action, November 1996.

6. Publications and Educational Activities

6.1 Optical Materials

6.1.1 Publications

Andersen, P.E.; Buchhave, P.; Petersen, P.M., Strong coupling between coherent gratings due to nonlinear spatial frequency mixing in $Bi_{12}SiO_{20}$. Opt. Commun. (1996) v. 128 pp 185-192.

Andersen, P.E.; Dam, J.S.; Petersen, P.M., Lysudbredelse i humant væv. DOPS-Nyt (1996) v. 11 (no.3) pp 10-11.

Andersen, P.E.; Petersen, P.M., Fundamental properties of nonlinear combinations of gratings in $Bi_{12}SiO_{20}$ and their applications. J. Opt. (India) (1995) v. 24 (no.4) pp 185-226.

Berg, R.H.; Hvilsted, S.; Ramanujam, P.S., Peptide oligomers for holographic data storage. Nature (1996) v. 383 pp 505-508.

Dam-Hansen, C., Magnetophotorefractive effect and interference filters in lithium niobate. Risø-R-880(EN) (1996) 90 p. (ph.d.- thesis).

Dam-Hansen, C.; Johansen, P.M.; Fridkin, V.M., Photorefractive grating formation in piezoelectric $La_3Ga_5SiO_{14}:Pr^{3+}$ crystals. Appl. Phys. Lett. (1996) v. 69 pp 2003-2005.

Dam-Hansen, C.; Johansen, P.M.; Petersen, P.M.; Fridkin, V.M., Magnetophotorefractive effect in $LiNbO_3$:Fe crystals: theory and experiments. J. Opt. Soc. Am. B (1996) v. 13 pp 2286-2298.

Dutkiewicz, L.; Pedrys, R.; Schou, J., Linear and nonlinear effects at low energy ion bombardment of solid xenon. Nucl. Instrum. Methods Phys. Res. B (1996) v. 115 pp.

Hanson, S.G.; Lindvold, L.R.; Lading, L., A surface velocimeter based on a holographic optical element and semiconductor components. Meas. Sci. Technol. (1996) v. 7 pp 69-78.

Holme, N.C.R.; Ramanujam, P.S.; Hvilsted, S., 10,000 optical write, read, and erase cycles in an azobenzene sidechain liquid-crystalline polyester. Opt. Lett. (1996) v. 21 pp. 902-904.

Holme, N.C.R.; Ramanujam, P.S.; Hvilsted, S., Photoinduced anisotropic measurements in liquid-crystalline azobenzene side-chain polyesters. Appl. Opt. (1996) v. 35 pp 4622-4627.

Hvilsted, S.; Ramanujam, P.S.; Andruzzi, F., Optical storage medium. US Patent 5,496,670 A (5 Mar 1996).

Johansen, P.M., Dam-Hansen, C., Petersen, P.M., and Fridkin, V.M., "Dynamic grating formation in $LinBO_5$:Fe crystals under influence of an enternally applied magnetic field", Lasers'96, December 2-6, 1996 Portland, Oregon, USA.

Lading, L., Optik og fluid dynamik - en mærkelig kombination?. DOPS-Nyt (1996) v. 11 (no.1) pp 49-50.

Lindvold, L., Aktiviteter indenfor biomedicinske anvendelser af optik på OFD, Risø. DOPS-Nyt (1996) v. 11 (no.3) p. 15.

Nikolova, L.; Todorov, T.; Ivanov, M.; Andruzzi, F.; Hvilsted, S.; Ramanujam, P.S., Polarization holographic gratings in side-chain azobenzene polyesters with linear and circular photoanisotropy. Appl. Opt. (1996) v. 35 pp 3835-3840.

Pedersen, H.C., Nonlinear parametric processes in photorefractive media. Risø-R-887(EN) (1996) 82 p. (ph.d. thesis).

Pedersen, H.C.; Andersen, P.E.; Petersen, P.M.; Johansen, P.M., Theory of nonlinear multiple-grating interaction in diffusion-dominated photorefractive media. J. Opt. Soc. Am. B (1996) v. 13 pp 2569-2579.

Pedersen, H.C.; Johansen, P.M., Degenerate parametric amplification in photorefractive media: Theoretical analysis. J. Opt. Soc. Am. B (1996) v. 13 pp 590-600.

Pedersen, H.C.; Johansen, P.M., Observation of non-degenerate photorefractive parametric amplification. Phys. Rev. Lett. (1996) v. 76 pp 4159-4162.

Pedersen, H.C.; Johansen, P.M., Longitudinal, degenerate, and transversal parametric oscillation in a photorefractive media. Phys. Rev. Lett. (1996) v. 77 pp 3106-3109.

Petersen, P.M., Optik i Danmark. DOPS-Nyt (1996) v. 11 (no.1) p. 4.

Petersen, P.M.; Andersen, P.E. (eds.), Biomedicinske anvendelser af optik. Risø-R-919(DA) (1996) 42 p.

Petersen, P.M.; Dam-Hansen, C.; Johansen, P.M., Fremtidens datalagring sker ved hjælp af hologrammer. Risønyt (1996) (no.3) pp 4-5.

Ramanujam, P.S.; Holme, N.C.R.; Hvilsted, S., Atomic force and optical near-field microscopic investigations of polarization holographic gratings in a liquid crystalline azobenzene side-chain polyester. Appl. Phys. Lett. (1996) v. 68 pp 1329-1331.

Ramanujam, P.S.; Holme, C.; Hvilsted, S.; Pedersen, M.; Andruzzi, F.; Paci, M.; Tassi, E.L.; Magagnini, P.; Hoffman, U.; Zebger, I.; Siesler, H.W., Side-chain liquid crystalline polyesters for optical information storage. Polym. Adv. Technol. (1996) v. 7 pp 768-776.

Ramanujam, P.S.; Hvilsted, S.; Berg, R.H., New polymer materials for erasable holographic storage. Holography. SPIE Int. Techn. Working Group Newslett. (1996) v. 6 (no.2) pp 2-3.

Rudd, M.E.; Kim, Y.-K.; Märk, T.; Schou, J.; Stolterfoht, N.; Toburen, L.H., Secondary electron spectra from charged particle interactions. (International Commission on Radiation Units and Measurements, Bethesda, MD, 1996) (ICRU-55) 108 p.

Schou, J., Electron emission from solids. In: Physical processes of the interaction of fusion plasmas with solids. Hofer, W.O.; Roth, J. (eds.), (Academic Press, San Diego, CA, 1996) pp 177-216.

Schou, J., Secondary electrons from heavy-ion tracks. In: Radiation research 1895 - 1995. Congress proceedings. Vol. 2: Congress lectures. 10. International congress of radiation research, Würzburg

(DE), 27 Aug - 1 Sep 1995. Hagen, U.; Harder, D.; Jung, H.; Streffer, C. (eds.), (ICRR Society, Würzburg, 1995) p 101-105.

Shi, M.; Baragiola, R.A.; Grosjean, D.E.; Johnson, R.E.; Jurac, S.; Schou, J., Sputtering of water ice surfaces and the production of extended neutral atmospheres. J. Geophys. Res. (1995) v. 100 (no.E12) pp 26387-26395.

Svendsen, W.; Ellegaard, O.; Schou, J., Laser ablation deposition measurements from silver and nickel. Appl. Phys. A (1996) v. 63 pp 247-255.

Svendsen, W.; Schou, J.; Thestrup, B.; Ellegaard, O., Ablation from metals induced by visible and UV laser irradiation. Appl. Surf. Sci. (1996) v. 96/98 pp 518-521.

Svendsen, W.E., Charged particle and laser irradiation of selected materials. Risø-R-924(EN) (1996) 102 p.

6.1.2 Unpublished Contributions

Dam-Hansen, C.; Johansen, P.M.; Petersen, P.M., Magnetophoto-refractive effect in photovoltaic $LiNbO_3$:Fe. Annual meeting of the Danish Physical Society, Nyborg (DK), 23-24 May 1996. Unpublished. Abstract available.

Dutkiewicz, L.; Pedrys, R.; Schou, J., Lattice dynamics during electronic sputtering of solid Ne. COSIRES. Computer simulation of radiation effects in solids conference, Guildford (GB), 22-26 Jul 1996. Unpublished. Abstract available.

Ellegaard, O.; Schou, J., Laser induced evaporation of volatile films from a multicomponent system. Gordon research conference on laser interactions with materials, Plymouth, NH (US), 9-14 Jun 1996. Unpublished.

Hansen, T.N.; Nordskov, A.; Thestrup, B., Angular resolved distribution of silver ablated from intense UV laser irradiation. Annual meeting of the Danish Optical Society, Risø (DK), 21-22 Nov 1996. Unpublished. Abstract available.

Holme, N.C.R.; Ramanujam, P.S.; Hvilsted, S.; Pedersen, M., Near-field microscopy on liquid crystalline side-chain polyesters. Annual meeting of the Danish Physical Society, Nyborg (DK), 23-24 May 1996. Unpublished. Abstract available.

Hvilsted, S.; Berg, R.H.; Ramanujam, P.S.; Hendann, C.; Rømer Holme, N.C.; Pedersen, M.; Rasmussen, R.; Kulinna, C., The researh group on new materials for optical information storage at Risø National Laboratory. NorFA Nordic-Baltic workshop on molecular electrooptic materials, Göteborg (SE), 17-18 Jun 1996. Unpublished. Abstract available.

Hvilsted, S.; Kulinna, C.; Ramanujam, P.S., Laser induced segmental orientation of side-chain liquid crystalline polyesters investigated by FTIR. In: 12th European symposium on polymer spectroscopy. Program. Book of abstracts. ESOPS 12, Lyon (FR), 8-10 Jul 1996. (Universite Claude Bernard, Lyon, 1996) p. 18.

Hvilsted, S.; Ramanujam, P.S., Optisk informationslagring. Ungdommens Naturvidenskabelige Forening. (UNF). H.C. Ørsted Institutet, København (DK), 26 Sep 1996. Unpublished. Abstract available

Johansen, P.M.; Pedersen, H.C., Holographic wave instabilities in photorefractive sillenite crystals. Annual meeting of the Danish Optical Society, Risø (DK), 21-22 Nov 1996. Unpublished. Abstract available.

Kulinna, C.; Hvilsted, S.; Ramanujam, P.S., Selective deuterium labeling as a tool for the investigation of laser induced segmental orientation in cyanoazobenzene side-chain polyesters. In: EPF'96. Book of abstracts. 6. European Polymer Federation symposium on polymeric materials, Crete (GR), 7-11 Oct 1996. (Eilenic Polymer Society, Athen, 1996) 2 p.

Lindvold, L., Miniaturization of optical chemical sensors. Grundfos sensor seminar, Bjerringbro (DK), 18 Apr 1996. Unpublished.

Madsen, S.; Birkelund, K.; Müllenborn, M.; Holme, N.C.R.; Hvam, J.M.; Grey, F., Optical near-field induced nano-scale pattering of hydrogen-passivated silicon. Annual meeting of the Danish Optical Society, Risø (DK), 21-22 Nov 1996. Unpublished. Abstract available

Petersen, P.M., Nonlinear self-refraction of Gaussian laser beams in silica sono-gels. Advanced topics in modern optics. Summerschool and workshop in optics, Humlebæk (DK), 2-8 Jun 1996. Unpublished.

Petersen, P.M., Grating couplers in optical waveguides. Advanced topics in modern optics. Summerschool and workshop in optics, Humlebæk (DK), 2-8 Jun 1996. Unpublished.

Schou, J., Electronic sputtering. International symposium on particle penetration and collision cascades, Odense (DK), 12-14 Apr 1996. Unpublished.

Schou, J.; Svendsen, W.; Ellegaard, O.; Nordskov, A.; Thestrup, B., Total yields and angular distributions from laser ablated silver. Gordon research conference on laser interactions with materials, Plymouth, NH (US), 9-14 Jun 1996. Unpublished.

Schou, J.; Svendsen, W.; Thestrup, B.; Ellegaard, O., Angular resolved UV laser ablation from silver. Annual meeting of the Danish Physical Society, Nyborg (DK), 23-24 May 1996. Unpublished. Abstract available.

Schou, J.; Svendsen, W.; Nordskov, A.; Thestrup, B.; Ellegaard, O., Angular resolved ablation from silver induced by intense UV laser irradiation. E-MRS 1996 spring meeting. Symposium K, Strasbourg (FR), 4-7 Jun 1996. Unpublished. Abstract available.

Svendsen, W.; Schou, J.; Ellegaard, O.; Thestrup, B., Yields and angular distributions of particles from UV laser-irradiated silver.

Thestrup Nielsen, B., Pulsed laser deposition of thin ITO films: the physics behind the experiment and the first promising results. Gruppemøde i atomfysikgruppen. Niels Bohr Institutet, København (DK), 22 Mar 1996. Unpublished.

Thestrup, B.; Nordskov, A.; Schou, J.; Svendsen, W.; Johansen, P.M., Thin films of ITO produced by pulsed laser deposition. Gordon research conference on laser interactions with materials, Plymouth, NH (US), 9-14 Jun 1996. Unpublished.

Thestrup, B.; Nordskov, A.; Schou, J.; Svendsen, W.; Johansen, P.M., Thin films of ITO produced by pulsed laser deposition. Annual meeting of the Danish Physical Society, Nyborg (DK), 23-24 May 1996. Unpublished. Abstract available.

Thestrup, B.; Nordskov, A.; Dam-Hansen, C.; Johansen, P.M.; Schou, J., Holographic gratings induced in laser ablated thin films of indium tin oxide. Annual meeting of the Danish Optical Society, Risø (DK), 21-22 Nov 1996. Unpublished. Abstract available. International symposium on particle penetration and collision cascades, Odense (DK), 12-14 Apr 1996. Unpublished.

Thestrup, B.; Svendsen, W.; Schou, J.; Ellegaard, O., Electronic sputtering and charge accumulation in thick deuterium films. International symposium on particle penetration and collision cascades, Odense (DK), 12-14 Apr 1996. Unpublished.

6.1.3 Internal Reports

Bidrag til Forskningscenter Risøs 3-årsplan 1997-1999 fra Afdelingen for Optik og Fluid Dynamik. Risø-Dok-470 (1996) 32 p.

6.2 Optical Diagnostics and Information Processing

6.2.1 Publications

Andersen, F., Resultatet af NIF audit D1 digitaltermometer. In: Den nordiske konferanse måleteknikk og kalibrering. 18. nordiske konferanse måleteknikk og kalibrering, Lillehammer (NO), 24-27 Nov 1996. (NJV, Lillehammer, 1996) Paper 8.

Andersen, P.E.; Buchhave, P.; Petersen, P.M., Strong coupling between coherent gratings due to nonlinear spatial frequency mixing in $Bi_{12}SiO_{20}$. Opt. Commun. (1996) v. 128 pp 185-192.

Andersen, P.E.; Dam, J.S.; Petersen, P.M., Lysudbredelse i humant væv. DOPS-Nyt (1996) v. 11 (no.3) pp 10-11.

Andersen, P.E.; Petersen, P.M., Fundamental properties of nonlinear combinations of gratings in $Bi_{12}SiO_{20}$ and their applications. J. Opt. (India) (1995) v. 24 (no.4) pp 185-226.

Boll Illerup, J.; Rathmann, O., CO_2 gasification of wheat straw, barley straw, willow and giganteus. Risø-R-873(EN) (1996) 32 pp.

Christensen, S.S.; Andersen, A.W.; Jørgensen, T.M.; Liisberg, C., Visual guidance of a pig evisceration robot using neural networks. Pattern Recognit. Lett. (1996) v. 17 pp 345-355.

Clausen S.; Sørensen, L.H., Improved temperature measurements of burning char and coal particles using an FT-IR spectrometer. Energy Fuels (1996) v. 10 pp 1133-1141.

Clausen, S., Infrarød temperaturmåling. Risø-R-862(DA) (1996) 21 pp.
Clausen, S., Measurements of particle temperature under combustion. Risø-R-861(EN) (1996) 22 pp.
Clausen, S., Infrarød gas- og temperaturmåling i affaldsforbrændings-anlæg. Risø-R-781(DA) (1996) 27 p.
Clausen, S., Mie calculations of the scattered light from laser doppler anemometers for a wide range of particle sizes. Risø-R-860(EN) (1996) 19 p.
Clausen, S., Local measurement of gas temperature with an infrared fibre-optic probe. Meas. Sci. Technol. (1996) v. 7 pp 888-896.
Clausen, S.; Kirkegaard, M., Kalibrering af infrarødt udstyr. In: Den 18. nordiske konferanse måleteknikk og kalibrering. 18. nordiske konferanse måleteknikk og kalibrering, Lillehammer (NO), 24-27 Nov 1996. (NJV, Lillehammer, 1996) Paper 30.
Clausen, S.; Morgenstjerne, A.; Rathmann, O., Measurement of surface temperature and emissivity by a multitemperature method for Fourier-transform infrared spectrometers. Appl. Opt. (1996) v. 35 pp 5683-5691.
Clausen, S.; Sørensen, L.H., Measurement of single moving particle temperatures with an FT-IR spectrometer. Appl. Spectros. (1996) v. 50 pp 1103-1111.
Flyvbjerg, H., Replies on comment on 'simplest possible self-organized critical system'. Phys. Rev. Lett. (1996) v. 77 p. 4274.
Flyvbjerg, H.; Holy, T.E.; Leibler, S., Microtubule dynamics: Caps, catastrophes, and coupled hydrolysis. Phys. Rev. E (1996) v. 54 pp 5538-5560.
Flyvbjerg, H.; Jobs, E.; Leibler, S., Kinetics of self-assembling microtubules: An 'inverse problem' in biochemistry. Proc. Nat. Acad. Sci. USA (1996) v. 93 pp 5975-5979.
Glückstad, J., Synthesis of arbitrary optical intensity distributions by use of extended phase contrast principle. In: 1996 International topical meeting on optical computing. Proceedings. OC '96, Sendai (JP), 21-25 Apr 1996. (Japan Society of Applied Physics, Tokyo, 1996) (Technical Digest, 1) pp 208-209.
Glückstad, J., Phase contrast image synthesis. Opt. Commun. (1996) v. 130 pp 225-230.
Glückstad, J., Phase contrast imaging. WO Patent 96/34307 (31 Oct 1996).
Glückstad, J.; Toyoda, H.; Igasaki, Y.; Yoshida, N.; Ooie, T.; Hara, T., Energy-efficient image projection by use of novel phase contrast technique. In: Holographic optical elements and displays. Conference on holographic optical elements and displays, Beijing (CN), 4-7 Nov 1996. Lin, F.S.; Xu, D. (eds.), (The International Society for Optical Engineering, Bellingham, WA, 1996) (SPIE Proceedings Series, 2885) pp 126-131.
Glückstad, J.; Toyoda, H.; Yoshida, N.; Takemori, T,.; Hara, T., Experimental verification of phase contrast image synthesis system. In: Optical information processing. 2. International conference on optical information processing, St. Petersburg (RU), 14-17 Jun 1996.

Alferov, Z.I.; Gulyaev, Y.V.; Pape, D.R. (eds.), (The International Society for Optical Engineering, Bellingham, WA, 1996) (SPIE Proceedings Series, 2969) pp 630-634.

Hanson, S.G., System for noncontact measurement of torsional vibrations of shafts. In: Optical velocimetry. OV-metry conference, Warsaw (PL), 29 May - 2 Jun 1995. Pluta, M.; Jabczynski, J.K. (eds.), (The International Society for Optical Engineering, Bellingham, WA, 1996) (SPIE Proceedings Series, 2729) pp 155-163.

Hanson, S.G.; Lading, L., Generics of systems for measuring linear and angular velocities of solid objects. In: Optical velocimetry. OV-metry conference, Warsaw (PL), 29 May - 2 Jun 1995. Pluta, M.; Jabczynski, J.K. (eds.), (The International Society for Optical Engineering, Bellingham, WA, 1996) (SPIE Proceedings Series, 2729) pp 81-90.

Hanson, S.G.; Lindvold, L.R.; Lading, L., A surface velocimeter based on a holographic optical element and semiconductor components. Meas. Sci. Technol. (1996) v. 7 pp 69-78.

Hanson, S.G.; Lindvold, L.R.; Hansen, B.H., Industrial implementation of diffractive optical elements for nondestructive testing. In: Vibration measurements by laser techniques: Advances and applications. 2. International conference on vibration measurements by laser techniques, Ancona (IT), 23-25 Sep 1996. Tomasini, E.P. (ed.), (The International Society for Optical Engineering, Bellingham, WA, 1996) (SPIE Proceedings Series, 2868) pp 216-224.

Hanson, S.G.; Lading, L.; Lynov, J.P.; Skaarup, B. (eds.), Optics and Fluid Dynamics Department annual progress report for 1995. Risø-R-865(EN) (1996) 90 p.

Holst Sørensen, L.; Clausen, S.; Astrup, P.; Rathmann, O.; Biede, O.; Swane Lund, J., Experimental high-temperature investigations of coal particles. Risø-R-871(EN) (1996) 82 p.

Imam, H.; Rose, B.; Lindvold, L.R.; Hanson, S.G.; Lading, L., Miniaturising and ruggedising laser anemometers. In: Eighth international symposium on applications of laser techniques to fluid mechanics. Vol. 2. 8. International symposium on applications of laser techniques to fluid mechanics, Lisbon (PT), 8-11 Jul 1996. (Instituto Superior Técnico. Departemento de Engenharia Mecanica, Lisboa Codex, 1996) Paper 40.2.

Jørgensen, T.M.; Andersen, A.W.; Christensen, S.S., Shape recognition system for automatic disassembly of TV-sets. In: International conference on image processing. Proceedings. Vol. 2. ICIP - 96, Lausanne (CH), 16-19 Sep 1996. (Institute of Electrical and Electronics Engineers, Piscataway, NJ, 1996) pp 653-656.

Jørgensen, T.M.; Christensen, S.S.; Andersen, A.W., Detecting danger labels with RAM-based neural networks. Pattern Recognit. Lett. (1996) v. 17 pp 399-412.

Kaiser, N.E., Måleusikkerhed ved temperaturkalibrering i væskebade. In: Den 18. nordiske konferanse måleteknikk og kalibrering. 18. nordiske konferanse måleteknikk og kalibrering, Lillehammer (NO), 24-27 Nov 1996. (NJV, Lillehammer, 1996) Paper 32.

Lading, L., A white light speed trap. Phys. World (1996) v. 9 (no.1) pp 19-20.
Lading, L., Optik og fluid dynamik - en mærkelig kombination?. DOPS-Nyt (1996) v. 11 (no.1) pp 49-50.
Lading, L., Doppler debate - reply. Phys. World (1996) v. 9 (no.4) p. 15.
Lading, L.; Earnshaw, J., Surface light scattering: Integrated technology and signal processing. In: Photon correlation and scattering. Summaries of the papers. Conference edition. Topical meeting on photon correlation and scattering, Capri (IT), 21-24 Aug 1996. (Optical Society of America, Washington, DC, 1996) (1996 Technical Digest Series, 14) pp 11-13.
Lading, L.; Saffman, M.; Hanson, S.G.; Edwards, R.V., A combined doppler and time-of-flight laser anemometer for measurement of density fluctuations in plasmas. J. Atmos. Terr. Phys. (1996) v. 58 pp 1013-1019.
Lindvold, L., Aktiviteter indenfor biomedicinske anvendelser af optik på OFD, Risø. DOPS-Nyt (1996) v. 11 (no.3) p. 15.
Martini Jørgensen, T.; Weimar Andersen, A.; Sloth Christensen, S., Neural net based image processing for disassembling TV-sets. In: Solving engineering problems with neural networks. Proceedings. 2. International conference EANN '96, London (GB), 17-19 Jun 1996. Bulsari, A.B.; Kallio, S.; Tsaptsinos, D. (eds.), (Systems Engineering Association, Turku, 1996) pp 213-216.
Martini Jørgensen, T., Classification of handwritten digits using a RAM neural net architecture. In: Solving engineering problems with neural networks. Proceedings. 2. International conference EANN '96, London (GB), 17-19 Jun 1996. Bulsari, A.B.; Kallio, S.; Tsaptsinos, D. (eds.), (Systems Engineering Association, Turku, 1996) pp 285-288.
Martini Jørgensen, T., A RAM-based neural net with inhibitory weights and its application to recognising handwritten digits. In: International workshop on neural networks for identification, control, robotics, and signal/image processing. Proceedings. NICROSP '96, Venice (IT), 21-23 Aug 1996. (IEEE Computer Society Press, Los Alamitos, CA, 1996) pp 228-232.
Pedersen, H.C.; Andersen, P.E.; Petersen, P.M.; Johansen, P.M., Theory of nonlinear multiple-grating interaction in diffusion-dominated photorefractive media. J. Opt. Soc. Am. B (1996) v. 13 pp 2569-2579.
Petersen, P.M., Optik i Danmark. DOPS-Nyt (1996) v. 11 (no.1) p. 4.
Petersen, P.M.; Andersen, P.E. (eds.), Biomedicinske anvendelser af optik. Risø-R-919(DA) (1996) 42 p.
Rathmann, O.; Biede, O.; Swane Lund, J.; Wolff, L.; Kirkegaard, M.; Holst Sørensen, L., Flame chars at different burnout degrees from tunnel furnace tests. Risø-R-872(EN) (1996) 82 p.
Rose, B.; Imam, H.; Lading, L.; Hanson, S.G., Time-of-flight velocimetry: Bias and robustness. In: Photon correlation and scattering. Summaries of the papers. Conference edition. Topical meeting on photon correlation and scattering, Capri (IT), 21-24 Aug

1996. (Optical Society of America, Washington, DC, 1996) (1996 Technical Digest Series, 14) pp 68-70.

Rose, B.; Leistiko, O., End-fire coupling between a buried waveguide structure and a Si photodetector. In: Integrated optics and microstructures 3. 3. Conference on integrated optics and microstructures, San Jose, CA (US), 27 Jan - 2 Feb 1996. Tabib-Azar, M. (ed.), (The International Society for Optical Engineering, Bellingham, WA, 1996) (SPIE Proceedings Series, 2686) pp 175-181.

Stenholm, M.; Arendt Jensen, P.; Hald, P., Biomasses brændsels- og fyringskarakteristika. Fyringsforsøg. (Forskningscenter Risø, Roskilde, dk-Teknik, Søborg, 1996) (Energiministeriets Forskningsudvalg for produktion og fordeling af el og varme. Brændsler og forbrændingsteknik) vp.

Stenholm, M.; Westborg, S.; Arendt Jensen, P., Biomasses brændsels- og fyringskarakteristika. Analysearbejde. (Forskningscenter Risø, Roskilde, dk-Teknik, Søborg, 1996) (Energiministeriets Forskningsudvalg for produktion og fordeling af el og varme. Brændsler og forbrændingsteknik) 42 p.

Taylor, T.W.; Meyer, W.V.; Tin, P.; Mann, J.A.; Cheung, H.M.; Rogers, R.B.; Lading, L., A new surface light scattering instrument with autotracking optics. In: Photon correlation and scattering. Summaries of the papers. Conference edition. Topical meeting on photon correlation and scattering, Capri (IT), 21-24 Aug 1996. (Optical Society of America, Washington, DC, 1996) (1996 Technical Digest Series, 14) pp 114-116.

Yura, H.T.; Hanson, S.G.; Lading, L., Comparison between the time-of-flight velocimeter and the laser doppler velocimeter for measurements on solid surfaces. In: Optical velocimetry. OV-metry conference, Warsaw (PL), 29 May - 2 Jun 1995. Pluta, M.; Jabczynski, J.K. (eds.), (The International Society for Optical Engineering, Bellingham, WA, 1996) (SPIE Proceedings Series, 2729) pp 91-102.

Yura, H.T.; Hanson, S.G., Effects of receiver optics contamination on the performance of laser velocimeter systems. J. Opt. Soc. Am. A (1996) v. 13 pp 1891-1902.

6.2.2 Unpublished Contributions

Bak, J., CO_2 emission from 2212 powders measured by TGA-FTIR. Pulvermøde. Afdelingen for Materialeforskning, Risø (DK), 16 Jan 1996. Unpublished.

Clausen, S., Measurement of particle and gas temperature with an FT-IR spectrometer. In: Proceedings of the 3rd workshop on infrared emission measurements by FTIR. Abstracts. 3. Workshop on infrared emission measurements by FTIR, Québec (CA), 7-9 Feb 1996. (Bomem Inc., Québec, 1996) p. 10.

Clausen, S., Infrared combustion diagnostics: Measurement of particle and gas temperature in flames. CANMET. Energy Research

Laboratories. Advanced Combustion Technologies, Ottawa (CA), 5 Feb 1996. Unpublished. Abstract available.

Clausen, S., Praktisk måling af overfladetemperaturer med IR-termometer. Måleteknisk temadag. Temperaturmåling i industrien. DTI Energi, Taastrup (DK), 30 Apr 1996. Unpublished.

Clausen, S., Fourier-transform infrared emission spectroscopy as a tool for temperature measurements - theory and application. Ph.d.-forelæsning. H.C. Ørsted Institutet, København (DK), 18 Jun 1996. Unpublished. Abstract available.

Flyvbjerg, H., Self-assembly of microtubules: An inverse problem in biochemistry. 3. European conference on mathematics applied to biology and medicine, Heidelberg (DE), 6-10 Oct 1996. Unpublished.

Flyvbjerg, H., Two simple self-organized critical systems. Max-Planck-Institute for Colloids and Interfaces, Berlin (DE), 8 Jul 1996. Unpublished.

Flyvbjerg, H., Error estimation on correlated data. International summer school and workshop on advances in computer simulations. Bolyai College. Eötvös University, Budapest (HU), 16-20 Jul 1996. Unpublished.

Flyvbjerg, H., Mean field and random neighbor approximations to simple evolution models. Workshop on distributed dynamical systems applied to ecology, genetics, and forestry, Les Houches (FR), 30 Sep - 6 Oct 1996. Unpublished.

Flyvbjerg, H., Modeling the complex dynamics of microtubules. Meeting on biophysics in the Copenhagen Area. Niels Bohr Institute, Copenhagen (DK), 11 Oct 1996. Unpublished.

Flyvbjerg, H., Self-assembly of microtubules: An inverse problem in biochemistry. Max-Planck-Institute for Colloids and Interfaces, Berlin (DE), 25 Nov 1996. Unpublished.

Flyvbjerg, H.; Holy, T.E.; Leibler, S., Microtubule dynamics: Caps, catastrophes, and coupled hydrolysis. 3. European conference on mathematics applied to biology and medicine, Heidelberg (DE), 6-10 Oct 1996. Unpublished.

Glückstad, J., Generalized phase contrast imaging. Hokkaido University. Department of Electronic Science, Sapporo, Hokkaido (JP), 6 Feb 1996. Unpublished.

Glückstad, J., Priliminary experiments performed with novel phase contrast imaging system. Hamamatsu Photonics K.K. Central Research Labs, Shizuoka (JP), 28 May 1996. Unpublished.

Glückstad, J., Joint research at Hamamatsu Photonics: generalized phase contrast techniques. Advanced Telecommunication Laboratories (ATR), Kansai Science City, Kyoto (JP), 4 Oct 1996. Unpublished.

Glückstad, J., New phase contrast techniques. Saitama University, Saitama (JP), 17 Oct 1996. Unpublished.

Glückstad, J., Phase contrast encoding and applications. LaSIE group. Department of Applied Physics. Osaka University, Osaka (JP), 29 Oct 1996. Unpublished.

Glückstad, J., Phase contrast image synthesis. Hamamatsu Photonics K.K. Central Research Laboratories, Shizuoka (JP), 15 Nov 1996. Unpublished.

Hanson, S.G., Matrix method for analyzing beam propagation through complex optical systems. Chernivtsy University, Chernivtsy (UA), 29 Feb 1996. Unpublished.

Hanson, S.G., Optical methods for measurement of linear and angular displacement. Chernivtsy University, Chernivtsy (UA), 1 Mar 1996. Unpublished.

Hanson, S.G., Tailoring coherence properties - space-time processing. Advanced topics in modern optics. Summerschool and workshop in optics, Humlebæk (DK), 2-8 Jun 1996. Unpublished.

Hanson, S.G., ABCD-metode. Konference om Fourier optik og dens anvendelser, Risø (DK), 17 Sep 1996. Unpublished.

Jánosi, I.M.; Chrétien, D.; Leibler, S.; Flyvbjerg, H., Mechanical model for microtubules. 3. European conference on mathematics applied to biology and medicine, Heidelberg (DE), 6-10 Oct 1996. Unpublished.

Jobs, E.; Leibler, S.; Flyvbjerg, H., Modeling microtubule oscillations. 3. European conference on mathematics applied to biology and medicine, Heidelberg (DE), 6-10 Oct 1996. Unpublished.

Lading, L., A white light speed trap. Physics World, 1996, Jan 1996, pp 19-20.

Lading, L., Doppler debate - reply. Physics World, 1996, vol. 9, No. 4, April 1996 pp 15-15.

Lading, L., Statistical description of optical fields. Advanced topics in modern optics. Summerschool and workshop in optics, Humlebæk (DK), 2-8 Jun 1996. Unpublished.

Lading, L., Speckle and related phenomena. Advanced topics in modern optics. Summerschool and workshop in optics, Humlebæk (DK), 2-8 Jun 1996. Unpublished.

Lindvold, L., Miniaturization of optical chemical sensors. Grundfos sensor seminar, Bjerringbro (DK), 18 Apr 1996. Unpublished.

Martini Jørgensen, T., Anvendelse af kunstige neurale net til vision opgaver. Knowledge at your fingertips. Seminar on applied machine intelligence. Zitech, Allerød (DK), 29 Oct 1996. Unpublished. Abstract available.

Peters, B.O.; Pfurtscheller, G.; Flyvbjerg, H., Classification of EEG signals with artificial neural networks. 3. European conference on mathematics applied to biology and medicine, Heidelberg (DE), 6-10 Oct 1996. Unpublished.

Rogaard, C., Styringer. Ordblindeinstituttet. Københavns Amt, Søborg (DK), 18 Apr 1996. Unpublished.

Rose, B., Scattering from solid surfaces: The effects of target structures. Advanced topics in modern optics. Summerschool and workshop in optics, Humlebæk (DK), 2-8 Jun 1996. Unpublished.

Weimar Andersen, A.; Martini Jørgensen, T., Examples of machine vision applications in the food industry. Advanced industrial food processing conference. Bristol University, Bristol (GB), 10-12 Jul 1996. Unpublished. Abstract available.

6.2.3 Internal Reports

Bidrag til Forskningscenter Risøs 3-årsplan 1997-1999 fra Afdelingen for Optik og Fluid Dynamik. Risø-Dok-470 (1996) 32 p.

6.3 Plasma and Fluid Dynamics

6.3.1 Publications

Bergé, L.; Kuznetsov, E.A.; Rasmussen, J. Juul, Defocusing regimes of nonlinear waves in media with negative dispersion. Phys. Rev. E (1996) v. 53 pp R1340-R1343.

Bergé, L.; Kuznetsov, E.A.; Rasmussen, J. Juul; Shapiro, E.G.; Turitsyn, S.K., Self-focusing of optical pulses in media with normal dispersion. Phys. Scr. (1996) v. T67 pp 17-20.

Bergé, L.; Rasmussen, J. Juul, Multisplitting and collapse of self-focusing anisotropic beams in normal/anomalous dispersive media. Phys. Plasmas (1996) v. 3 pp 824-843.

Bergé, L.; Rasmussen, J. Juul, Pulse splitting of self-focusing-beams in normally dispersive media. Phys. Rev. A (1996) v. 53 pp 4476-4480.

Bergé, L.; Rasmussen, J. Juul; Wyller, J., Dynamics of localized solutions to the Raman-extended derivative nonlinear Schrödinger equation. J. Phys. A (1996) v. 29 pp 3581-3595.

Bergé, L.; Rasmussen, J. Juul; Kuznetsov, E.A.; Shapiro, E.G.; Turitsyn, S.K., Self-focusing of chirped optical pulses in media with normal dispersion. J. Opt. Soc. Am. B (1996) v. 13 pp 1879-1891.

Bergeron, K.; Coutsias, E.A.; Lynov, J.P.; Nielsen, A.H., Self-organization in circular shear layers. Phys. Scr. (1996) v. T67 pp 33-37.

Christiansen, P.L.; Gaididei, Y.B.; Rasmussen, K.Ø.; Mezentsev, V.K.; Rasmussen, J. Juul, Dynamics in discrete two-dimensional nonlinear Schrödinger equations in the presence of point defects. Phys. Rev. B (1996) v. 54 pp 900-912.

Christiansen, P.L.; Gaididei, Y.B.; Mezentsev, V.K.; Musher, S.L.; Rasmussen, K.Ø.; Rasmussen, J. Juul; Ryzhenkova, I.V.; Turitsyn, S.K., Discrete localized states and localization dynamics in discrete nonlinear Schrödinger equations. Phys. Scr. (1996) v. T67 pp 160-166.

Coutsias, E.A.; Hagstrom, T.; Hesthaven, J.S.; Torres, D., Integration preconditioners for differential operators in spectral *tau*-methods. In: ICOSAHOM-95. Proceedings. 3. International conference on spectral and high order methods, Houston, TX (US), 5-9 Jun 1995. Ilin, A.V.; Ridgway Scott, L. (eds.), (Houston Journal of Mathematics, Houston, TX, 1996) (Houston Journal of Mathematics) pp 21-38.

Coutsias, E.A.; Hesthaven, J.S.; Lynov, J.P., New spectral algorithms for accurate simulations of bounded flows. In: Advanced concepts and techniques in thermal modelling. Eurotherm seminar 36, Poitiers (FR),

21-23 Sep 1994. Lemonnier, D.; Saulnier, J.B.; Fiebig, M. (eds.), (Elsevier, Amsterdam, 1996) pp 119-127.

Coutsias, E.A.; Hesthaven, J.S.; Lynov, J.P., An accurate and efficient spectral tau method for the incompressible Navier-Stokes equations in a planar channel. In: ICOSAHOM-95. Proceedings. 3. International conference on spectral and high order methods, Houston, TX (US), 5-9 Jun 1995. Ilin, A.V.; Ridgway Scott, L. (eds.), (Houston Journal of Mathematics, Houston, TX, 1996) (Houston Journal of Mathematics) pp 39-54.

Hesthaven, J.S., An asymptotically stable penalty method for multi-domain solution of the unsteady compressible Navier-Stokes equations. In: ICOSAHOM-95. Proceedings. 3. International conference on spectral and high order methods, Houston, TX (US), 5-9 Jun 1995. Ilin, A.V.; Ridgway Scott, L. (eds.), (Houston Journal of Mathematics, Houston, TX, 1996) (Houston Journal of Mathematics) pp 445-456.

Hesthaven, J.S.; Gottlieb, D., A stable penalty method for the compressible Navier-Stokes equations: I. Open boundary conditions. SIAM J. Sci. Comput. (1996) v. 17 pp 579-612.

Jensen, V.O., Fusionsenergien: Kommer den, og hvad kommer den til at betyde?. EL og Energi (1996) v. 92 (no.9) pp 34-35.

Karpman, V.I.; Lynov, J.P.; Michelsen, P.K.; Rasmussen, J.J., Modulational instability of plasma waves in two dimensions. Math. Comput. Simul. (1996) v. 40 pp 223-234.

Lading, L.; Saffman, M.; Hanson, S.G.; Edwards, R.V., A combined doppler and time-of-flight laser anemometer for measurement of density fluctuations in plasmas. J. Atmos. Terr. Phys. (1996) v. 58 pp 1013-1019.

Lynov, J.P.; Singh, B.N. (eds.), Association Euratom - Risø National Laboratory annual progress report 1995. Risø-R-897(EN) (1996) 70 p.

Mamaev, A.V.; Saffman, M.; Zozulya, A.A., Propagation of dark stripe beams in nonlinear media: Snake instability and creation of optical vortices. Phys. Rev. Lett. (1996) v. 76 pp 2262-2265.

Mamaev, A.V.; Saffman, M., Hexagonal optical patterns in anisotropic non-linear media. Europhys. Lett. (1996) v. 34 pp 669-674 .

Mamaev, A.V.; Saffman, M., Pattern formation in a linear photorefractive oscillator. Opt. Commun. (1996) v. 128 pp 281-286.

Mamaev, A.V.; Saffman, M.; Anderson, D.Z.; Zozulya, A.A., Propagation of light beams in anisotropic nonlinear media: From symmetry breaking to spatial turbulence. Phys. Rev. A (1996) v. 54 pp 870-879.

Mamaev, A.V.; Saffman, M.; Zozulya, A.A., Break-up of two-dimensional bright spatial solutions due to transverse modulation instability. Europhys. Lett. (1996) v. 35 pp 25-30.

Mamaev, A.V.; Saffman, M., Periodic and irregular patterns in linear and ring photorefractive oscillators. In: International quantum electronics conference 1996. IQEC conference, Sydney (AU), Jul 1996. (Optical Society of America, Washington, DC, 1996) (OSA Technical Digest Series) Paper WL71.

Mamaev, A.V.; Saffman, M.; Zozulya, A.A., Breakup and spatial dynamics of light beams in anisotropic bulk nonlinear media. In: International quantum electronics conference 1996. IQEC conference, Sydney (AU), Jul 1996. (Optical Society of America, Washington, DC, 1996) (OSA Technical Digest Series) Paper ThJ3.

Mamaev, A.V.; Saffman, M.; Zozulya, A.A., Vortex evolution and bound pair formation in anisotropic nonlinear optical media. Phys. Rev. Lett. (1996) v. 77 pp 4544-4547.

Mamaev, A.V.; Saffman, M., Optical vortex patterns in a unidirectional ring oscillator. Phys. Scr. (1996) v. T67 p 21-25.

McCluskey, D.R.; Laursen, T.S.; Rasmussen, J.J.; Stenum, B., Damping of a vortex ring in a stratified fluid. In: Eighth international symposium on applications of laser techniques to fluid mechanics. Vol. 2. 8. International symposium on applications of laser techniques to fluid mechanics, Lisbon (PT), 8-11 Jul 1996. (Instituto Superior Técnico. Departemento de Engenharia Mecanica, Lisboa Codex, 1996) Paper 35.4.

Nielsen, A.H.; He, X.; Rasmussen, J. Juul; Bohr, T., Vortex merging and spectral cascade in two-dimensional flows. Phys. Fluids (1996) v. 8 pp 2263-2265.

Nielsen, A.H.; Pécseli, H.L.; Rasmussen, J.J., Turbulent transport in low-beta plasmas. Phys. Plasmas (1996) v. 3 pp 1530-1544.

Nielsen, A.H.; Rasmussen, J. Juul; Schmidt, M.R., Self-organization and coherent structures in plasmas and fluids. Phys. Scr. (1996) v. T63 pp 49-58.

Hanson, S.G.; Lading, L.; Lynov, J.P.; Skaarup, B. (eds.), Optics and Fluid Dynamics Department annual progress report for 1995. Risø-R-865(EN) (1996) 90 p.

Pedersen, T.S.; Michelsen, P.K.; Rasmussen, J.J., Lyapunov exponents and particle dispersion in drift wave turbulence. Phys. Plasmas (1996) v. 3 pp 2939-2950.

Pedersen, T.S.; Michelsen, P.K.; Rasmussen, J. Juul, Resistive coupling in drift wave turbulence. Plasma Phys. Control. Fusion (1996) v. 38 pp 2143-2154.

Pedersen, T.S.; Michelsen, P.K.; Rasmussen, J. Juul, Analysis of chaos in plasma turbulence. Phys. Scr. (1996) v. T67 p 30-32.

Rasmussen, J.J.; Hesthaven, J.S.; Lynov, J.P.; Nielsen, A.H.; Schmidt, M.R., Dipolar vortices in two-dimensional flows. Math. Comput. Simul. (1996) v. 40 pp 207-221.

Saffman, M., Book review: Self-organization in optical systems and applications in information technology. Eds. Vorontsov, M.A.; Miller, W.B. (Springer-Verlag, New York, 1995). Opt. Photonics News (1996) v. 7 p. 43.

Saffman, M., Quantum noise reduction by beam coupling in photorefractive media. In: Atomic and quantum optics: High-precision measurements. ICONO '95, St. Petersburg (RU), 27 Jun - 1 Jul 1995. Bagayev, S.N.; Chirkin, A.S. (eds.), (The International Society for Optical Engineering, Bellingham, WA (US), 1996) (SPIE Proceedings Series, 2799) pp 198-202.

Saffman, M., Tunable twin beam generation by beam coupling in photorefractive media. In: Coherence and quantum optics 7. Proceedings. 7. Rochester conference on coherence and quantum optics, Rochester, NY (US), 7-10 Jun 1995. Eberly, J.H.; Mandel, L.; Wolf, E. (eds.), (Plenum Press, New York, NY, 1996) pp 639-640.

Sørensen, L.H.; Gjernes, E.; Jessen, T.; Fjellerup, J., Determination of reactivity parameters of model carbons, cokes and flame-chars. Fuel (1996) v. 75 p. 31-38.

Tachon, J.; Lawson, J.; Jensen, M.I.; Jensen, V.O. (eds.), Fusion expo. Energi fra solens egen energikilde. (Europa-Kommissionen. DG XII. Europæiske Fusionsprogram, Bruxelles, 1996) 43 p.

Zozulya, A.A.; Anderson, D.Z.; Saffman, M., Control of mutual spatial coherence of temporal features by reflexive photorefractive coupling. J. Opt. Soc. Am. B (1996) v. 13 pp 41-49.

Zozulya, A.A.; Anderson, D.Z.; Mamaev, A.V.; Saffman, M., Self-focusing and soliton formation in media with anisotropic nonlocal material response. Europhys. Lett. (1996) v. 36 pp 419-424.

6.3.2 Unpublished Contributions

Bang, O.; Bergé, L.; Rasmussen, J.J.; Mezentsev,V.K., Self-focusing of CW-beams in bulk media with both quadratic and cubic nonlinearities. ACOFT 96. 21. Australian conference on optical fibre technology, Gold Coast, Queensland (AU), 1-4 Dec 1996. Unpublished. Abstract available.

Bergé, L.; Juul Rasmussen, J.; Schmidt, M.R., Amalgamation of interacting light beams in Kerr-type media. Annual meeting of the Danish Optical Society, Risø (DK), 21-22 Nov 1996. Unpublished. Abstract available.

Jensen, S.J.; Saffman, M., Transfer of temporal fluctuations in photorefractive two-beam coupling. Annual meeting of the Danish Optical Society, Risø (DK), 21-22 Nov 1996. Unpublished. Abstract available.

Jensen, V.O., EU's fusionsprogram set ud fra et forskningssynspunkt. Møde om EU's fusionsprogram, incl. ITER. Forskningsministeriet, København (DK), 26 Feb 1996. Unpublished.

Jensen, V.O., Fusionsforskning. Kursus for fysiklærere fra 'Kursusregion Syd', Risø (DK), 15 Mar 1996. Unpublished.

Jensen, V.O., Fusion energy - the solution of the future. Seminar for project Lycée Carriat and Herlev Gymnasium, Risø (DK), 11 Apr 1996. Unpublished.

Jensen, V.O., Fusion. Seminar for lærere fra Hässleholm Tekniska Skole, Risø (DK), 2 May 1996. Unpublished.

Jensen, V.O., Fusionsenergi i fortid, nutid og fremtid. Fusion expo - solens kraftværk til jordens folk. Åbningsceremoni. Elmuseet, Bjerringbro (DK), 16 Aug 1996. Unpublished. Abstract available.

Jensen, V.O., Fusion work at Risø, future plans. Fusion Expo Consortium meeting. Centre de Recherches en Physique des Plasmas, Lausanne (CH), 23-24 Oct 1996. Unpublished.

Junker, W.; Saffman, M.; Lading, L., Spatially resolved measurements of density fluctuations with a hybrid doppler/time-of-flight laser anemometer. In: 1996 CLEO/Europe. Technical digest. Conference on lasers and electro-optics Europe, Hamburg (DE), 8-13 Sep 1996. (IEEE, Piscataway, NJ, 1996) p. 151.

Juul Jensen, S.; Saffman, M., Correlation enhancement by nonlinear optical three beam coupling. Annual meeting of the Danish Physical Society, Nyborg (DK), 23-24 May 1996. Unpublished. Abstract available.

Lynov, J.-P., Experimental and numerical studies of coherent structures in fluids and plasmas. ERCOFTAC Nordic pilot center meeting, Stockholm (SE), 5-6 Sep 1996. Unpublished.

Lynov, J.-P., Numeriske Strømningsstudier i Afdelingen for Optik og Fluid Dynamik, Foss Electric, Hillerød, Denmark, 12 November 1996.

Mamaev, A.V.; Saffman, M., Multiple scale hexagonal patterns. In: QELS '96. Summaries of papers presented at the quantum electronics and laser science conference. Conference edition. Quantum electronics and laser science conference, Anaheim, CA (US), 2-7 Jun 1996. (Optical Society of America, Washington, DC, 1996) (1996 Technical Digest Series, 10) p. 129.

Mamaev, A.V.; Saffman, M.; Zozulya, A.A., Three-dimensional breakup and spatial dynamics of two-dimensional beams in bulk nonlinear media. In: QELS '96. Summaries of papers presented at the quantum electronics and laser science conference. Conference edition. Quantum electronics and laser science conference, Anaheim, CA (US), 2-7 Jun 1996. (Optical Society of America, Washington, DC, 1996) (1996 Technical Digest Series, 10) pp 221-222.

Mamaev, A.V.; Saffman, M., Optical patterns in linear and ring photorefractive oscillators: from rolls to rotating flowers. In: QELS '96. Summaries of papers presented at the quantum electronics and laser science conference. Conference edition. Quantum electronics and laser science conference, Anaheim, CA (US), 2-7 Jun 1996. (Optical Society of America, Washington, DC, 1996) (1996 Technical Digest Series, 10) p. 222.

Mamaev, A.V.; Saffman, M., Hexagonal pattern formation in anisotropic nonlinear media. In: EQEC '96. Technical digest. European quantum electronics conference, Hamburg (DE), 8-13 Sep 1996. (IEEE, Piscataway, NJ, 1996) p. 30.

Mamaev, A.V.; Saffman, M.; Zozulya, A.A., Instability of planar solitary waves in anisotropic bulk nonlinear media. In: EQEC '96. Technical digest. European quantum electronics conference, Hamburg (DE), 8-13 Sep 1996. (IEEE, Piscataway, NJ, 1996) p. 232.

Michelsen, P.K., Numerical studies of drift wave turbulence. Joint Varenna - Lausanne international workshop on theory of fusion plasmas, Varenna (IT), 26-30 Aug 1996. Unpublished.

Michelsen, P.K.; Juul Rasmussen, J., Vortex dynamics in low-frequency electrostatic turbulence. 5. Symposium on double layers - potential formation and related nonlinear phenomena in plasmas. Tohoku

University, Sendai (JP), 17-19 Sep 1996. Unpublished. Abstract available.

Michelsen, P.K.; Sunn Pedersen, T.; Juul Rasmussen, J., Lyapunov exponents and particle dispersion in drift-wave turbulence. 1996 International conference on plasma physics, Nagoya (JP), 9-13 Sep 1996. Unpublished. Abstract available.

Michelsen, P.K.; Sunn Pedersen, T.; Juul Rasmussen, J., Resistive coupling in drift wave plasma turbulence. 1996 International conference on plasma physics, Nagoya (JP), 9-13 Sep 1996. Unpublished. Abstract available.

Naulin, V., Vortex structures and transport in drift-wave turbulence. Düsseldorf University, Düsseldorf (DE), 19 Dec 1996. Unpublished.

Naulin, V., Structures in drift-wave turbulence and their impact on particle transport. Joint Varenna-Lausanne International workshop on Theory of Fusion Plasma, Varenne, Italy, 26-30 August 1996.

Naulin, V., Contribution of coherent structures to particle transport in driftwave turbulence. Euroconference on Supercomputation in Nonlinear and Disordered Systems: Algorithms, Applications and Architectures San Lorenzo de El Escorial, Marid, Spain, 23-28 September 1996.

Nielsen, A.H.; Rasmussen, J. Juul, Trapped passive particles in two-dimensional coherent structures. 21. General assembly of the European Geophysical Society, The Hague (NL), 6-10 May 1996. Ann. Geophys. Suppl. 2 (1996) v. 14 p. C612

Nielsen, A.H.; Rasmussen, J.J.; He, X., Trapped passive particles in two-dimensional coherent structures. Annual meeting of the Danish Physical Society, Nyborg (DK), 23-24 May 1996. Unpublished. Abstract available.

Nijs, R. de; Stoltze Laursen, T.; Rasmussen, J.J.; Stenum, B., Shear flow instability in a parabolic vessel. Annual meeting of the Danish Physical Society, Nyborg (DK), 23-24 May 1996. Unpublished.

Nijs, R. de; Stolze Laursen, T.; Rasmussen, J. Juul; Stenum, B., Shear flow instability in a parabolic vessel. 21. General assembly of the European Geophysical Society, The Hague (NL), 6-10 May 1996. Ann. Geophys. Suppl. 2 (1996) v. 14 p. C674.

Rasmussen, J. Juul, Electron beam instabilities in plasmas. Royal Institute of Technology. Alfvén Laboratory, Stockholm (SE), 2 Feb 1996. Unpublished.

Rasmussen, J. Juul, Self-organization and coherent vortical structures in plasmas, fluids and optics. Seminar Ionenphysik. Universität Innsbruck. Institut für Ionenphysik, Innsbruck (AT), 4 Jun 1996. Unpublished.

Rasmussen, J. Juul, Transport and turbulence in a low-beta plasma. Seminar Energie- und Plasmaphysik. Universität Innsbruck. Institut für Ionenphysik, Innsbruck (AT), 5 Jun 1996. Unpublished.

Rasmussen, J. Juul, Turbulence and transport in fluids and plasmas. EPS 10. Trends in physics. 10. General conference of the European Physical Society, Sevilla (ES), 9-13 Sep 1996. Unpublished. Abstract available.

Rasmussen, J. Juul, Vortex merging and spectral cascade in two-dimensional flows. Isaac Newton Institute for Mathematical Sciences.

University of Cambridge, Cambridge (GB), 21 Oct - 1 Nov 1996. Unpublished.

Saffman, M., Optical patterns in linear and ring photorefractive oscillators: rolls to rotating flowers. Institut for Matematisk Modellering. DTU, Lyngby (DK), 25 Jan 1996. Unpublished.

Saffman, M., Dynamics of spatial solitons and patterns in nonlinear optics. Nordic summer school on complexity, coherence and non-equilibrium systems, Humlebæk (DK), 24-27 Aug 1996. Unpublished.

Schmidt, M.R.; Rasmussen, J. Juul; Nielsen, A.H., Inverse cascade and intermittency in 2D turbulence. 21. General assembly of the European Geophysical Society, The Hague (NL), 6-10 May 1996. Ann. Geophys. Suppl. 2 (1996) v. 14 p. C676.

Schmidt, M.R.; Rasmussen, J.J.; Nielsen, A.H., Inverse cascade and intermittency in 2D turbulence. Annual meeting of the Danish Physical Society, Nyborg (DK), 23-24 May 1996. Unpublished. Abstract available

Stenum, B.; Stoltze Laursen, T.; Rasmussen, J. Juul; Snezhkin, E.N., Drift velocities of forced monopoles in rotating shallow water. 21. General assembly of the European Geophysical Society, The Hague (NL), 6-10 May 1996. Ann. Geophys. Suppl. 2 (1996) v. 14 p. C676.

Stenum, B.; Stoltze Laursen, T.; Rasmussen, J.J.; Snezhkin, E.N., Drift velocities of forced monopoles in rotating shallow water. Annual meeting of the Danish Physical Society, Nyborg (DK), 23-24 May 1996. Unpublished.

Zozulya, A.A.; Anderson, D.Z.; Mamaev, A.V.; Saffman, M., Self-focusing and convergence to elliptical solitons in anisotropic bulk nonlinear media. In: CLEO-Europe/EQEC '96. Postdeadline papers. CLEO-Europe '96, Hamburg (DE), 8-13 Sep 1996. (IEEE, Piscataway, NJ, 1996) Paper EPD2.5.

6.3.3 Internal Reports

Bidrag til Forskningscenter Risøs 3-årsplan 1997-1999 fra Afdelingen for Optik og Fluid Dynamik. Risø-Dok-470 (1996) 32 p.

7. Personnel

Scientific Staff

Bak, Jimmy
Christensen, Steen Sloth (until 31 January)
Clausen, Sønnik
Flyvbjerg, Henrik (from 1 April, on leave from 1 July - 31 December)
Hansen, Lars Kresten (1 January - 30 November)
Hanson, Steen Grüner
Jensen, Arne Skov
Jensen, Vagn O.
Jensen, Peter Arendt (1 January - 30 April)
Johansen, Per Michael
Junker, Wolfgang (until 30 April)
Jørgensen, Thomas Martini
Kaiser, N.E.
Kirkegaard, Mogens
Lading, Lars
Lindvold, Lars R.
Linneberg, Christian (from 1 April)
Lynov, Jens-Peter
Michelsen, Poul K.
Nielsen, Anders H.
Olsen, Aksel
Petersen, Paul Michael
Ramanujam, P.S.
Rasmussen, Jens Juul
Rogaard, Carsten (until 30 September)
Saffman, Mark
Schou, Jørgen
Stenum, Bjarne

Post Docs

Konijnenberg, Johan Antoon van de (from 1 August)
Kristensen, Jesper Glückstad
Laursen, Thorkild S. (until 29 February)
Naulin, Volker (from 1 September)
Pedersen, Thomas Garm (from 1 September)
Pedersen, Henrik C. (from 1 June)
Svendsen, Winnie E. (from 1 May)

Industrial Post Docs

Andersen, Peter E.
Dam-Hansen, Carsten (from 1 March)

Hazell, Irene (until 28 February)
Imam, Husein

Ph.D. Students

Dam-Hansen, Carsten (until 29 February)
Holme, Niels Christian Rømer
Jensen, Sussie Juul
Jessen, Thomas
Løbel, Martin
Nielsen, Birgitte Thestrup
Pedersen, Henrik C. (until 31 May)
Rose, Bjarke
Schmidt, Michel R.
Svendsen, Winnie E. (until 30 April)

Technical Staff

Andersen, Finn
Bækmark, Lars
Eilertsen, Erik
Ethelfeld, Joel
Hansen, Bengt Hurup
Jensen, Monika (1-28 February)
Nordskov, Arne
Pedersen, Søren Peo (until 31 July)
Petersen, Torben D.
Poulsen, Karin
Rasmussen, Erling
Reher, Børge
Sass, Bjarne
Stubager, Jørgen
Thorsen, Jess

Secretaries

Astradsson, Lone
Skaarup, Bitten

Guest Scientists

Chakrabarti, Nikhil, Institute of Plasma Research, Bhat, India
Fridken, Vladimir, Institute of Crystallography, Moscow, Russia
Hesthaven, Jan, Brown University, Rhode Island, USA
Mamaev, Alexander, Russian Academy of Sciences, Russia
Mezentsev, Vladimir, Institute of Automation and Electrometry, Russian Academy of Sciences, Novosibirsk, Russia

Nikolova, Ludmila, Bulgarian Academy of Sciences, Bulgaria
Podivilov, E.V., Institute of Automation and Electrometry, Russian Academy of Sciences, Novosibirsk, Russia
Rypdal, Kristoffer, University of Tromsø, Norway
Saeki, Koichi, Shizuoka University, Japan
Snezhkin, E.N., Russian Research Center Kurchatov Institute, Moscow, Russia
Ul'yanov, Sergey Sergeevitch, Saratov State University, Russia
Zozulya, Alexei, University of Colorado at Boulder, Boulder, USA
Yura, Harold T., The Aerospace Corporation, Los Angeles, USA

Short-term Visitors

Bergé, Luc, Commissariat á l'Energie Atomique, Centre d'Etudes de Limeil-Valenton, France
Clercx, Herman, Eindhoven Technical University, The Netherlands
Grauer, Rainer, Heinrich-Heine-Universität, Düsseldorf, Germany
Karpman, Vladimir I., Racah Institute of Physics, Hebrew University, Jerusalem, Israel
Kuznetsov, Evgenii A., Landau Institute, Moscow, Russia
Nezlin, M.V., Russian Research Center Kurchatov Institute, Moscow, Russia
Pécseli, H.L., University of Oslo, Norway
Shivamoggi, B.K., University of Central Florida, USA
Stegner, Alexander, Ecole Normale Superieure, Paris, France
Tsinober, Arkady, Tel Aviv University, Israel
Turitsyn, Sergei K., Institute of Automation and Electrometry, Russian Academy of Sciences, Novosibirsk, Russia
Wyller, John, Narvik Institute of Technology, Norway
Yankov, V.V., Russian Research Center Kurchatov Institute, Moscow, Russia
Zakharov, V.E., Landau Institute, Moscow, Russia

Students Working for the Master's Degree

Büchmann, Nanna
Hansen, Tue Normann
de Nijs, Robin
Leerbech, Lars
Lomholt, Sune

Student Assistants

Christensen, Max Peter Mørk
Leerbech, Lars